

# **Composition Prediction of Debutanizer Column using Neural Network**

by

Ima Syafiah Binti Isnu

16841

Dissertation submitted in partial fulfilment of  
the requirements for the  
Bachelor of Engineering (Hons)  
(Chemical Engineering)

MAY 2015

Universiti Teknologi PETRONAS  
32610, Bandar Seri Iskandar,  
Perak

# CERTIFICATION OF APPROVAL

## **Composition Prediction of Debutanizer Column using Neural Network**

by

Ima Syafiah Binti Isnu

16841

A project dissertation submitted to the  
Chemical Engineering Programme  
Universiti Teknologi PETRONAS  
in partial fulfillment of the requirement for the  
BACHELOR OF ENGINEERING (Hons)  
(CHEMICAL ENGINEERING)

Approved by,

---

(Nasser B M Ramli)

UNIVERSITI TEKNOLOGI PETRONAS

BANDAR SERI ISKANDAR, PERAK

May 2015

## CERTIFICATION OF ORIGINALITY

This is to certify that I am responsible for the work submitted in this project, that the original work is my own except as specified in the references and acknowledgements, and that the original work contained herein have not been undertaken or done by unspecified sources or persons.

---

IMA SYAFIAH BINTI ISNU

## **ABSTRACT**

In oil refining industries, debutanizer column is one of the important unit operations. Debutanizer column is the main column used to produce the main product in oil refinery process. The online composition prediction of top and bottom product of debutanizer column using neural network will be an aid to increase product quality monitoring in oil refining industry. In this work, a single dynamic neural network model is used in order to achieve the objective which is to generate composition prediction online of the top and bottom product of debutanizer column. Neural network is a computing system with several of simple and highly interconnected processing elements that will process information using their dynamic state response to external inputs. It is a software based sensor method or known as “soft sensor” which is a helpful technology that utilizes software techniques to infer the value of important but difficult-to-measure process variables from available process variables which are requisite from physical sensor observation or lab measurements. The neural network development and equation based model for i-butane, i-pentane, n-butane, n-pentane and propane has been obtained. Then, these results will be compared with proportional integral derivatives (PID) controller design to show its supremacy over this method.

## **ACKNOWLEDGEMENT**

In the name of ALLAH S.W.T, the most merciful and compassionate, praise to ALLAH, He is the almighty, eternal blessing and peace upon the Glory of the Universe, our beloved prophet Muhammad (S.A.W), and his family and companions.

First and foremost, all praise and glory to ALLAH Almighty for giving me healthiness and strength to undergo this final year final semester period as well as to complete this report. My deep appreciation goes to Universiti Teknologi PETRONAS and the Chemical Engineering Department for giving me this opportunity to learn and undergo this project which is widely researched in the oil and gas industry.

Special appreciation and gratitude is extended my supervisor, Mr. Nasser Bin M Ramli, Lecturer at Chemical Engineering Department for guiding, monitoring and teaching me throughout the Final Year Project. His attention, guidance, willingness and kindness have made the journey of my project a pleasant and successful one.

Last but not least, I also would like to thank my beloved family and friends for their support and encouragement in order for me to complete this phase of learning.

## TABLE OF CONTENTS

<b>CERTIFICATION OF APPROVAL</b>	ii
<b>CERTIFICATION OF ORIGINALITY</b>	iii
<b>ABSTRACT</b>	iv
<b>ACKNOWLEDGEMENT</b>	v
<b>TABLE OF CONTENTS</b>	vi
<b>LIST OF FIGURES</b>	viii
<b>LIST OF TABLES</b>	xi
<b>LIST OF APPENDICES</b>	xi
<b>CHAPTER 1: INTRODUCTION</b>	1
1.1 Problem Statement	1
1.2 Objective	3
1.3 Scope of Study	3
<b>CHAPTER 2: LITERATURE REVIEW</b>	4
2.1 Overview of Crude Oil Processing Plant & Debutanizer Column	11
2.2 Overview of Neural Network	14
2.3 Overview of Feedforward Neural Network	16
<b>CHAPTER 3: METHODOLOGY</b>	18
3.1 Model Data Generation	18
3.2 Neural Network Data Sets	18
3.3 Gantt Chart	22

3.4	Key Milestone	24
<b>CHAPTER 4:</b>	<b>RESULTS AND DISCUSSION</b>	<b>26</b>
4.1	Top (Reflux) and Bottom (Reboiler) Composition of the Components	26
4.2	Neural Network Development	32
4.2.1	Neural Network Forward Model	32
4.2.2	Neural Network Inverse Model	44
4.3	Transfer Function Equation Development	54
<b>CHAPTER 5:</b>	<b>CONCLUSION AND RECOMMENDATION</b>	<b>57</b>
<b>REFERENCES</b>		<b>58</b>
<b>APPENDICES</b>		<b>61</b>

## LIST OF FIGURES

Figure 1:	Oil refinery industry block diagram	11
Figure 2:	Debutanizer column configuration	13
Figure 3:	General structure of neural network	14
Figure 4:	Flow of neural network	15
Figure 5:	Two layer FTDNN	15
Figure 6:	A single-layer network	15
Figure 7:	Two-layer <i>tansig/purelin</i> network	16
Figure 8:	Top composition of i-butane	24
Figure 9:	Bottom composition of i-butane	25
Figure 10:	Top composition of i-pentane	25
Figure 11:	Bottom composition of i-pentane	26
Figure 12:	Top composition of n-butane	26
Figure 13:	Bottom composition of n-butane	27
Figure 14:	Top composition of n-pentane	27
Figure 15:	Bottom composition of n-pentane	28
Figure 16:	Top composition of propane	28
Figure 17:	Bottom composition of propane	29
Figure 18:	Neural network forward model	29
Figure 19:	MSE vs. Epoch for i-butane at number of neuron 20	31
Figure 20:	Regression for i-butane at number of neuron 20	31
Figure 21:	Actual and simulated plot for top composition of i-butane	31

Figure 22:	Actual and simulated plot for bottom composition of i-butane	32
Figure 23:	MSE vs. Epoch for i-pentane at number of neuron 56	32
Figure 24:	Regression for i-pentane at number of neuron 56	33
Figure 25:	Actual and simulated plot for top composition of i-pentane	33
Figure 26:	Actual and simulated plot for bottom composition of i-pentane	33
Figure 27:	MSE vs. Epoch for n-butane at number of neuron 40	34
Figure 28:	Regression for n-butane at number of neuron 40	34
Figure 29:	Actual and simulated plot for top composition of n-butane	35
Figure 30:	Actual and simulated plot for bottom composition of n-butane	35
Figure 31:	MSE vs. Epoch for n-pentane at number of neuron 36	36
Figure 32:	Regression for n-pentane at number of neuron 36	36
Figure 33:	Actual and simulated plot for top composition of n-pentane	36
Figure 34:	Actual and simulated plot for bottom composition of n-pentane	37
Figure 35:	MSE vs. Epoch for propane at number of neuron 48	37
Figure 36:	Regression for propane at number of neuron 48	38
Figure 37:	Actual and simulated plot for top composition of propane	38
Figure 38:	Actual and simulated plot for bottom composition of propane	38
Figure 39:	Neural network inverse model	39
Figure 40:	MSE vs. Epoch for i-butane at number of neuron 4	40
Figure 41:	Regression for i-butane at number of neuron 4	40
Figure 42:	Actual and simulated plot for top composition of i-butane	40
Figure 43:	Actual and simulated plot for bottom composition of i-butane	41
Figure 44:	MSE vs. Epoch for i-pentane at number of neuron 48	41

Figure 45:	Regression for i-pentane at number of neuron 48	42
Figure 46:	Actual and simulated plot for top composition of i-pentane	42
Figure 47:	Actual and simulated plot for bottom composition of i-pentane	42
Figure 48:	MSE vs. Epoch for n-butane at number of neuron 28	43
Figure 49:	Regression for n-butane at number of neuron 28	43
Figure 50:	Actual and simulated plot for top composition of n-butane	44
Figure 51:	Actual and simulated plot for bottom composition of n-butane	44
Figure 52:	MSE vs. Epoch for n-pentane at number of neuron 64	45
Figure 53:	Regression for n-pentane at number of neuron 64	45
Figure 54:	Actual and simulated plot for top composition of n-pentane	45
Figure 55:	Actual and simulated plot for bottom composition of n-pentane	46
Figure 56:	MSE vs. Epoch for propane at number of neuron 20	46
Figure 57:	Regression for propane at number of neuron 20	47
Figure 58:	Actual and simulated plot for top composition of propane	47
Figure 59:	Actual and simulated plot for bottom composition of propane	47

## **LIST OF TABLES**

Table 1:	Debutanizer column specification	12
Table 2:	Description of the variables for the column	13
Table 3:	Variables involved in the neural network	21

## **LIST OF APPENDICES**

Appendix 1:	Top and Bottom Output Plot	61
Appendix 2:	Training State	71
Appendix 3:	Trial and Error Hidden Nodes	75
Appendix 4:	Overall Algorithm/Coding for neural network	78

# CHAPTER 1

## INTRODUCTION

The industry of chemical process plant involves many type of operation unit. A number of equipments such as reactor and distillation column have been used in their chemical process to produce required product. In oil refinery process, the debutanizer column is the main column unit functioning to produce products such as petroleum product, liquefied petroleum gas, naphtha and low sulphur waxy residue. Debutanizer column is a type of fractional distillation column used to separate butane from natural gas. Distillation column is the most common unit in the chemical industry that has an integrated and complex system. Its integrated and complex system has made the operation and control of column become very difficult. In recent years, an interest in development of distillation column system to produce high quality of product has emerged. Hence it becomes important to design the debutanizer column system in oil refinery process to help improve product quality by predicting the top and bottom composition. In relation to this requirement, a robust and cheaper method such as online soft sensor has to be developed by using suitable approach.

### 1.1 Problem Statement

Debutanizer column used in petroleum refining industries is one of the distillation column that has the complex behaviour, high non-linearity and complexity in control loops. These unique behaviour or characteristics of distillation column becomes complicated and difficult to handle by chemical engineers. The most problem encounter by chemical industry is in controlling and monitoring the debutanizer column. Principally, there are five basic variables required to be control to achieve efficient operation which are liquid level of reflux drum, liquid level of

bottom stream, composition of bottom stream, composition of distillate stream and column pressure (de Canete, Gonzalez-Perez, & del Saz-Orozco, 2008). These variables have to be controlled in order to achieve accurate operation and high quality of product. However, chemical engineers nowadays facing difficulty to control and monitoring these variables due to column non-linearity issues, multivariate issues, open loop instability issues, and the difficulty to measure a certain variable directly.

Currently, the top and bottom composition of column are measured by normal laboratory sampling which is monotonous and time consuming. The time taken to measure the compositions by laboratory sampling normally takes one day (Mohamed Ramli, Hussain, Mohamed Jan, & Abdullah, 2014). In past decades, the distillation dynamics and control especially for composition control have been studied (Skogestad, 1997). One of the composition control used was the online measurement or online analyzer. In order to achieve the monitoring and controlling purpose in chemical process operation, an accurate online measurement of quality variables are required and many manipulated variables could be used, such as distillate flow, reflux flow, vapour flow, and bottom flow. From this, many control strategy with different combination of manipulated variables and configurations have to be developed (Skogestad, 2004). Unfortunately, the key obstacles in implementation online measurement are the large time delays of measurement and the expensive cost of its measurement devices (Fortuna, Graziani, & Xibilia, 2005). Since most of chemical industry processes are nonlinear in nature, a continuous robust method that can solve these problems is therefore needed to be developed.

In recent times, the soft sensor method is widely used to develop model for non-linearity problem in chemical process industry. Principal component analysis (PCA) and partial least square (PLS) which are the multivariate statistical methods based on linear projection have been the efficient methods for the constructing empirical model (Park & Han, 2000a). In addition, there are also well-known nonlinear regression methods such as neural network or artificial neural network (ANN), projection pursuit regression (PPR), nonlinear PLS, and alternating conditional expectations (ACC) (Hussain, 1999).

## 1.2 Objectives

In this day and age the purity of distillate, the quality of products and the time to estimate the distillate composition are the main objectives of chemical process industries. For debutanizer column used in petroleum refining industries, the design for composition prediction is important in order to improve the product quality.

This paper is intended to generate the composition prediction online of the top and bottom product of debutanizer column using neural network method or also known as artificial neural network (ANN). Throughout this method, an equation based neural network models will be developed. Singh et al. (2006) have design ANN-based estimator for distillation process using Levenberg-Marquardt (LM) approach (Singh, Gupta, & Gupta, 2007). The column pressure, reboiler duty and reflux flow together with the temperature profile of the distillation column as the input were used to predict the composition of distillate for this approach. ANN equation shown that it is more efficient method than the partial least square (PLS) and regression analysis (RA) equation based methods (Mohamed Ramli et al., 2014). The soft sensor of equation based ANN also a fast and practical route for debutanizer column system. Therefore, the alternative online method which is neural network is used in this study to predict the composition of debutanizer column since it is expected to generate more precise and robust results within a faster period. The composition prediction using neural network will be compared with PID controller method.

## 1.3 Scope of Study

In achieving objective of the project, a comprehensive study has to be conducted and it covers the following scopes of study:

- i. Gathering information of chemical process plant, distillation column, soft sensor, and neural network by conducting literature survey; the background of crude oil processing plant, debutanizer column, soft sensor and neural network.
- ii. Observe the composition predicted of debutanizer column by single dynamic neural network approach or development.

## **CHAPTER 2**

### **LITERATURE REVIEW**

The intensity and complexity of chemical process plant operations have been exponentially increasing as the demands for the production level as well as more stringent product quality specification are increasing. In order to achieve these requirements, chemical process plant industries mostly relying on the automatic control systems. In recent years, a vigorous in the development and application of nonlinear control methodologies has become known. The remarkable increase in the number of research papers published in this area recently made the nonlinear control now as an important position in the area of chemical engineering as well as process control engineering. However, most of nonlinear system it is very difficult and expensive to achieve an accurate model of the process that had made limited usage of nonlinear models. Indeed, the cost of model development and validation is one of the barriers to the more pervasive use of nonlinear models in advanced modelling and control techniques in the chemical or petroleum industry. Hence a number of cheaper and accurate methods such as neural network for identifying nonlinear processes have been introduced. This low cost and accurate alternative of soft sensor has attracted plant designers and engineers to use it in their process plant operations.

The recent rise in research of neural networks has made it readily available as an attractive soft sensor method since it can learn by examples, offer a cost-effective method of developing useful process models (Hussain, 1999). Neural network is attractive because of its information processing characteristics such as high parallelism, nonlinearity, fault tolerance and capability to generalize and handle imprecise information (Basheer & Hajmeer, 2000). These characteristics have made neural network fit for solving a variety of problems. Neural network model also can learn the frequently complex dynamic behaviour of a physical system. A recent work

by Cybenko (Cybenko, 1989) Hornik et al. (Hornik, Stinchcombe, & White, 1989) proved that a feedforward neural network consists of two hidden layers and a fixed, continuous non-linearity can approximate any continuous functions to an arbitrary degree of exactness on a compact set. Pioneering works is a began application of neural network in chemical engineering (Hoskins & Himmelblau, 1988) and the number of research publications on neural network in chemical engineering was gradually increased in the following years. The five major areas which are process control, dynamic modelling, forecasting, fault diagnosis and optimization are the most covered in these publications. Other soft sensor method such as fuzzy neural network (FNN), partial least square (PLS), support vector regression (SVR), least square support vector machines (LS-SVM) and etc. also used recently.

A black-box modelling scheme to predict melt index (MI) in the industrial polymerization process has been proposed by Liu and Zhao (Liu & Zhao, 2012). Product specification can be determined by MI which is one of the most important quality variables and is influence by a large number of process variables. Since measurement of MI in laboratory is quite expensive and time consuming, they presented MI online prediction where it is much cheaper and faster statistical modelling method. The technologies involved including FNN, particle swarm optimization (PSO) algorithm and online correction strategy (OCS). Global PSO (GPSO) algorithm, best-neighbour PSO (BNPSO) and BNPSO with OCS have been applied in their study to optimize parameters of FNN. BNPSO algorithm that used square topological structure shows advantage of high convergence speed and optimization precision than GPSO algorithm that used global structure. Their study shows the reliability and efficiency of the BPNSO algorithm and proves the proposed FNN model can express the relationship between process variables measured at the beginning of the production cycle and the quality of the final product. An adaptive soft sensor using FNN for online monitoring MI in the industrial propylene polymerization process has been developed by Zhang and Liu (Zhang & Liu, 2013). An adaptive fuzzy neural network (A-FNN) is subsequently developed to help determine the number of fuzzy values since the structure of FNN is difficult to determine. SVR also introduced for a better generalization ability of soft sensor. SVR acts as the parameter tuning and the output function is converted into an SVR based optimization problem. The different of soft sensor such as SVR, FNN-SVR

and A-FNN-SVR models also compared in their study using real industrial PP plant in order to obtain a good performance in MI prediction. A-FNN-SVR models give the most accurate result and all the proposed soft sensor models supposed to have a promising potential for practical use.

The prediction of MI is also important in quality control of propylene polymerization process. Shi and Liu using a LS-SVM soft sensor model of propylene polymerization process (Shi & Liu, 2006). LS-SVM is used to infer the MI of polypropylene from other process variables. In order to achieve a robust estimation of MI, the weighted LS-SVM (weighted LS-SVM) approach of propylene polymerization is further proposed in Shi and Liu work. A standard SVM model is used as a basis comparison of LS-SVM and weighted LS-SVM models. Another method proposed by Shi and co-workers to infer the MI of polypropylene from other process variables is a novel soft sensor architecture based on radial basis function networks (RBF). This RBF network combined with independent component analysis (ICA) and multi-scale analysis (MSA). The nonlinearity in every scale is characterized by RBF networks. ICA is introduced to select the most independent process features as well as to eliminate the correlations of the input variables while MSA is carried out to make the model more robust to mismatches and to acquire approximate scale information of the process. Furthermore, the LS-SVM with Ant Colony-Immune Clone Particle Swarm Optimization (AC-ICPSO-LSSVM) which is an optimal soft sensor is also studied by Jiang and co-workers (Jiang, Yan, & Liu, 2013). The soft sensor used to estimate the top and bottom composition of column is PLS regression. The work done by Kano et al. is the inferential models for estimating product compositions which is PLS regression with the simulated time series data as basis (Kano, Miyazaki, Hasebe, & Hashimoto, 2000). They also investigated the influence of selection measurements and sampling intervals on the performance. The result of their study shows that cascade control system based on proposed PLS model is better than the usual control system and tray temperature.

For low-density polyethylene (LDPE) and ethylene vinyl acetate (EVA) copolymers plant, the constant control and monitoring of reactors are required to minimize undesirable process excursions and meet severe product specifications. Both LDPE and EVA are produced in free radical polymerization using reactors at highly pressure. A work developed by Sharmin and co-workers is the application of

PLS as a soft sensor in order to predict melt flow index using data from an industrial autoclave reactor by introducing the data-based multivariable regression methods (Sharmin, Sundararaj, Shah, Vande Griend, & Sun, 2006). The product composition profiles for batch distillation column has been proposed by Zamprognna and co-workers using PLS regression (Zamprognna, Barolo, & Seborg, 2004). In their study, the composition of the distillate stream and the bottom product of batch distillation process are estimated using PLS based soft sensor. Principal component analysis (PCA) also used to analyse the available process data. A design methodology to build a soft sensor for chemical processes that can handle the nonlinearities and the correlation among many process variables is proposed by Park and Han (Park & Han, 2000b). The method proposed is the locally weighted regression (LWR) to estimate a regression surface through multivariate smoothing and the result obtained is then compared with other methods. A soft sensor developed using LWR approach shows an excellent way for chemical plants with high nonlinearity and colinearity. However, this approach cannot assure the good performance than other online methods such as NN and PLS. An online soft sensor modelling using the three different just-in-time-learning (JITL) methods is performed by Ge and Song (Ge & Song, 2010). The different JITL methods are PLS, SVR and LSSVR. Besides, a real-time performance improvement strategy also studied for modelling efficiency enhancement of JITL-based soft sensor. The real-time performance can be easily determined using JILT methods.

The product quality control and monitoring is the focus of oil refinery process plants recently. The product of oil refinery with high quality will depends on the performance of column system. Zilouchian and Bawazeer propose the application of neural networks in oil refineries to improve product quality (Zilouchian & Bawazeer, 2001). The information required for neural network models such as the input data, training data set, and selection of process variables etc. explained in their study. Various neural network architectures are proposed to predict product quality and the models show reliability to be implementing in oil refineries. A nonlinear system identification and model reduction technique using neural network has been developed by Prasad and Bequette (Prasad & Bequette, 2003). Plant input-output data is created using neural network and singular value decomposition (SVD) based technique to the weight matrices of neural network is applied to obtain model

reduction. A novel hybrid artificial neural network (HANN) based on BP-PLSR and its application in development of soft sensors is introduced in Xuefeng work (Xuefeng, 2010). The main flaws of neural network such as the difficulty to determine the optimal number of the hidden nodes and tendency of overfitting are overcome by applying HANN. The results of HANN model shown that it can solve overfitting problem and has the robust character. From the good results achieved by using neural network modelling, the neural network has been widely used in chemical process plant. The paper work presented by Hussain is on the application of neural networks in chemical process control in both simulation and online implementation (Hussain, 1999). The three major control schemes which are predictive control, adaptive control and inverse-model-based controls methods have been reviewed in his study.

Prediction control method is the most commonly found control method that used neural network models. Neural network based predictive method is a control scheme where the controller determines a manipulated variable profile that optimized some open-loop performance objective on a time interval, from the current time up to a prediction horizon. The attraction of using neural network models instead of other forms of model to efficiently correspond to the complex nonlinear systems within the predictive methodology is the reason of increasing esteem of the neural network based predictive method (Morris, Montague, & Willis, 1994). To achieve the objective and the usual limitation required upon it, this predictive control algorithm basically involves minimizing future output deviations from the set point whilst taking proper account of the control sequence needed. Psychogios and Ungar (Psychogios & Ungar, 1991) operated a neural network model of a continuous stirred-tank reactor (CSTR) to control the product composition in the conventional model predictive scheme. They found that steady state offsets were obtained during set point tracking. Hence, they made corrections to the output, accounting for unmeasured disturbances and modelling errors ingoing the process and they acquired offset-free tracking. The plant-model variance at each sampling instant estimated by Hunt and Sbarbaro (Hunt & Sbarbaro, 1991), Turner et al. (Turner, Montague, & Morris, 1995) and Willis et al. (Willis, Montague, Di Massimo, Tham, & Morris, 1992), and used it to correct the predictions from the model in their predictive control schemes. Hunt and Sbarbaro applied the scheme for control of pH in a neutralizing

reactor; Turner applied it for the control of concentration in a distillation column while Willies applied it for the control of concentration in a CSTR. All the set point tracking results obtained in these cases are offset-free. A steady-state multilayered neural network model to substitute the tray-to-tray model used in predictive model based controller to control the product compositions in a propylene-propane splitter utilized by Gokhale et al. (Gokhale, Hurowitz, & Riggs, 1995). They found that the set point changes in the top and bottom compositions using neural network scheme with online filtering presented slightly better than nonlinear model-based controller.

The recurrent networks also used in the model predictive method. The three different optimizing methods for design an external recurrent neural network predictive controller based on Smith-type prediction was compared by Tan and VanCauwenberghe (Tan & Van Cauwenberghe, 1996). This method used successfully by them to reimburse for large time delays in the control of anaerobic digester process under set point tracking. MacMurray and Himmelblau (MacMurray & Himmelblau, 1995) studied on the external recurrent neural network to predict and control the product compositions in a packed distillation column within the model predictive control technique. A result with less computation time compared to using first principle model is achieved in this study. The studies of using neural networks in the dynamic matrix control (DMC) algorithm have also been reported. The disturbance due to the presence of nonlinearities is estimated by implementing neural networks. This study is done by Hernandez and Arkun (Hernandez & Arkun, 1990) where it was then added to the linear model in the DMC formulation with online learning of the neural network models. The two cases applied this algorithm are the control of concentration in a CSTR system for set point tracking and disturbance-rejection. A better results is obtained for both cases as compared with the conventional linear DMC method.

Other than that, neural networks can also be adopted into the conventional adaptive control part in the control of nonlinear dynamic systems. There are two approaches normally categorized under these adaptive methods which are direct adaptive and indirect adaptive schemes. The controller parameters are directly adjusted on-line with no explicit attempt to find out the model of the system to obtain the necessary tracking and stability of the closed loop system for the direct adaptive control scheme. The controller in this scheme is the weights of the neural network

that are adjusted on-line to control the plant by reducing some cost function involving the desired response and plant output. Most of the applications of this method utilized the feedforward multilayered neural network. An adaptive control scheme where the controller models that updated on-line in the special inverse and error feedback learning method respectively is utilized by Watanabe (Watanabe, 2014). These methods were implemented successfully in controlling the number of average molecular weight of the polymer product and the temperature in a multiple-input multiple-output (MIMO) continuous polymerization reactor under set point tracking conditions. Neural network along with PID in a model reference adaptive strategy is use by Loh et al. (Loh, Looi, & Fong, 1995) to control a process pH where the network comprise of a cascade of two single hidden layer nets. The first net is a recurrent network to reveal the dynamic nature of the neutralizing reactor while the second net is a static one to reveal the static nature of filtration characteristics. Even under external load disturbances, their results showed good set point tracking performance. Lightbody and Irwin (Lightbody & Irwin, 1995) control the product composition of a CSTR system using neural network in parallel with a rigid gain linear controller in a direct model-reference adaptive control configuration. Under linear model reference output tracking, this method presented significantly improved performances over the conventional PI controller. Neural network in both direct adaptive and indirect adaptive control type methods for a CSTR with second order reactions take place between sodium thiosulphate and hydrogen peroxide studied by Ydstie (Ydstie, 1990). The objective of this study is to make the temperature follow a predetermined reference by controlling the reactant flow rate and it is successfully achieved. The neural network with linear bypass was used as the controller in the direct adaptive method while the numerical techniques at each step were used to solve the control action in the indirect adaptive method.



The top of debutanizer is the reflux that consists of the collected condensed hydrocarbon and lighter hydrocarbon is stripped by reboiler section.

TABLE 1. Debutanizer column specification (Mohamed Ramli *et al.*, 2014)

Number of tray of the column	35
Feed tray – stage number	23
Type of tray used	Valve
Column diameter	1.3 m
Column height	23.95 m
Condenser type	Partial
Feed mass flowrate	44106 kg $hr^{-1}$
Feed temperature	113 °C
Feed pressure	823.8 kPa
Overhead vapour mass flowrate	11286 kg $hr^{-1}$
Overhead liquid mass flowrate	5040 kg $hr^{-1}$
Condenser pressure	823.8 kPa
Reboiler pressure	853.2 kPa

The feed flow rate, reflux flow rate and reboiler flow rate are the main manipulated variables for debutanizer column. Debutanizer column is difficult to handle due to it deals with non-linearity, involves a great deal of interactions between the variables, is a highly multivariable process, and has lag in many of control system (Mohamed Ramli *et al.*, 2014).

TABLE 2. Description of the variables for the column (Mohamed Ramli *et al.*, 2014)

Tag	Description	Units
Temp 1	Debutanizer top temperature	°C
Temp 2	Debutanizer bottom temperature	°C
Temp 3	Debutanizer receiver bottom temperature	°C
Temp 4	Light Naphta temperature after condenser E 1	°C
Temp 5	Reboiler outlet temperature to column	°C
Temp 6	Debutanizer feed temperature	°C
Level 1	Debutanizer level	%
Level 2	Debutanizer condenser level	%
Level 3	Debutanizer level indicator	%
Level 4	Condenser level indicator	%
Flow 1	Light Naphta flow to storage	m <sup>3</sup> /hr
Flow 2	LPG flow to storage	m <sup>3</sup> /hr
Pressure 1	Debutanizer receiver overhead pressure	kPa

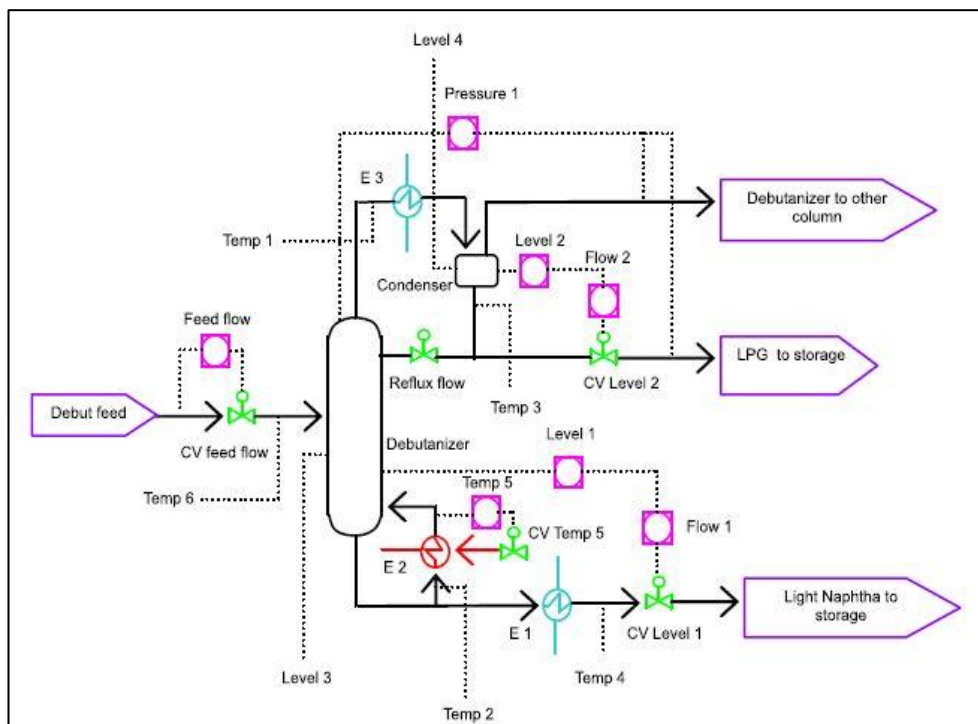


FIGURE 2. Debutanizer column configuration (Mohamed Ramli *et al.*, 2014)

## 2.2 Overview of Neural Network

Neural network or also referred as artificial neural network is a computing system with a various of simple and highly interconnected processing elements that will process information using their dynamic state response to external inputs (Beale, Hagan, & Demuth, 1992). The elements are inspired by biological nervous system. The structure of neural network consist of input layer that connected to one or more hidden layers and ending with an output layer where the actual processing is done via a system of weighted connections as shown in FIGURE 3. Neural network can be trained by adjusting the values of the connections or known as weights between elements to perform a particular function. It is adjusted or trained so that a particular input produce to a specific target output. The output and the target will be compared during the network is adjusted. They will be compared until the network output matches the target. Neural network has the ability as an arbitrary function approximation mechanism that acquire from observed data. In contrast, a very deep understanding of the neural network system and theory is required in order to develop an efficient and accurate neural network model as a soft sensor.

There are two categories of neural network; static and dynamic networks (Beale et al., 1992). Static network has no feedback elements and contain no delays. Its output is calculated directly from the input through feedforward connections. For dynamic network, the output depends on the current input and also previous input, output or states of the network. In short, dynamic network has a memory and it consists of feedforward and feedback connections. For this paper, the dynamic network is used and there are four types of dynamic network defined by Beale et al.; focused time-delay neural network (FTDNN), distributed time-delay, nonlinear autoregressive network with exogenous inputs (NARX) and layer-recurrent network (LRN). Dynamic network of FTDNN (newfftd) type is utilized to generate the composition prediction of the top and bottom debutanizer column. FTDNN is a dynamic neural network where the dynamic appear only at the input layer of a static multilayer feedforward network. It is start with the most straightforward dynamic network that consists of a feedforward network with a tapped delay line at the input. FIGURE 5 illustrates a two-layer FTDNN.

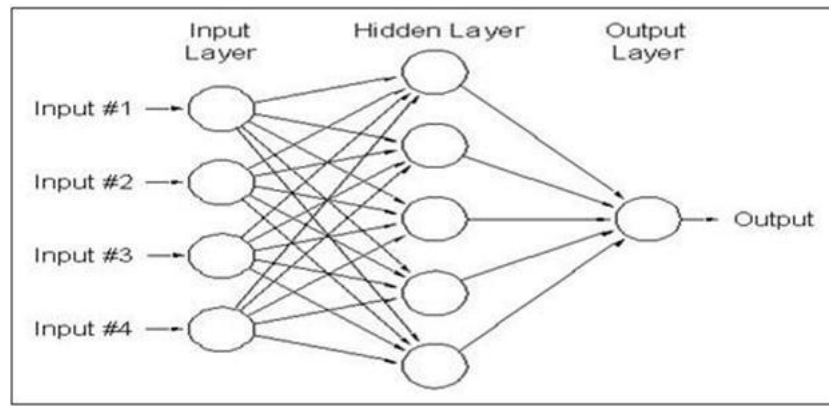


FIGURE 3. General structure of neural network (Prasad & Bequette, 2003)

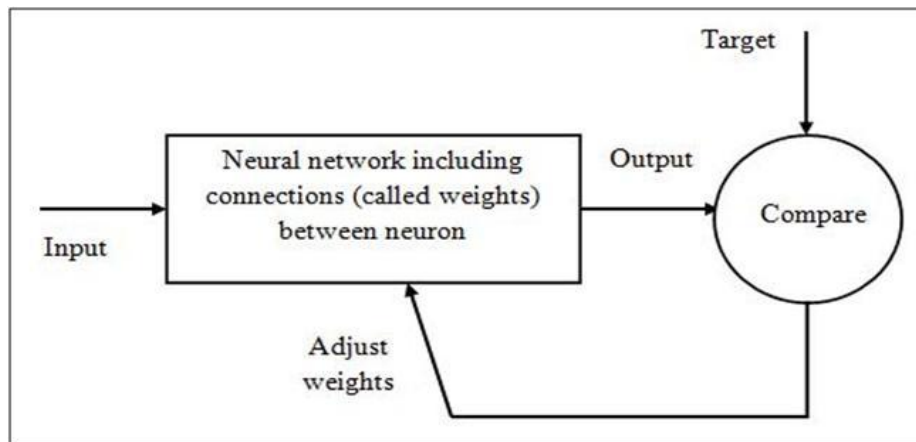


FIGURE 4. Flow of neural network structure (Beale *et al.*, 1992)

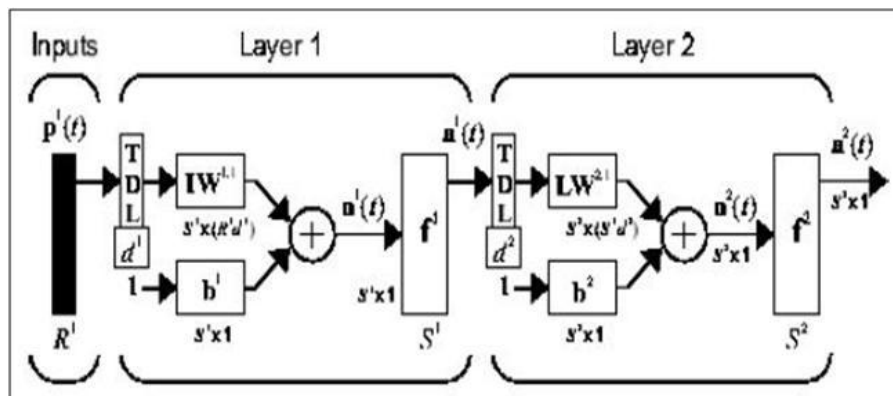


FIGURE 5. Two layer FTDNN (Beale *et al.*, 1992)

### 2.3 Overview of Feedforward Network

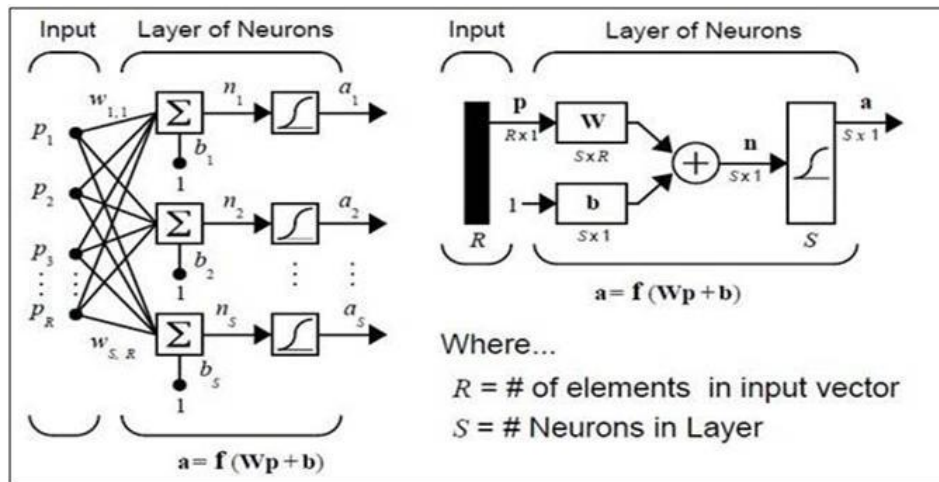


FIGURE 6. A single-layer network

FIGURE 6 is a single-layer network of  $S$  *logsig* neuron containing  $R$  inputs where on the left is the full detail and with a layer diagram on the right. Feedforward networks generally have one or more hidden layers of sigmoid neurons. The nonlinear and linear relationships between input and output vectors can be learned by network using nonlinear transfer functions with multiple layers of neuron. The network can produce values outside the range -1 to +1 by linear layer.

In contrast, the output layer should use a sigmoid transfer function such as *logsig* if it is desirable to limit the outputs of a network (i.e. between 0 and 1). For multiple-layer network, the number of layers is used to determine the superscript on the weight matrices. The suitable notation is used in two-layer *tansig/purelin* network as shown below.

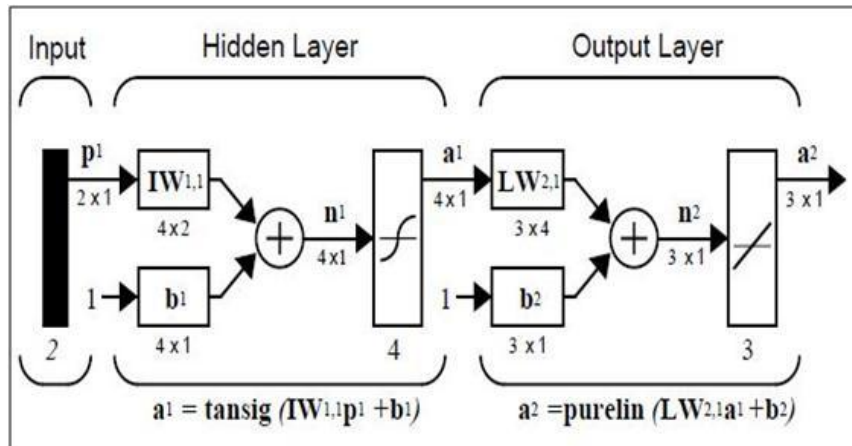


FIGURE 7. Two-layer *tansig/purelin* network

This network can be used as a common function approximator as it can approximate any function with a finite number of discontinuities, arbitrary well, given sufficient neurons in the hidden layer.

## **CHAPTER 3**

### **METHODOLOGY**

#### **3.1 Model Data Generation**

The online open loop response is mostly available from the plant surrounding the column. However, there are also some variables that are not available for open loop response surrounding this column. The variables that are not available are Temp 5, Pressure 1 and both top and bottom composition of the column. For this paper, these unavailable variables will be acquired by synthesizing the dynamic simulation of a debutanizer column using the plant process simulator HYSYS. The simulated close loop response of the composition of i-butane, i-pentane, n-butane, n-pentane and propane at the top and bottom of the column will be compared with the online close loop data. The simulated close loop response data will be determined prior to comparison with the online close loop data. For the simulation, the dynamic state will be developed by specifying additional engineering details such as equipment dimensions and pressure/flow relationships. For the selected unit operation in the simulation, the set of data including feed compositions, feed conditions, reflux ratio, reboiler pressure, and condenser pressure are needed. The manipulated variables for this simulation are reboiler and reflux flow rates. All variables surrounding the column were summarized in TABLE 2.

#### **3.2 Neural Network Data Sets**

Neural network is chosen for composition prediction of debutanizer due to it is expected to generate more robust, accurate and stable result than other online methods such as PLS and RA. The dynamic neural network architecture will be developed using open loop responses of the reboiler and reflux data sets. The outputs

of the neural network controller are the future predictions of i-butane, i-pentane, n-butane, n-pentane and propane while the composition of these components as well as the time delayed will be the output variables. For the numbers of past values, 1 will be considered for every input variable. This was determined by trial and error method.

In this work, Lavenberg-Marquard (LM) method is used for the training algorithm and the FTDNN is the type of dynamic network used. Furthermore, the mean square error criteria are the performance function that has been computed for this work. Other than that, the adaption learning function with momentum also will be performed. All the data is used for the training. The mean square performance with 100 number of epoch (training cycle) is used to obtain the network. The linear transfer function used for the whole layers with 10 number of inputs to the network (mv2, mv2\_lag, mv3, mv3\_lag, x, x1, x\_top, x\_top1, x\_bot, x\_bot1) and 2 outputs (x\_top+1, x\_bot\_1) as shown in TABLE 3.

The data set for open loop responses of the reboiler flow rate and reflux flow rate are obtained from plant and simulation. The composition of the components is the simulated data while the actual plant data is for the rest of the variables. The important variables involved in the neural network shows in TABLE 2. The input, hidden and output are the 3 layers of architecture. The training of the neural network has to be performed first to achieve the weights (values of the connections between element) and biases (network parameter) value used in the neural network equation. For the hidden nodes the trial and error method is used with initial guess of the hidden nodes at 4 and then it is increased by a factor 2 until 80. This step is performed using MATLAB 2013 simulation. The final number of hidden nodes is then determined by monitoring the Root Mean Square Error (RMSE). The one with the lowest RMSE value is selected to be used as hidden nodes. Analysis of variance (ANOVA) is also will be performed by using the test statistic method in MATLAB. RMSE is given by;

$$RMSE = \sqrt{\frac{(X_{measured} - X_{predicted})^2}{N}} \quad (1)$$

The general equation for the output from the neural network of 3 layer network given as

$$y = f^i(LW^{3,i}f^i(LW^{2,i}f^i(IW^{1,i}p + b^1) + b^2) + b^3) \quad (2)$$

Where,

$IW^{1,i}$  = input weight at layer 1 (input layer)

$b^1$  = bias values at layer 1

$LW^{2,i}$  = layer weight at layer 2 (hidden layer)

$b^2$  = bias values at layer 2

$LW^{3,i}$  = layer weight at layer 3 (output layer)

$b^3$  = bias values at layer 3

$p$  = vector inputs to the neural network

$y$  = vector outputs from the neural network

$f^i$  = activation function at layer i

TABLE 3. Variables involved in the neural network (Mohamed Ramli *et al.*, 2014)

mv2 (k)	Manipulated reboiler flow rate
mv2 (k-1)	Lag mv2
mv3 (k)	Manipulated reflux flow rate
mv3 (k-1)	Lag mv3
f (k)	Debutanizer feed temperature
f (k-1)	Lag feed temperature
p_top (k)	Top composition n-butane
p_top (k-1)	Lag top composition
p_bot (k)	Bottom composition n-butane
p_bot (k-1)	Lag bottom composition
p_top (k+1)	Future predictions top composition n-butane
p_bot (k+1)	Future predictions bottom composition n-butane

### 3.3 Gantt Chart

#### FYP 1

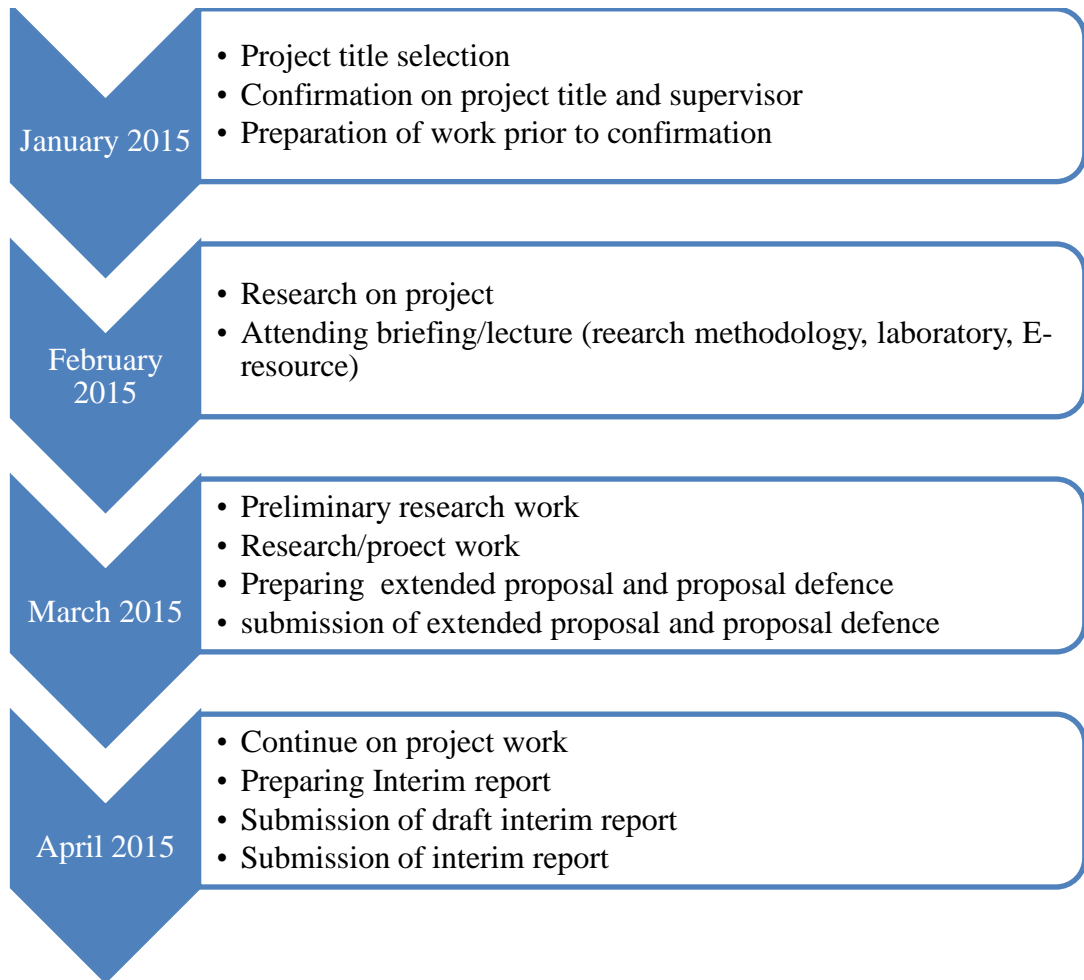
Week Number	1	2	3	4	5	6	7	8	9	10	11	12	13	14
Introductory lecture with coordinator	■													
Research titles submission by supervisors	■													
Title selection		■												
Research methodology lecture		■												
Laboratory briefing			■											
Preliminary research work and preparing proposal			■	■	■	■	■	■						
E-resource briefing			■											
Research work using Excel			■	■										
Endnote tutorial				■										
Research work using MATLAB					■	■	■	■	■					
Submission of Extended Proposal to supervisor								■						
Research proposal defence										■				
Project work continue														
Submission of Interim Draft Report to supervisors												■		
Submission of Final Interim Report													■	

FYP 2

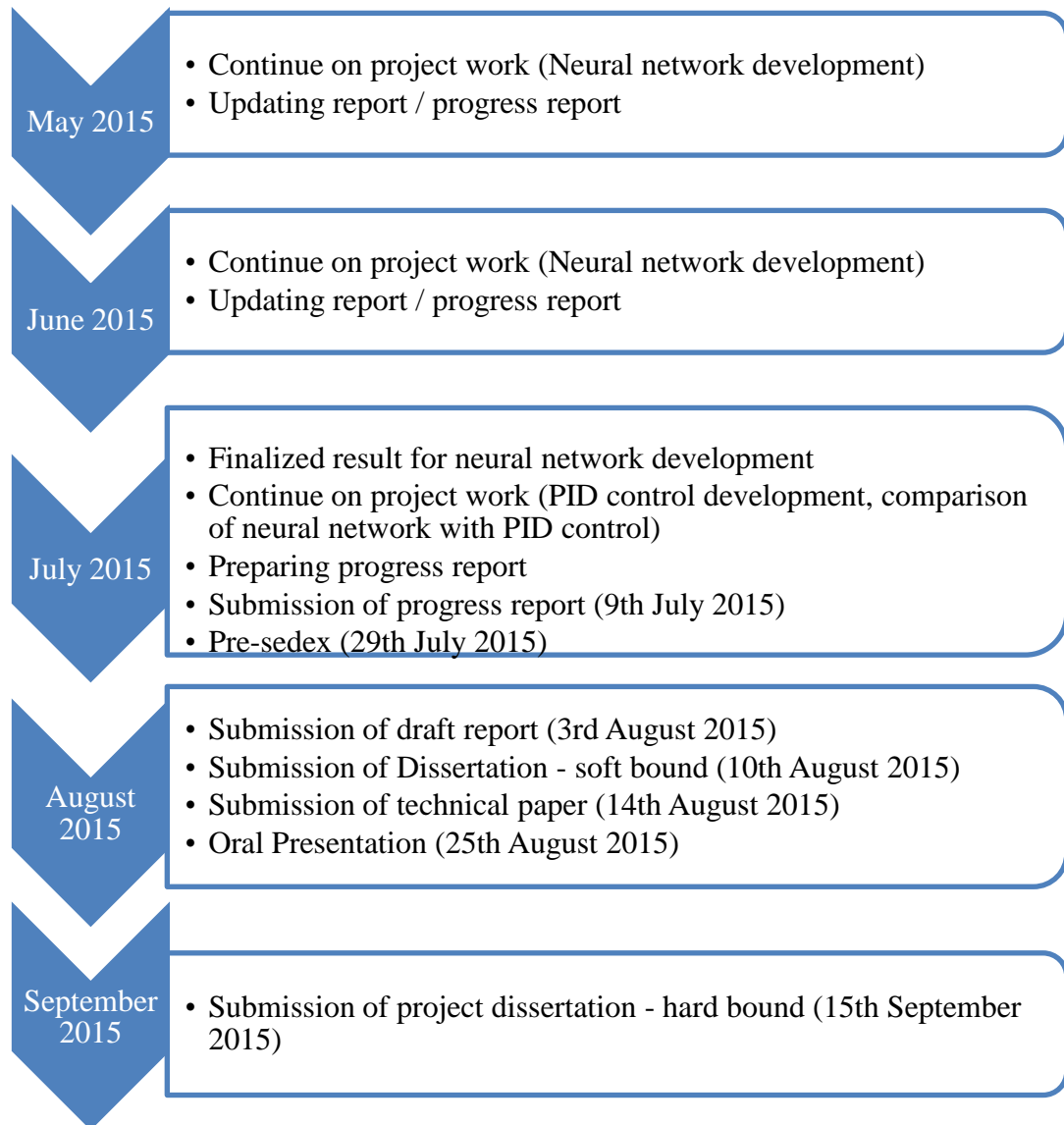
<b>Week Number</b>	<b>1</b>	<b>2</b>	<b>3</b>	<b>4</b>	<b>5</b>	<b>6</b>	<b>7</b>	<b>8</b>	<b>9</b>	<b>10</b>	<b>11</b>	<b>12</b>	<b>13</b>	<b>14</b>	<b>15</b>	<b>18</b>
<b>Activities</b>																
Project work continues																
Submission of Progress Report																
Project work continues																
Pre-SEDEX																
Submission of Draft Final Report																
Submission of Dissertation (soft bound)																
Submission of Technical Paper																
Oral Presentation																
Submission of Project Dissertation (hard bound)																

### 3.4 Key Milestone

#### FYP 1



## FYP 2



## CHAPTER 4

### RESULTS & DISCUSSION

#### 4.1 Top (Reflux) and Bottom (Reboiler) Composition of the Components

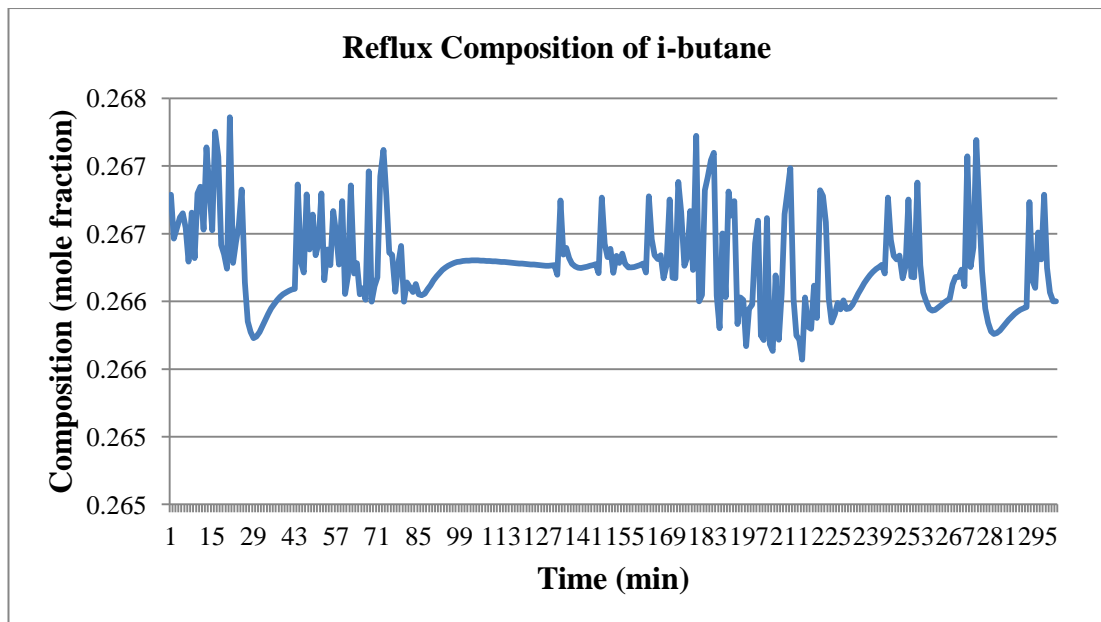


FIGURE 8. Top composition of i-butane

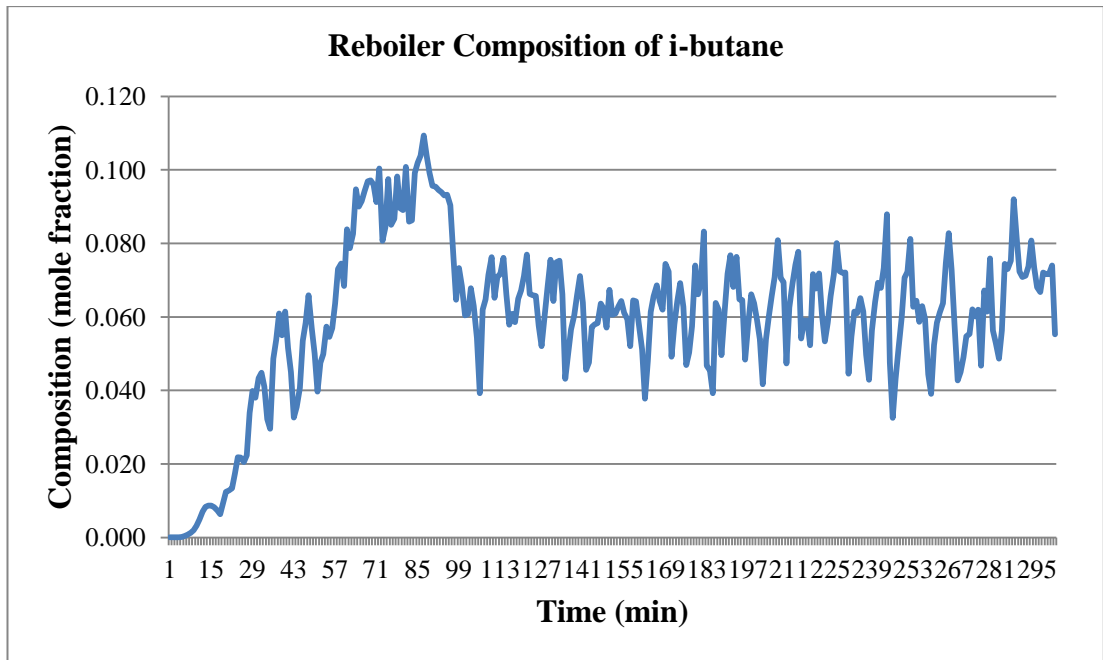


FIGURE 9. Bottom composition of i-butane

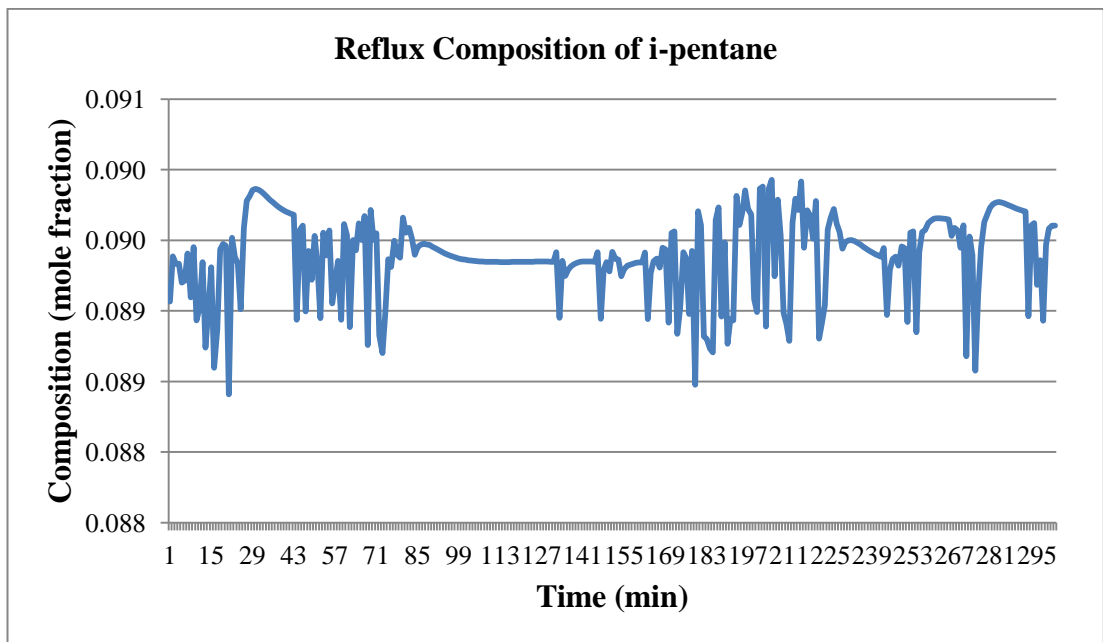


FIGURE 10. Top composition of i-pentane

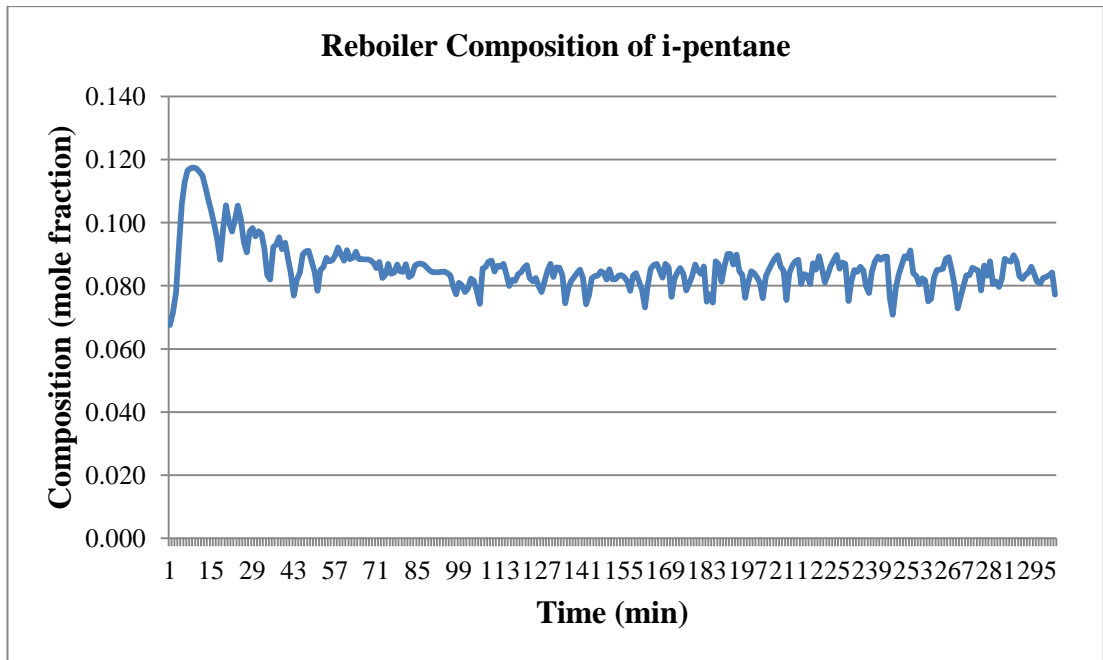


FIGURE 11. Bottom composition of i-pentane

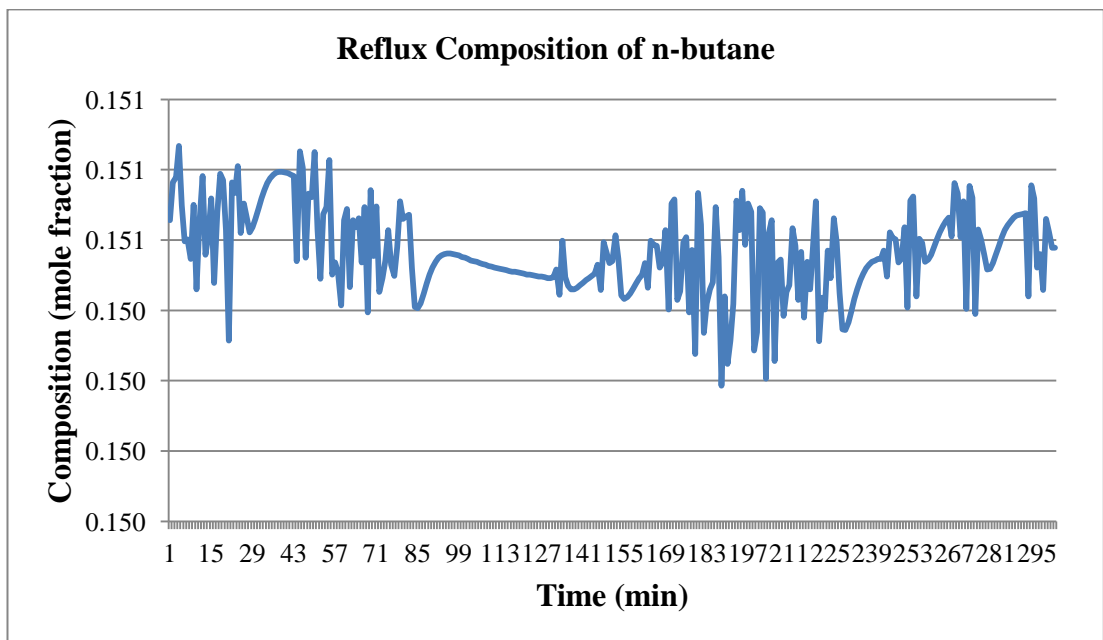


FIGURE 12. Top composition of n-butane

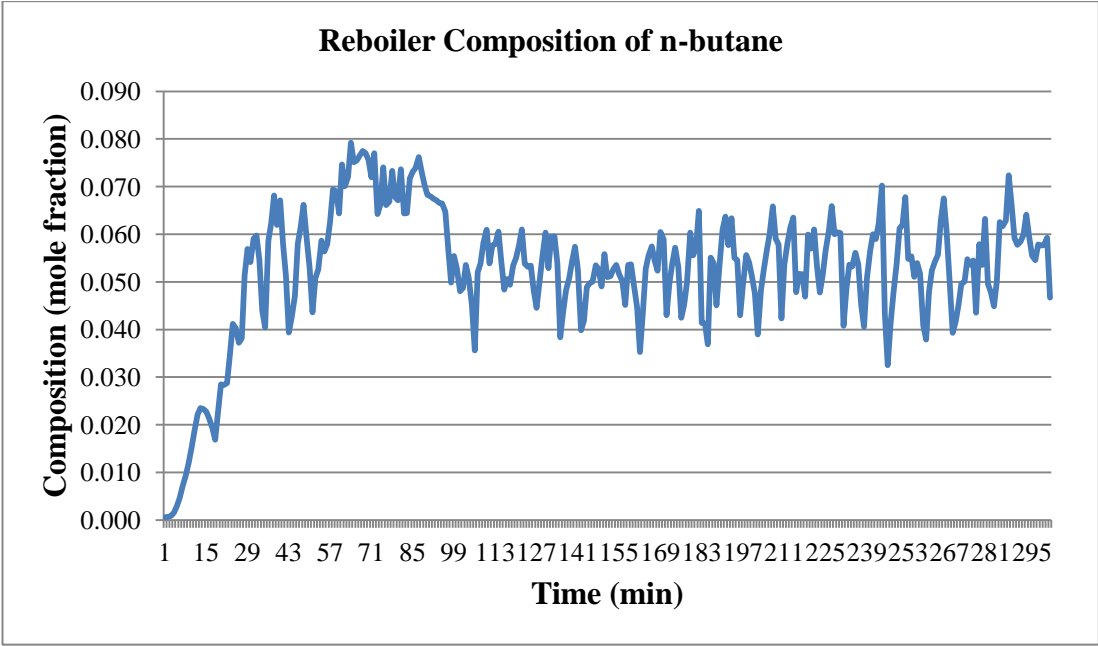
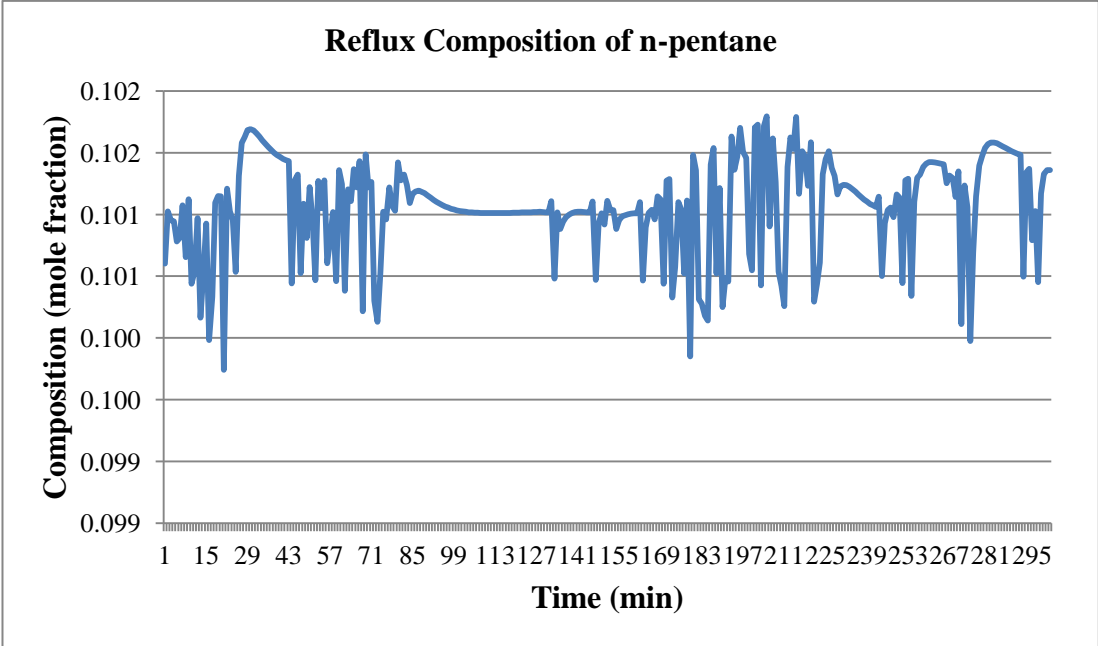


FIGURE 13. Bottom composition of n-butane



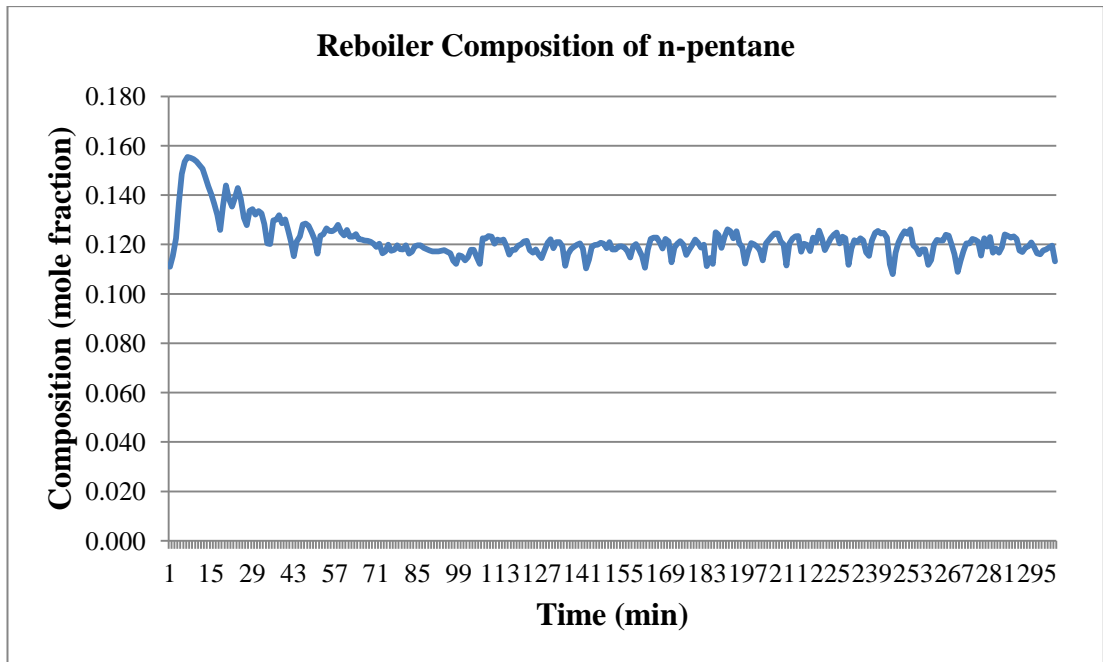


FIGURE 15. Bottom composition of n-pentane

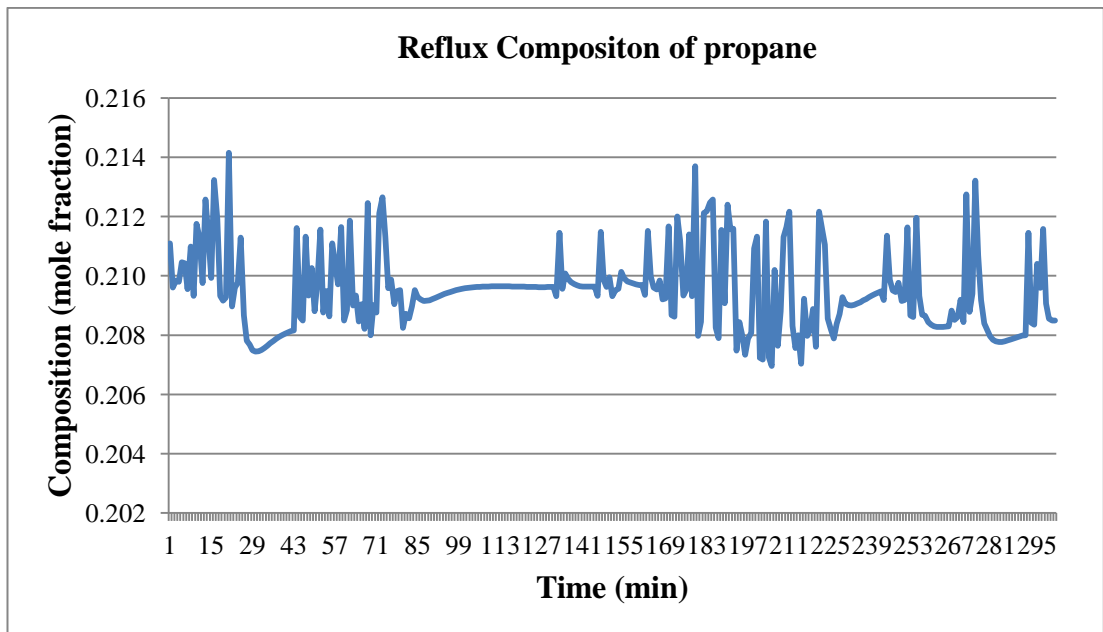


FIGURE 16. Top composition of propane

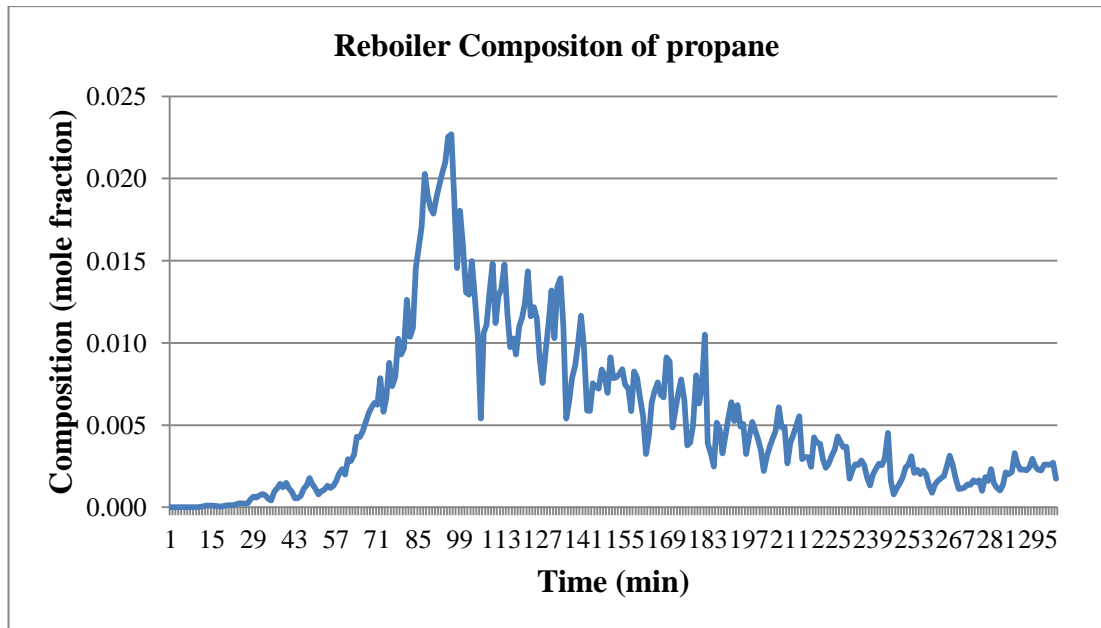


FIGURE 17. Bottom composition of propane

The reflux and reboiler composition of i-butane, i-pentane, n-butane, n-pentane and propane are plotted by using Microsoft EXCEL as shown in FIGURE 8 until FIGURE 17. The data of debutanizer column for these graphs can be obtained in the appendices where the step changes are applied to the inputs to get the corresponding output. The step test is needed in order to monitor the fluctuation and the effect of the process variables when making changes to the manipulated variable.

## 4.2 Neural Network Development

### 4.2.1 Neural Network Forward Model

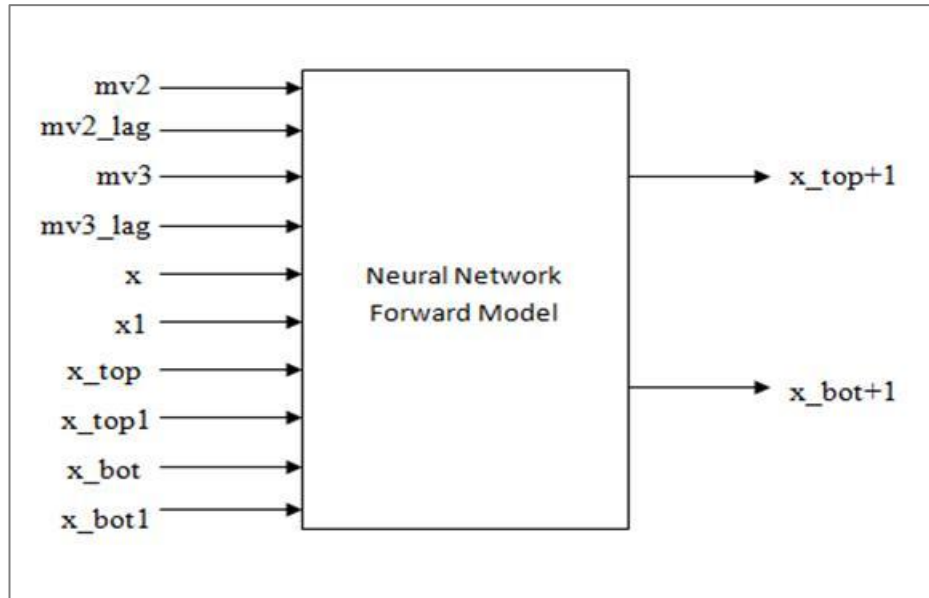


FIGURE 18. Neural network forward model

FIGURE 19 to FIGURE 38 shown below are the results obtained from the simulation of forward neural network control whereas FIGURE 40 to FIGURE 59 are from the simulation of inverse neural network control using MATLAB Simulation 2013 for i-butane, i-pentane, n-butane, n-pentane and propane. The optimum number of neuron selected is based on the MSE value by using trial and error method. MSE is the average squared difference between outputs and targets. The number of neuron tested that shows MSE value approach the target of 0.01 is chosen as the optimum number of neuron which also indicates the optimum prediction of the output. Zero means no error whereas MSE value over 0.6667 means high error.

#### i. i-Butane

For i-butane, 20 is the number of neuron that gives the optimum predictions of the output. FIGURE 19 shows the performance curve for the 20 number of neuron with 0.062119 MSE. FIGURE 4.12 is the regression, R values where it

measures the correlation between outputs and targets. The output for i-butane seems to track the target reasonably well. FIGURE 21 and 22 represent the differences between actual and simulated of the top and bottom composition of i-butane. From the both graphs it can be seen that there is a small deviation between the actual and simulation data.

Optimum number of neuron	20
Maximum number of epochs set	100
MSE	0.062119
R	0.80122

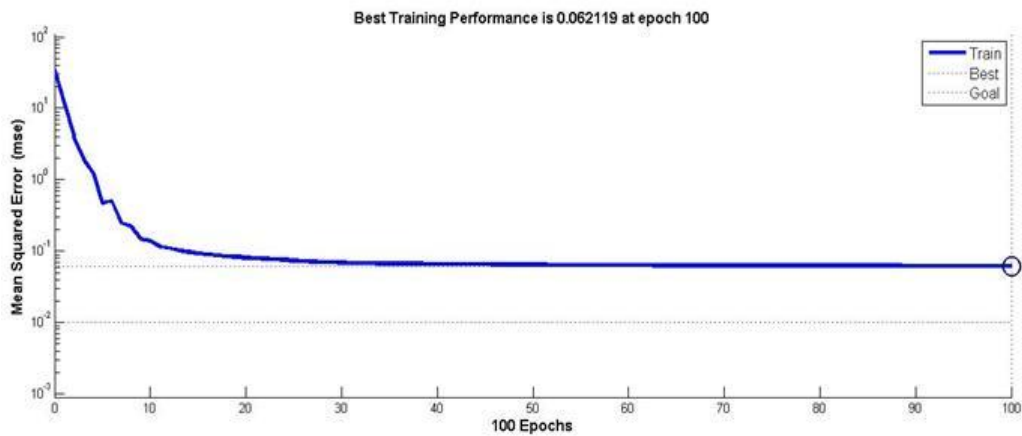


FIGURE 19. MSE vs. Epoch for i-butane at number of neuron 20

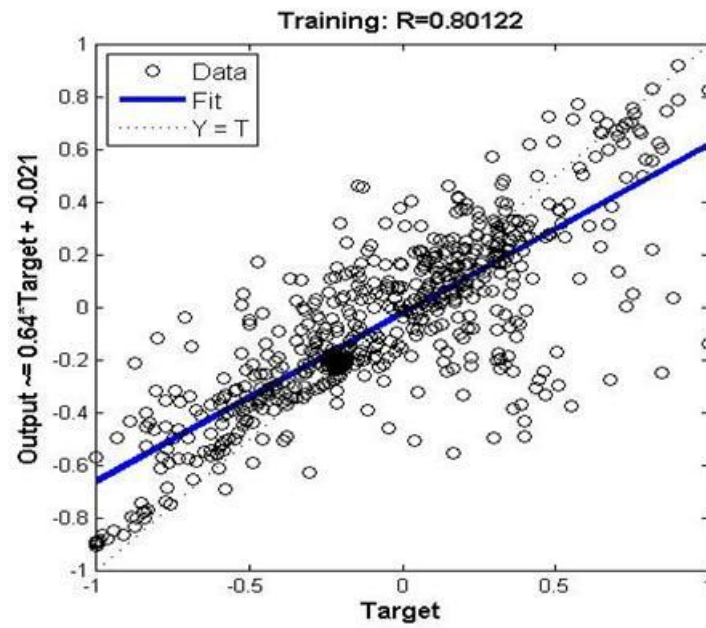


FIGURE 20. Regression for i-butane at number of neuron 20

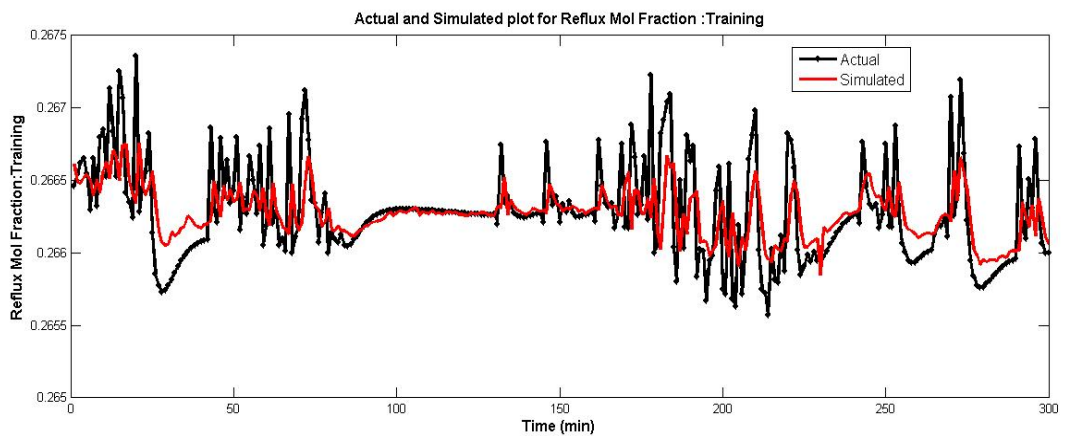


FIGURE 21. Actual and simulated plot for top composition of i-butane

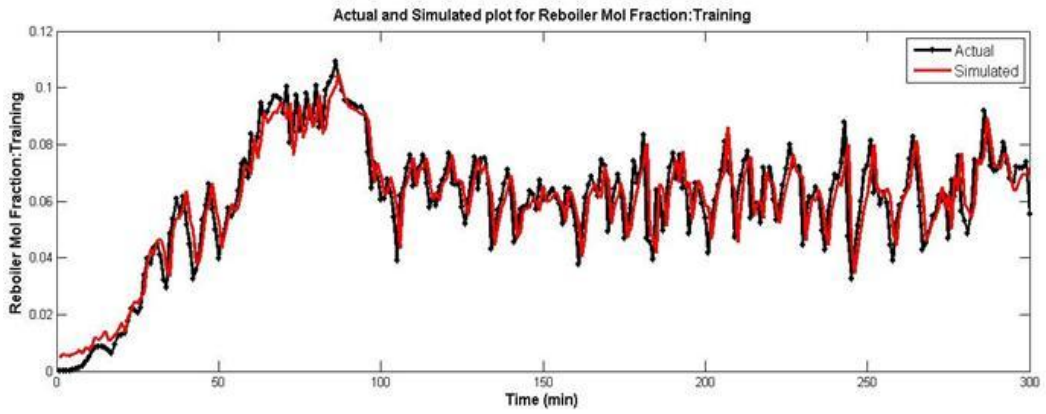


FIGURE 22. Actual and simulated plot for bottom composition of i-butane

**ii. i-Pentane**

For i-pentane, 56 is the number of neuron that gives the optimum predictions of the output. FIGURE 23 shows the performance curve for the 56 number of neuron with 0.042857 MSE. The regression value for i-pentane also seems to track the target reasonably and R-value is more than 0.9. FIGURE 25 and 26 represent the differences between actual and simulated of the top and bottom composition of i-pentane. From the both graphs it can be seen that there is a small deviation between the actual and simulation data.

Optimum number of neuron	56
Maximum number of epochs set	100
MSE	0.042857
R	0.90164

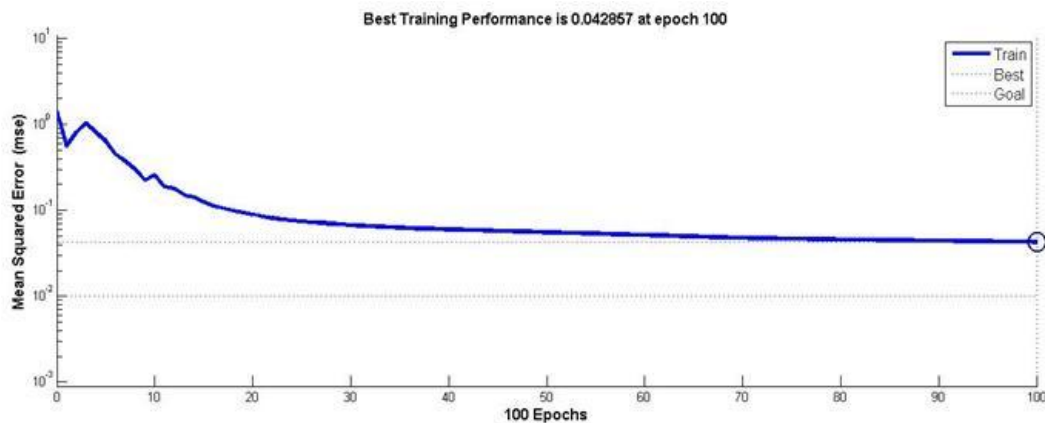


FIGURE 23. MSE vs. Epoch for i-pentane at number of neuron 56

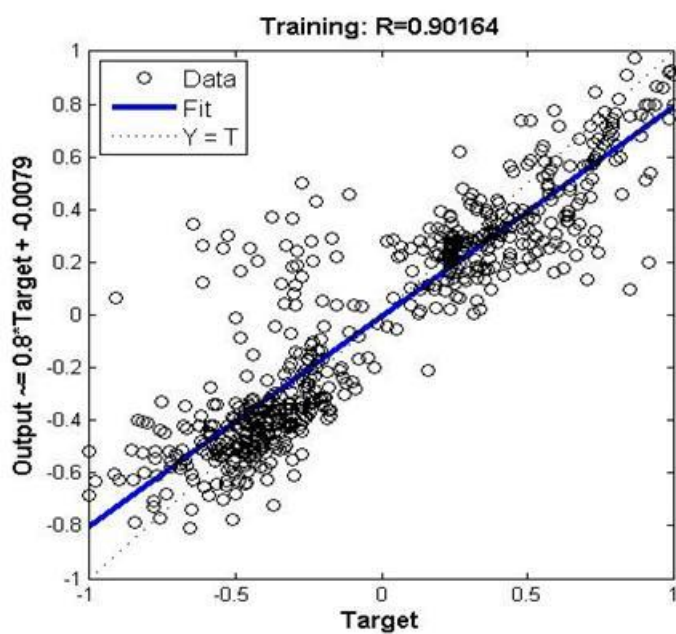


FIGURE 24. Regression for i-pentane at number of neuron 56

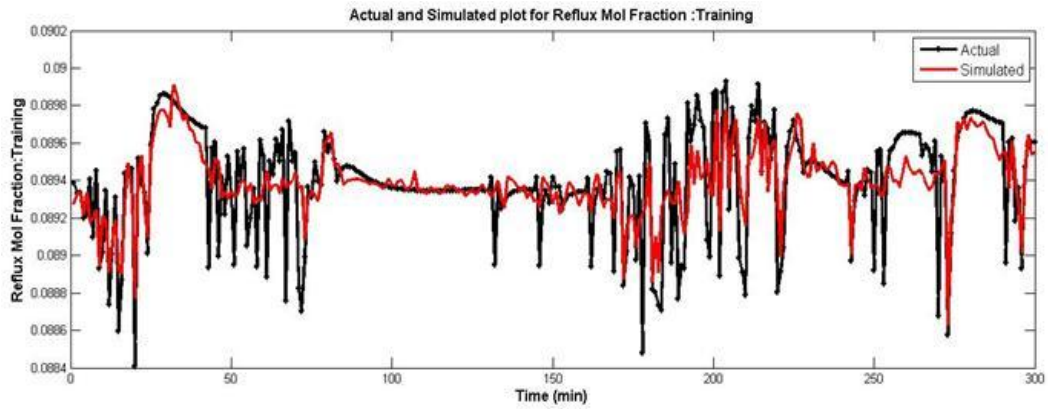


FIGURE 25. Actual and simulated plot for top composition of i-pentane

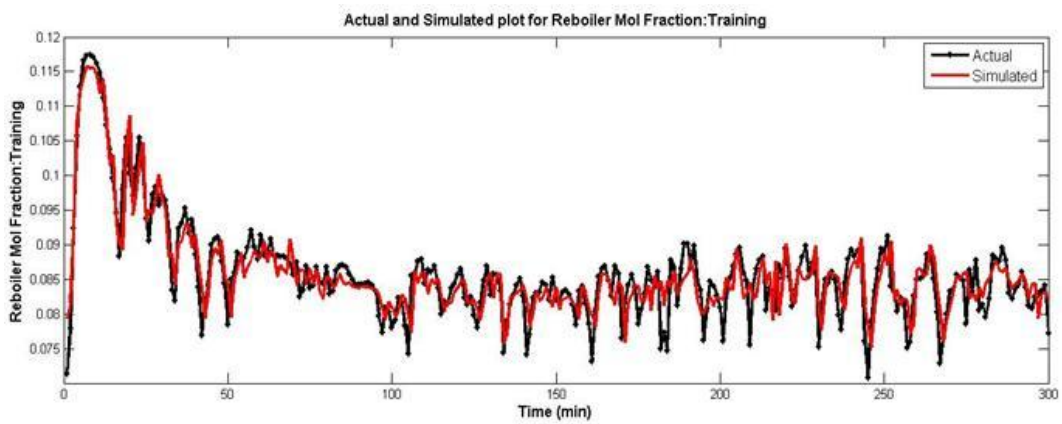


FIGURE 26. Actual and simulated plot for bottom composition of i-pentane

### iii. n-Butane

For n-butane, 40 is the number of neuron that gives the optimum predictions of the output. FIGURE 27 shows the performance curve for the 40 number of neuron with 0.037897 MSE. For n-butane R-value, its approach 0.9 and also track the target practically well. FIGURE 29 and 30 represent the differences between actual and simulated of the top and bottom composition of the n-butane. From the both graphs it can be seen that there is a small deviation between the actual and simulation data.

Optimum number of neuron	40
Maximum number of epochs set	100
MSE	0.037897
R	0.85134

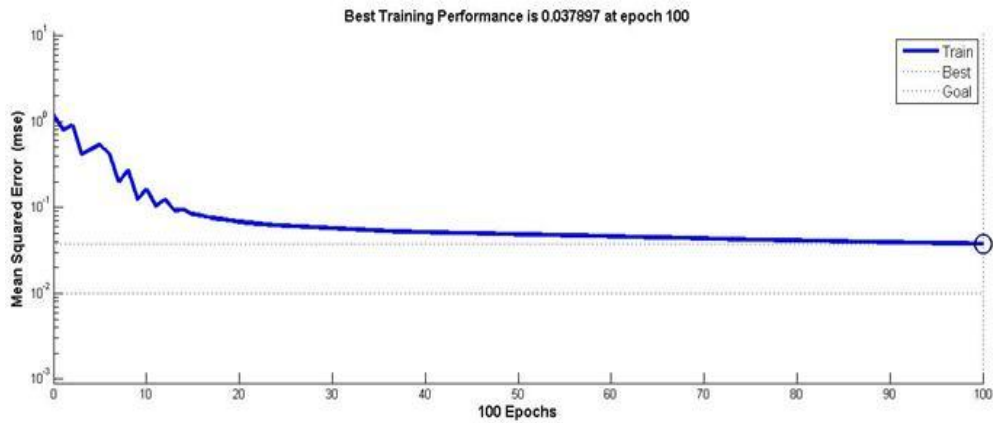


FIGURE 27. MSE vs. Epoch for n-butane at number of neuron 40

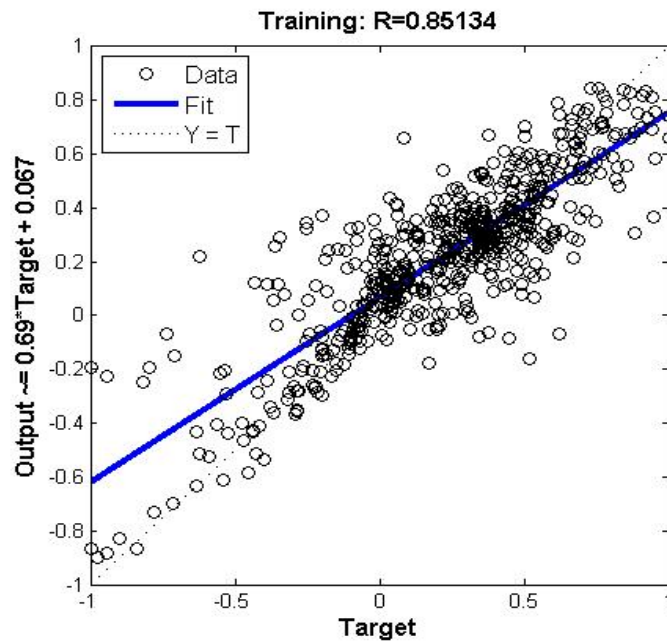


FIGURE 28. Regression for n-butane at number of neuron 40

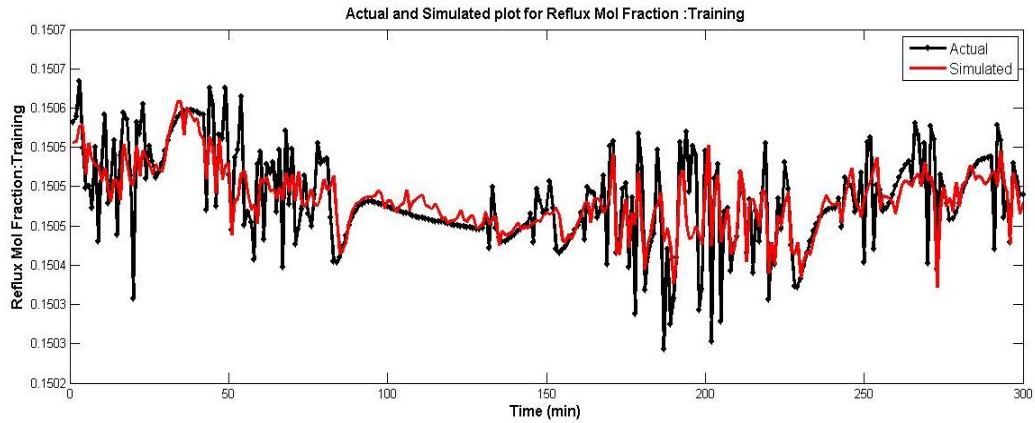


FIGURE 29. Actual and simulated plot for top composition of n-butane

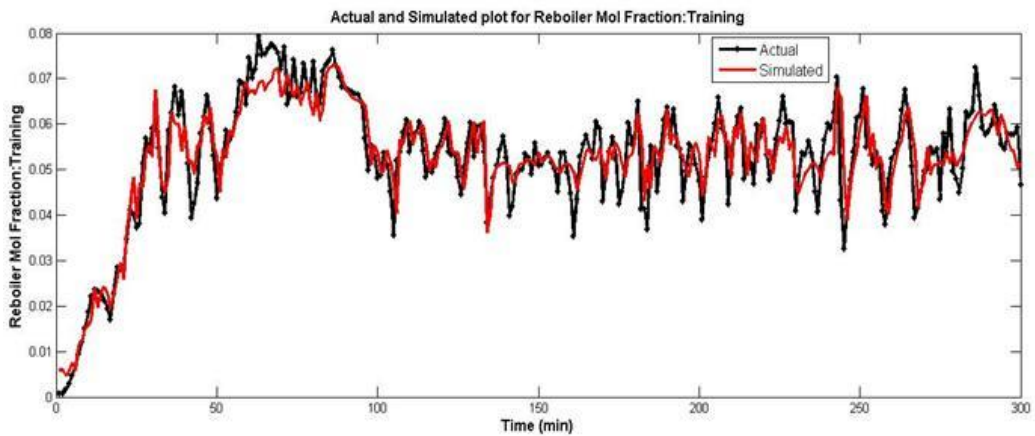


FIGURE 30. Actual and simulated plot for bottom composition of n-butane

#### iv. n-Pentane

For n-pentane, 36 is the number of neuron that gives the optimum predictions of the output. FIGURE 31 shows the performance curve for the 36 number of neuron with 0.041974 MSE. FIGURE 31 is the R-value for n-pentane with more than 0.9 and it can be concluded that its output track the target reasonably well. FIGURE 33 and 34 represent the differences between actual and simulated of the top and bottom composition of the n-pentane. From the both graphs it can be seen that there is a small deviation between the actual and simulation data.

Optimum number of neuron	36
Maximum number of epochs set	100
MSE	0.041974
R	0.91188

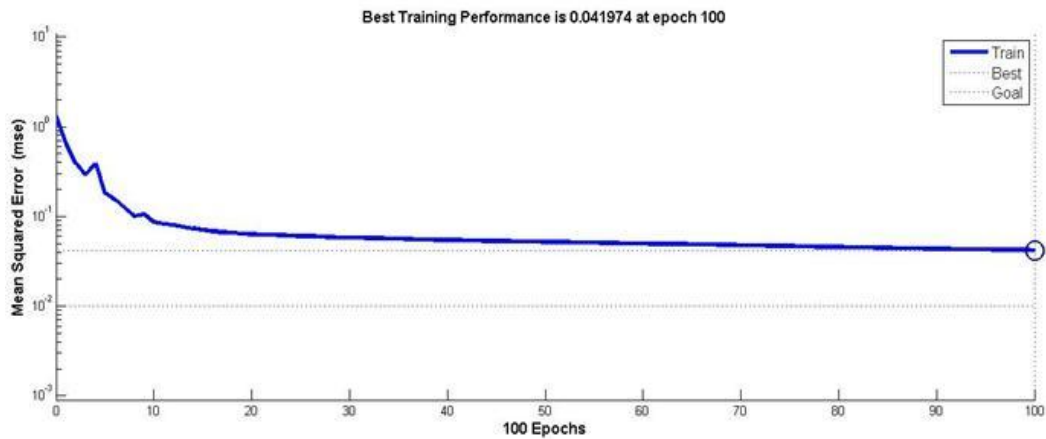


FIGURE 31. MSE vs. Epoch for n-pentane at number of neuron 36

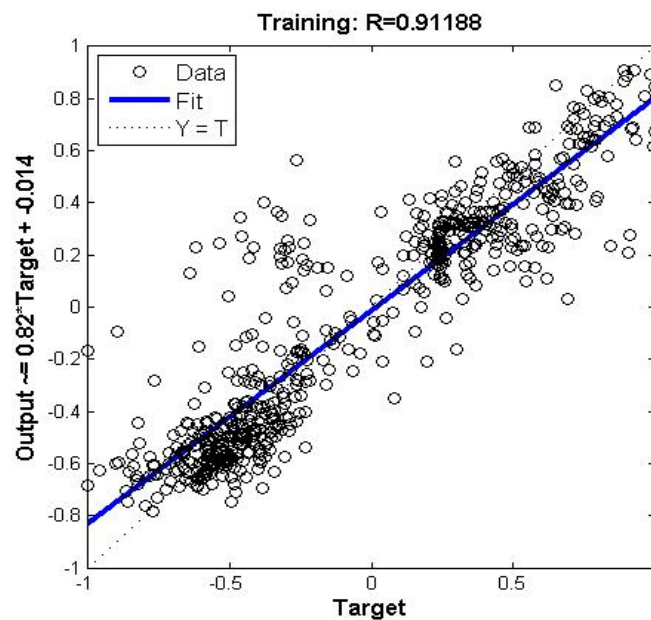


FIGURE 32. Regression for n-pentane at number of neuron 36

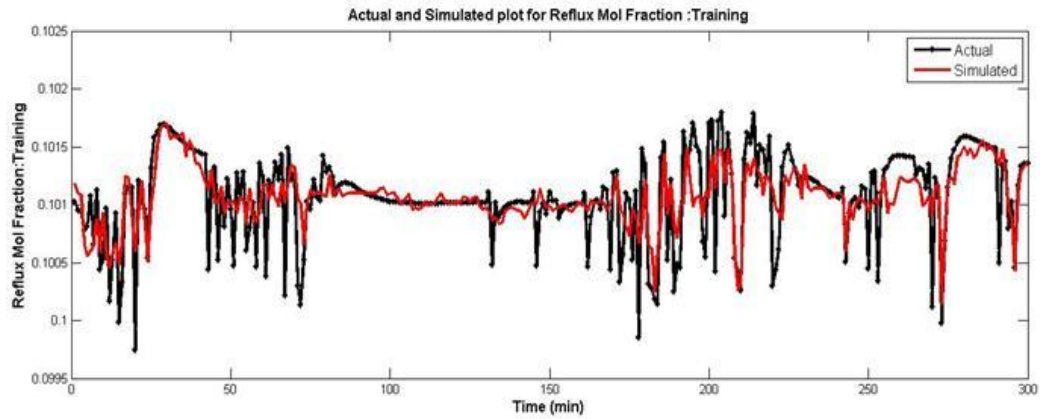


FIGURE 33. Actual and simulated plot for top composition of n-pentane

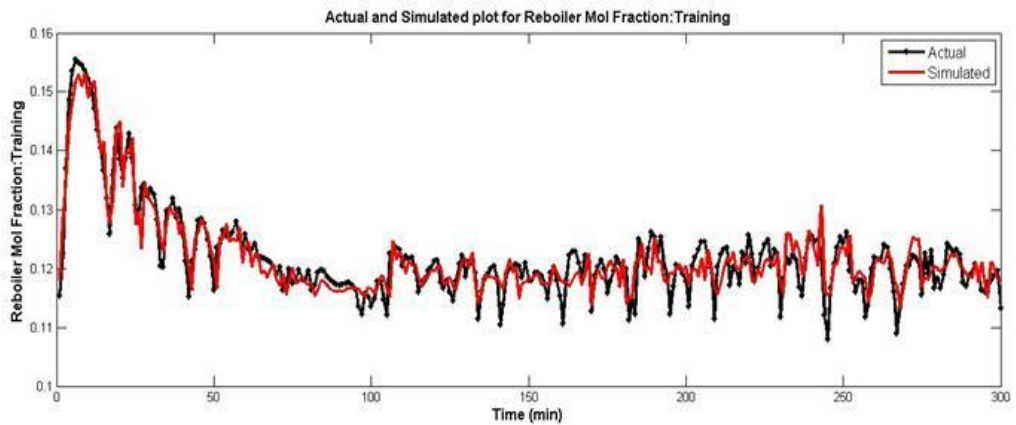


FIGURE 34. Actual and simulated plot for bottom composition of n-pentane

#### v. Propane

For propane, 48 is the number of neuron that gives the optimum predictions of the output. FIGURE 35 shows the performance curve for the 48 number of neuron with 0.043903 MSE. For R-value of pentane, its approach 0.9 and also track the target well. FIGURE 37 and 38 represent the differences between actual and simulated of the top and bottom composition of the propane. From the both graphs it can be seen that there is a small deviation between the actual and simulation data.

Optimum number of neuron	48
Maximum number of epochs set	100
MSE	0.043903
R	0.86647

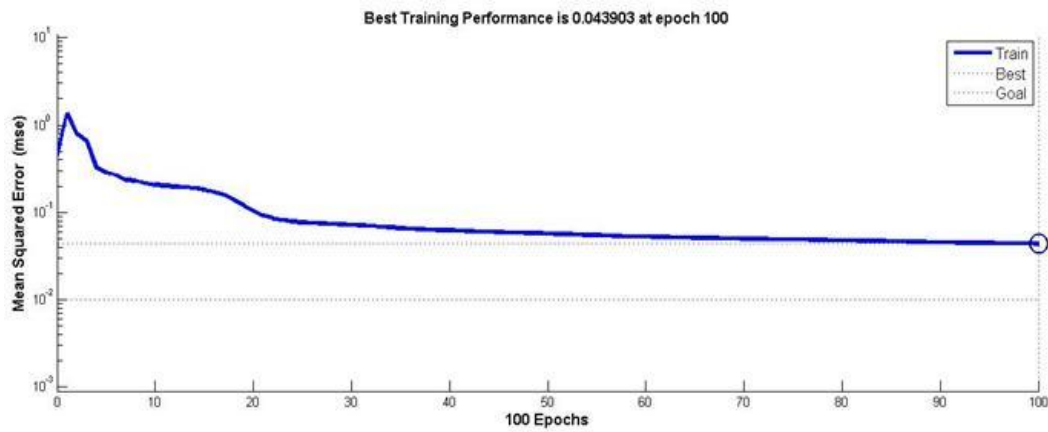


FIGURE 35. MSE vs. Epoch for propane at number of neuron 48

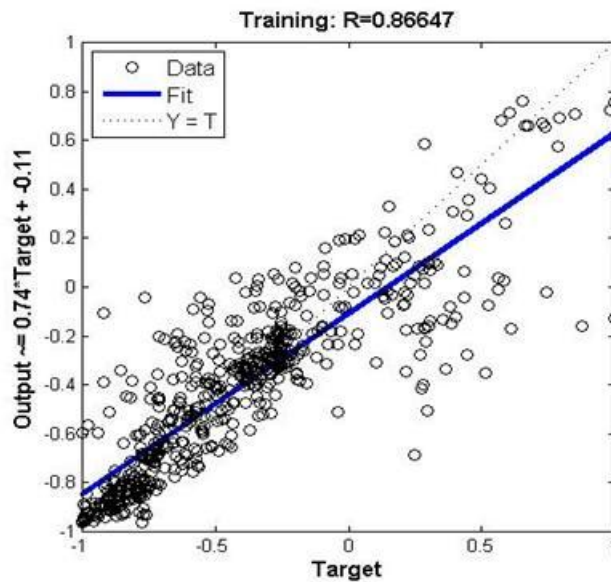


FIGURE 36. Regression for propane at number of neuron 48

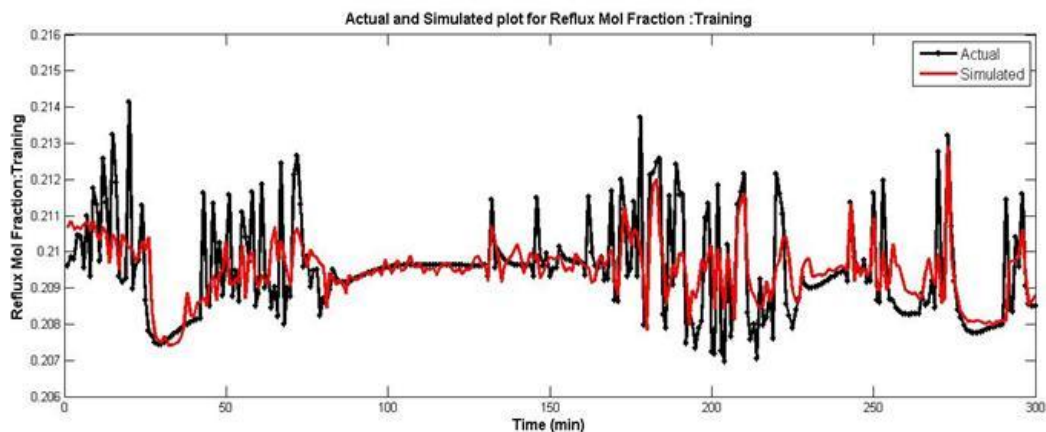


FIGURE 37. Actual and simulated plot for top composition of propane

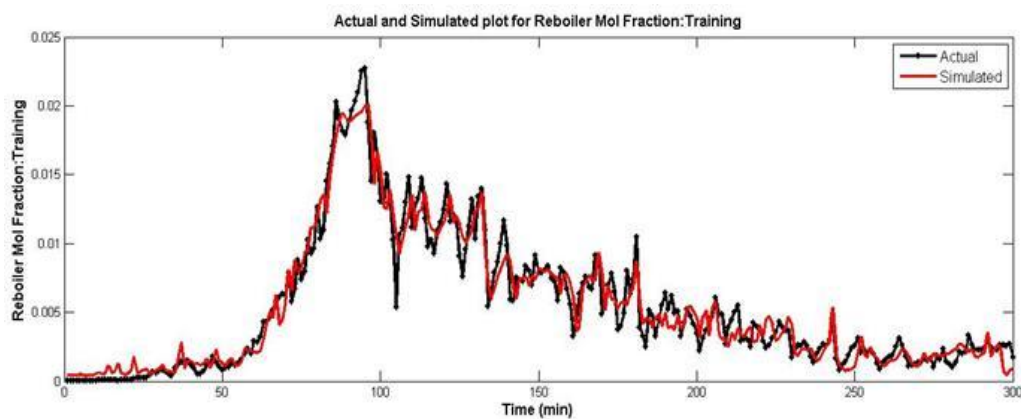


FIGURE 38. Actual and simulated plot for bottom composition of propane

All the results for neural network development are obtained by using trial and error method. The number of hidden layer is manipulated from 4 to 80 (Appendix 4) to determine the optimum number of hidden layer for neural network architecture. The RMSE value and regression (R) are observed in order to analyse the performance of the network. Based on the results, the deviation between the actual and simulated of the top and bottom composition of all five components (i-butane, i-pentane, n-butane, n-pentane and propane) is small. Besides, the feed forward neural network also capable of producing a very low RMSE with optimum number of hidden layer. For regression, the slope for i-butane, i-pentane, n-butane, n-pentane and propane are approaching 1. An R-value of 1 means a close relationship while 0 represents random relationship. From these results, it can be indicated that the

network is efficient to predict the top and bottom composition of debutanizer column.

#### 4.2.2 Neural Network Inverse Model

For inverse model, it is developed by inverse the inputs variable and outputs. The reboiler flowrate (mv2) and reflux flowrate (mv3) are the two outputs and the future composition of the top and bottom are the inputs variable.

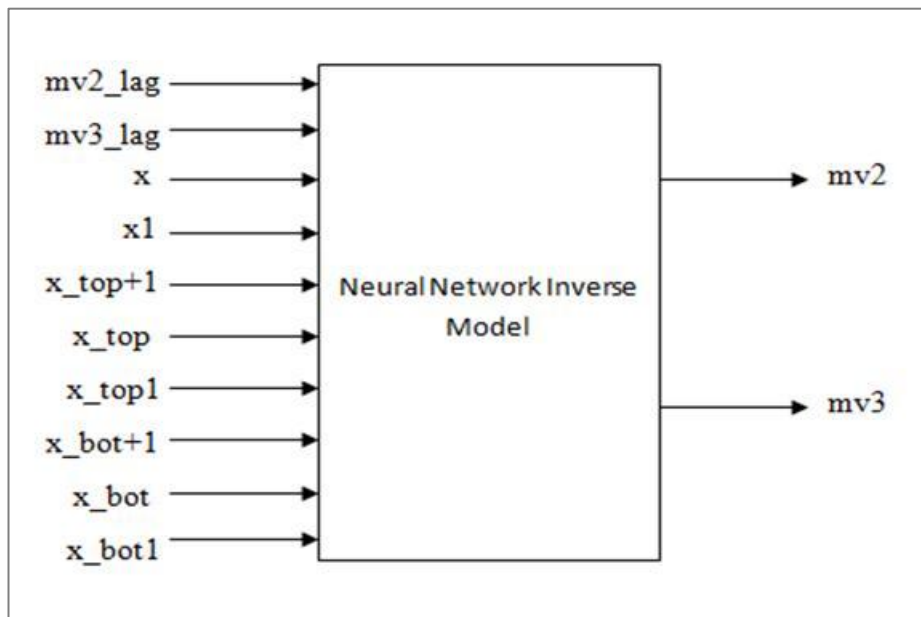


FIGURE 39. Neural network inverse model

#### i. i-Butane

Optimum number of neuron	4
Maximum number of epochs set	100
MSE	0.039633
R	0.97366

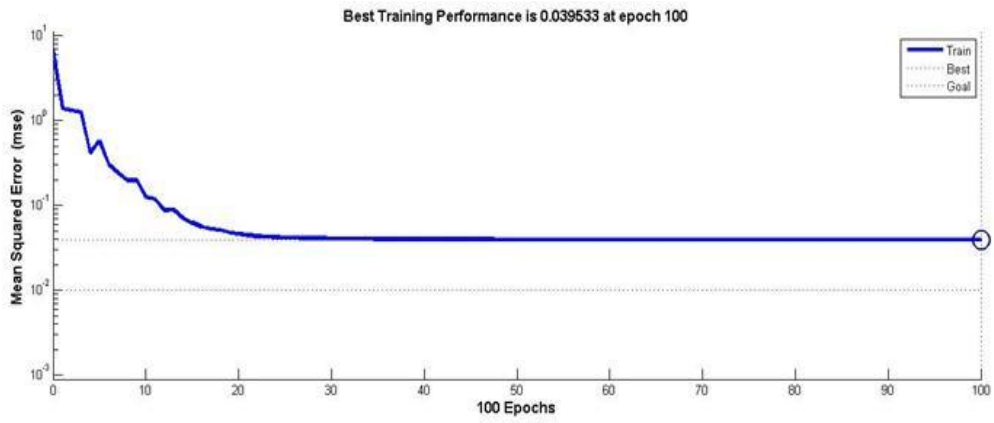


FIGURE 40. MSE vs. Epoch for i-butane at number of neuron 4

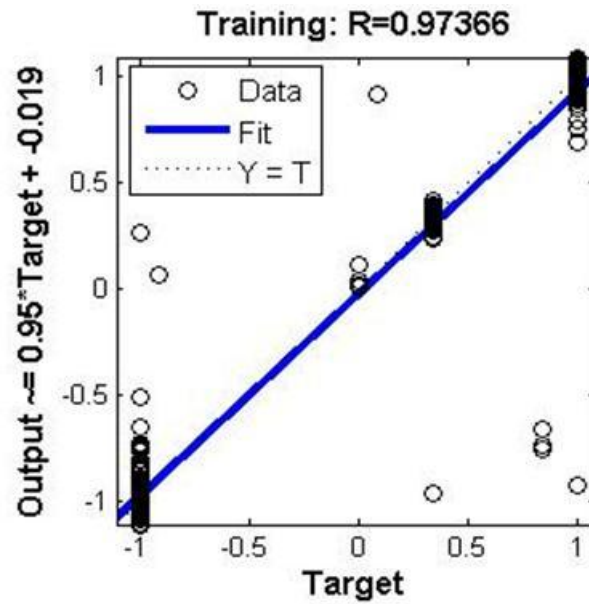


FIGURE 41. Regression for i-butane at number of neuron 4

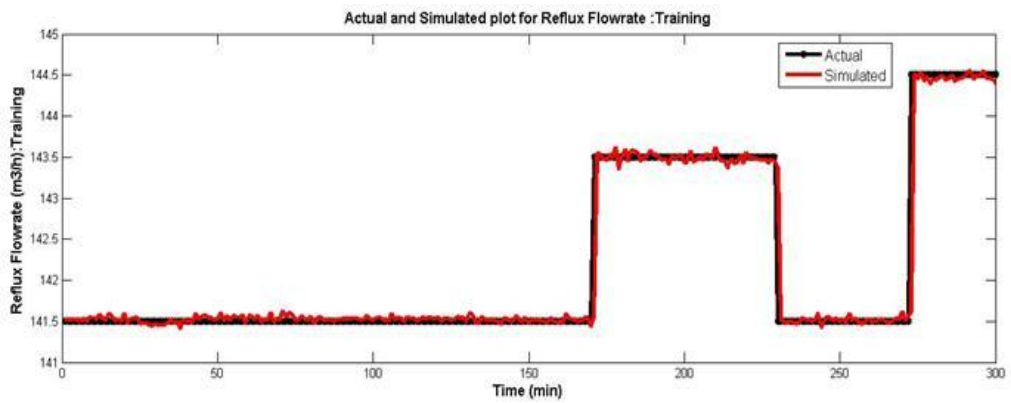


FIGURE 42. Actual and simulated plot for top flowrate of i-butane

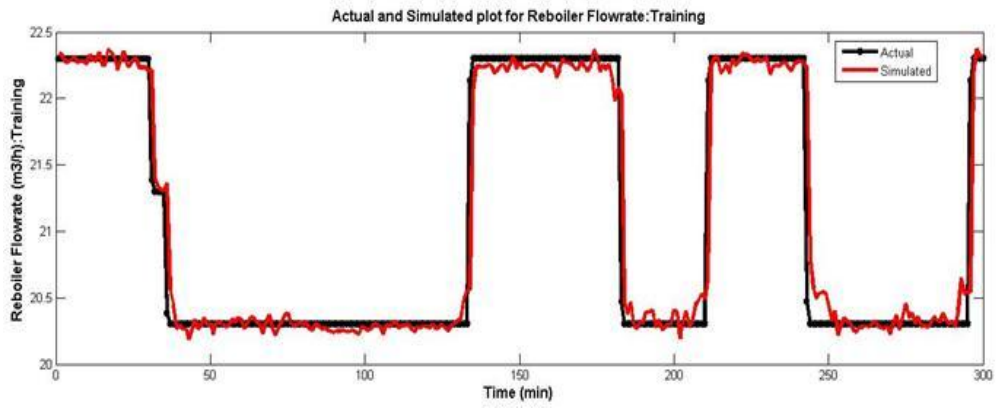


FIGURE 43. Actual and simulated plot for bottom flowrate of i-butane

ii. i-Pentane

Optimum number of neuron	48
Maximum number of epochs set	100
MSE	0.014842
R	0.99031

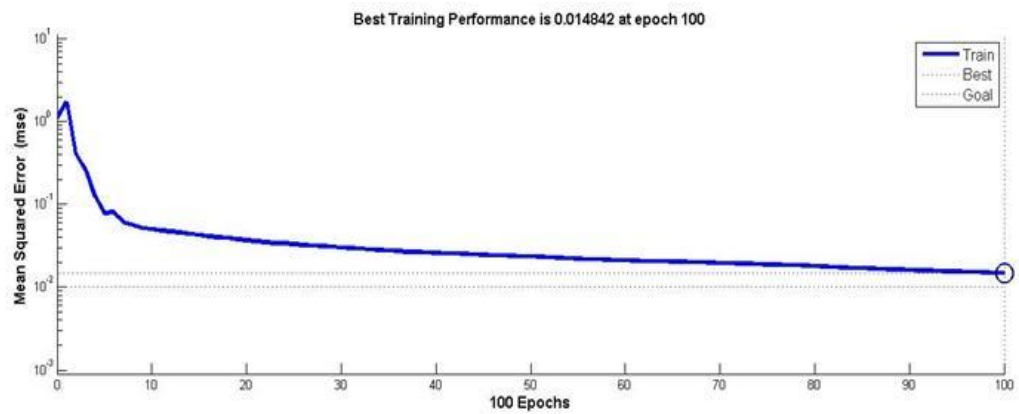


FIGURE 44. MSE vs. Epoch for i-pentane at number of neuron 48

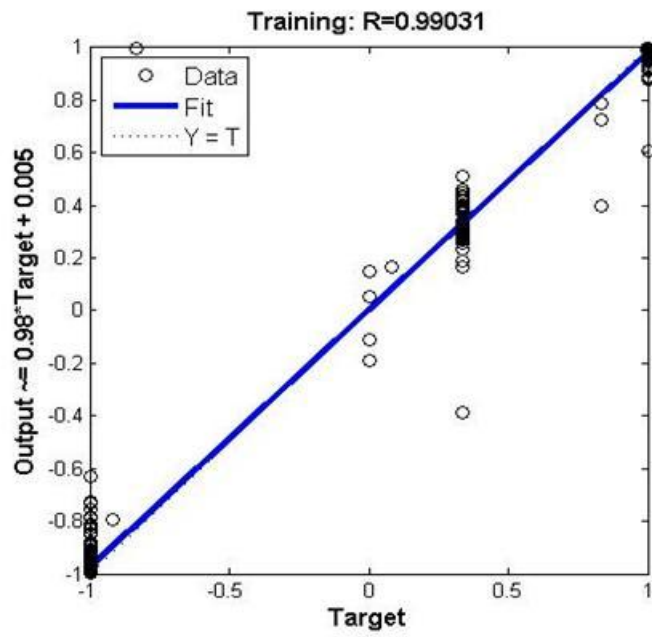


FIGURE 45. Regression for i-pentane at number of neuron 48

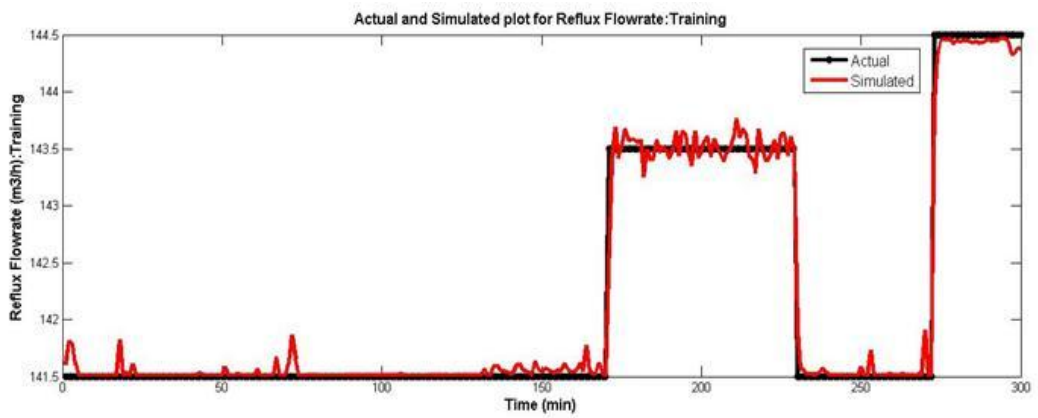


FIGURE 46. Actual and simulated plot for top flowrate of i-pentane

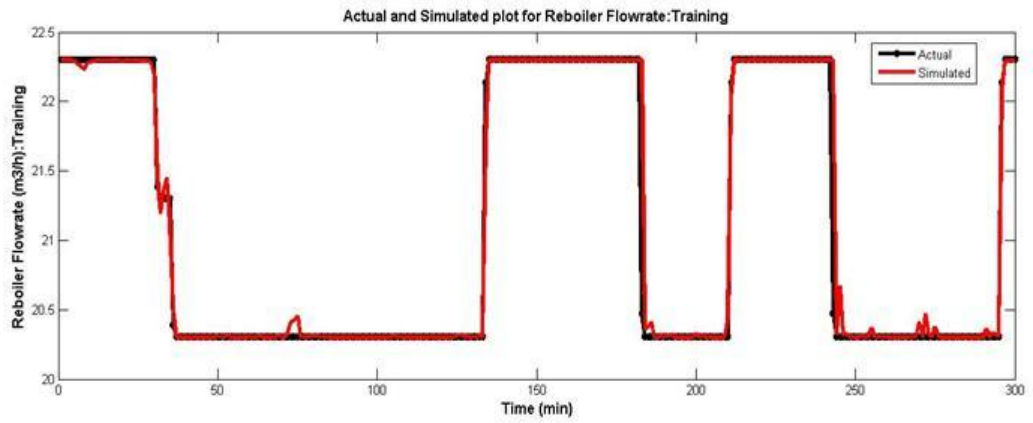


FIGURE 47. Actual and simulated plot for bottom flowrate of i-butane

**iii. n-Butane**

Optimum number of neuron	28
Maximum number of epochs set	100
MSE	0.014824
R	0.99029

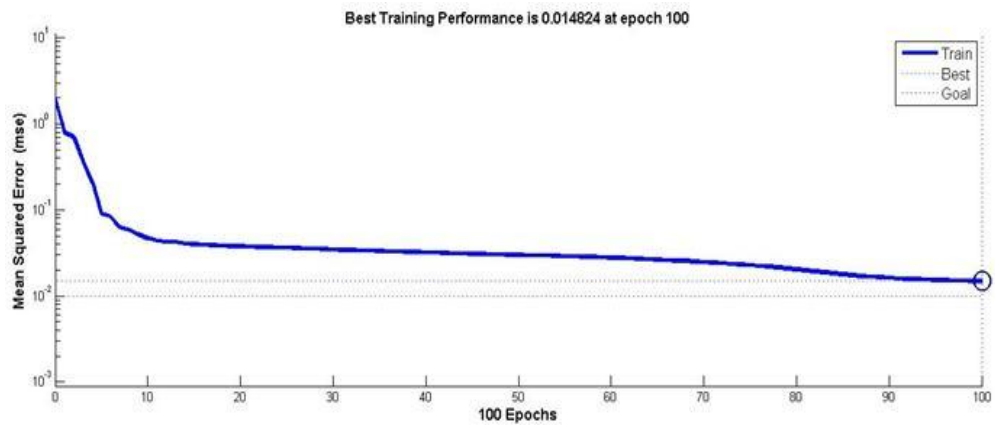


FIGURE 48. MSE vs. Epoch for n-butane at number of neuron 28

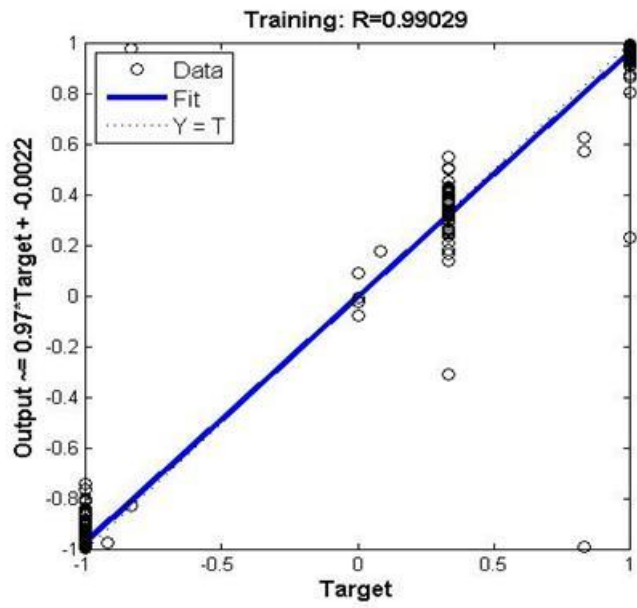


FIGURE 49. Regression for n-butane at number of neuron 28

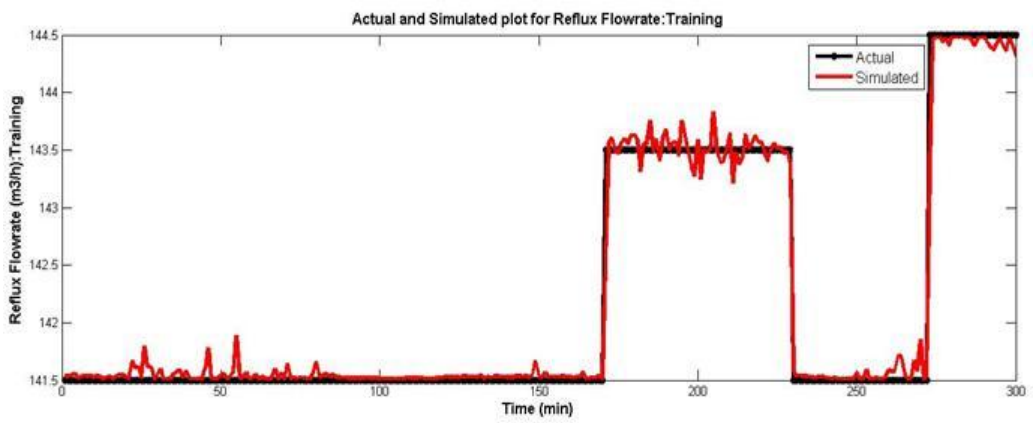


FIGURE 50. Actual and simulated plot for top flowrate of n-butane

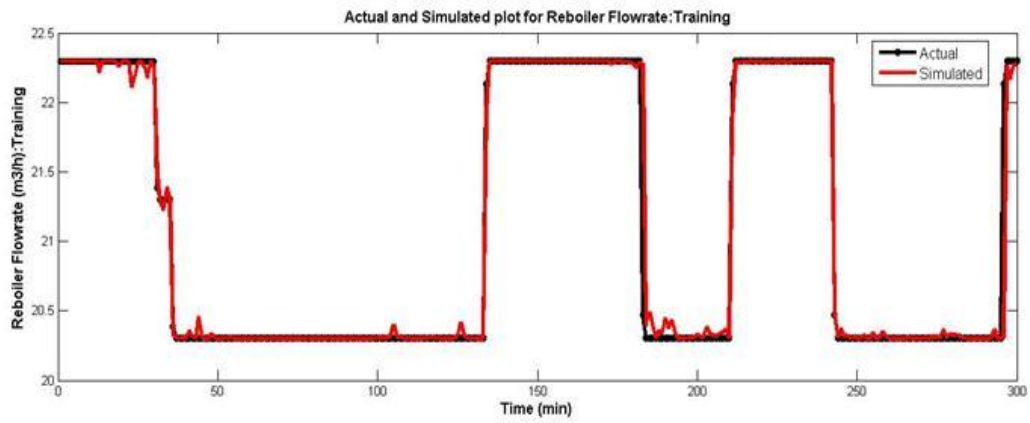


FIGURE 51. Actual and simulated plot for bottom flowrate of n-butane

**iv. n-Pentane**

Optimum number of neuron	64
Maximum number of epochs set	100
MSE	0.0099543
R	0.99353

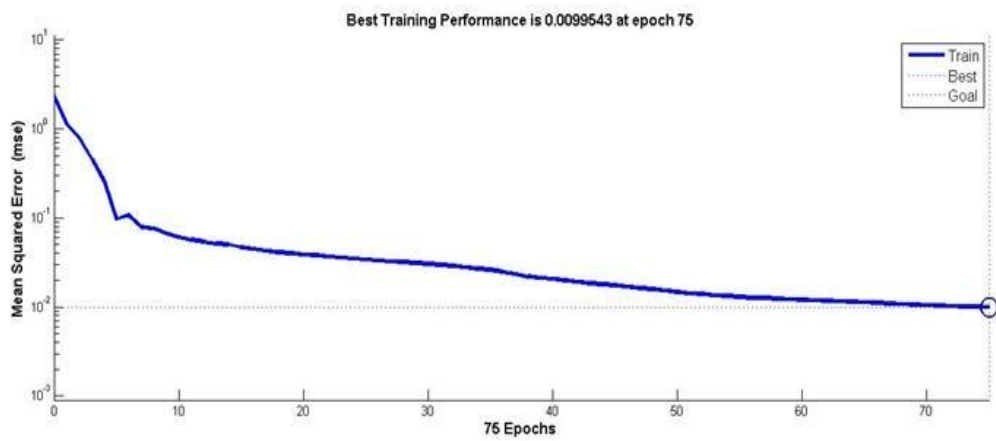


FIGURE 52. MSE vs. Epoch for n-pentane at number of neuron 64

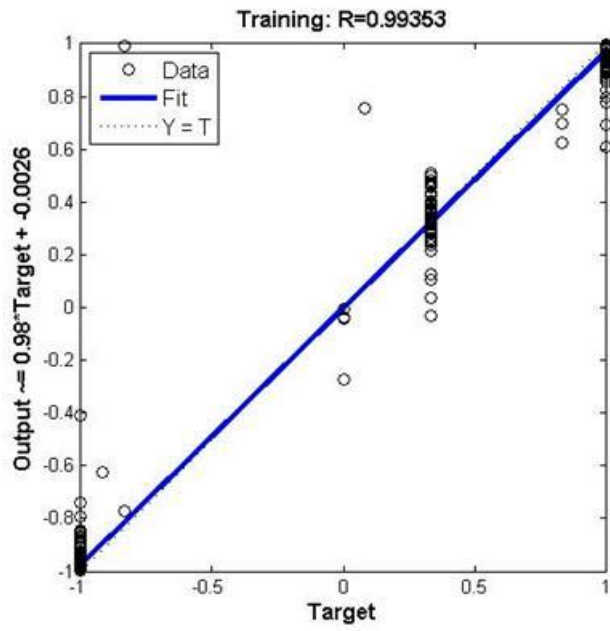


FIGURE 53. Regression for n-pentane at number of neuron 64

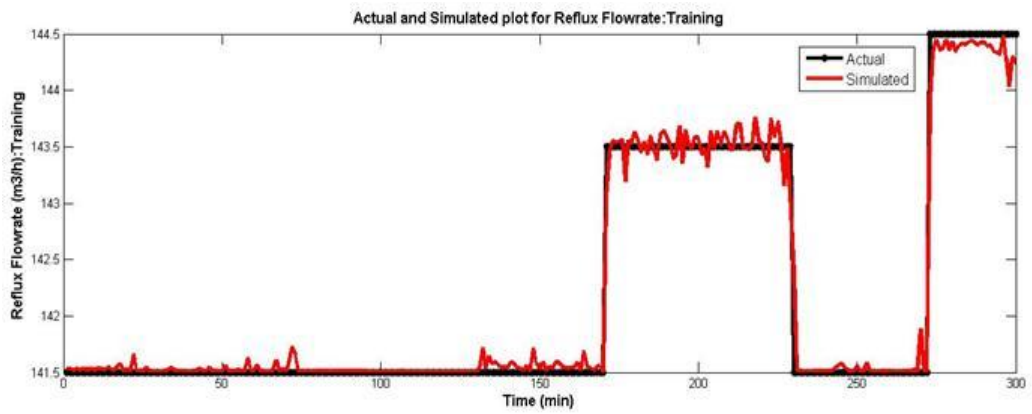


FIGURE 54. Actual and simulated plot for top flowrate of n-pentane

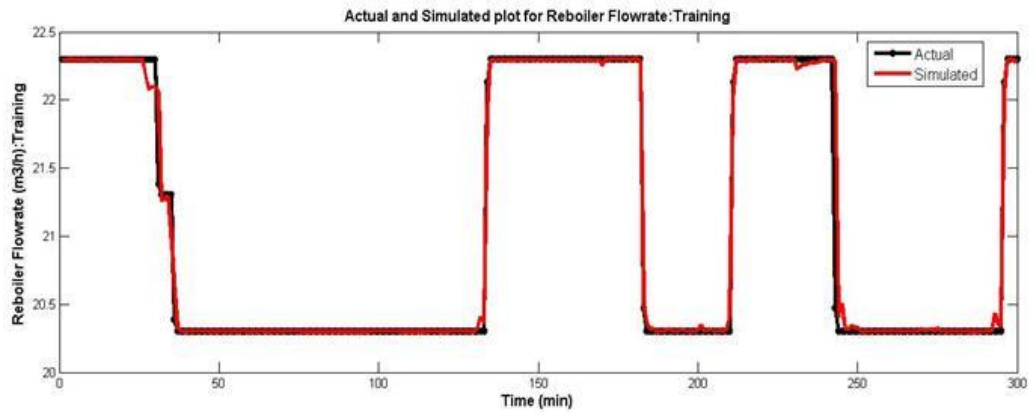


FIGURE 55. Actual and simulated plot for bottom flowrate of n-pentane

v. Propane

Optimum number of neuron	20
Maximum number of epochs set	100
MSE	0.012947
R	0.99152

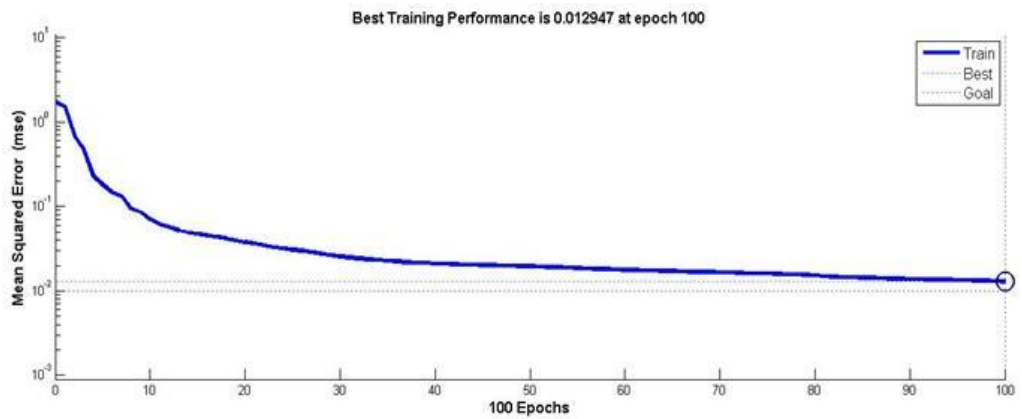


FIGURE 56. MSE vs. Epoch for propane at number of neuron 20

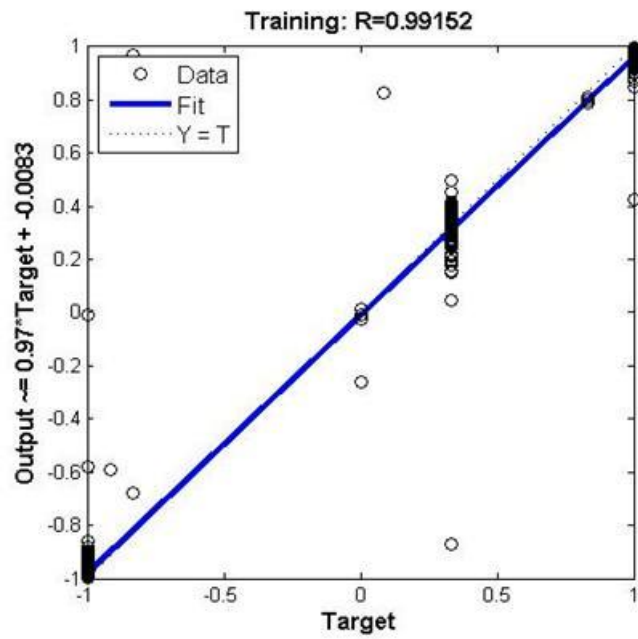


FIGURE 57. Regression for propane at number of neuron 20

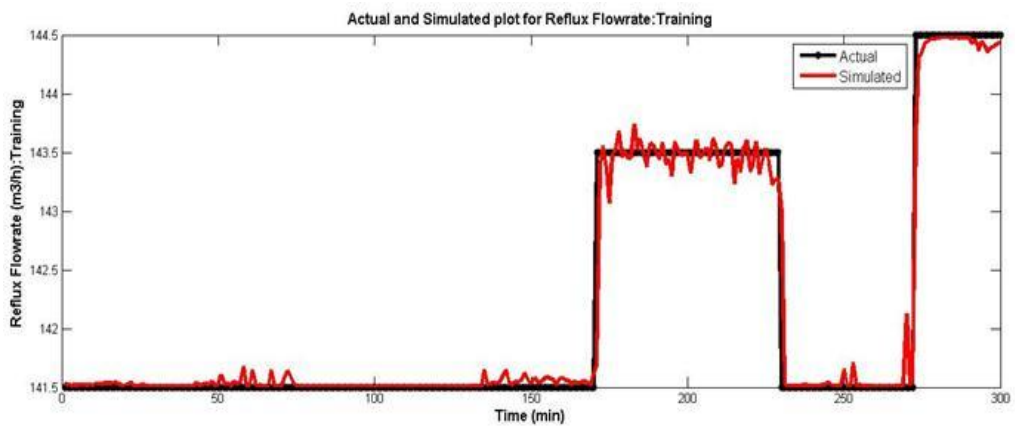


FIGURE 58. Actual and simulated plot for top flowrate of propane

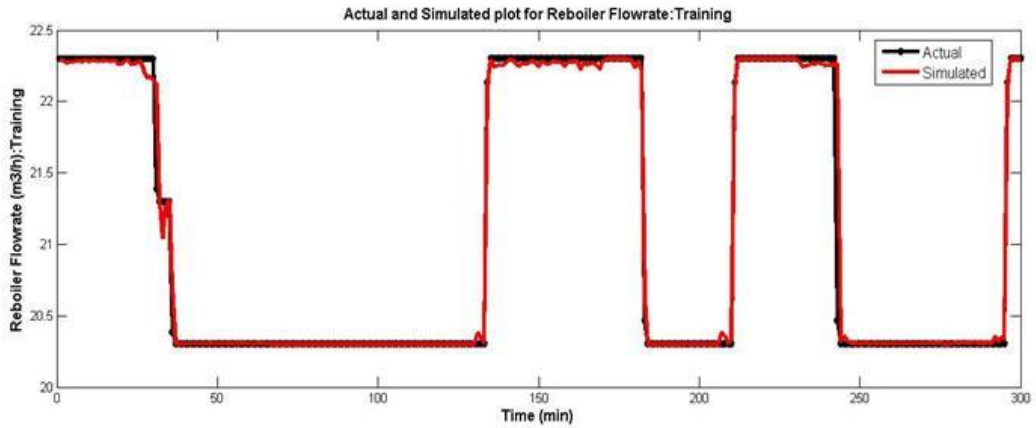


FIGURE 59. Actual and simulated plot for bottom flowrate of propane

### 4.3 Transfer Function Equation Development

1. i-Butane

a) Top

Best poles for model function: All real, 2, Zero, Integrator

$$a = \frac{0.00002466s - 0.0000002999}{42.98s^3 + 8828s^2 + s} \quad (3)$$

b) Bottom

Best poles for model function: Underdamped, 2, Zero

$$b = \frac{0.05777s + 0.0004494}{521s^2 + 15.11s + 1} \quad (4)$$

2. i-Pentane

a) Top

Best poles for model function: Underdamped, 3, Delay

$$c = \exp(-3.96s) \frac{0.004285}{970.5s^3 + 2121s^2 + 2193s + 1} \quad (5)$$

b) Bottom

Best poles for model function: Underdamped, 3, Zero

$$d = \frac{0.001908s + 0.0005856}{151.4s^3 + 56.77s^2 + 27.62s + 1} \quad (6)$$

3. n-Butane

a) Top

Best poles for model function: All real, 3, Delay, Integrator

$$e = \exp(-30s) \frac{0.0001487}{1650000s^4 + 61950000s^3 + 72140s^2 + s} \quad (7)$$

b) Bottom

Best poles for model function: Underdamped, 2, Zero

$$f = \frac{0.04053s + 0.0003762}{608.7s^2 + 21.72s + 1} \quad (8)$$

4. n-Pentane

a) Top

Best poles for model function: Underdamped, 2, Zero

$$g = \frac{0.035s + 0.004805}{37590s^2 + 464.4s + 1} \quad (9)$$

b) Bottom

Best poles for model function: All real, 2, Zero, Integrator

$$h = \frac{-0.0009262s + 0.0008376}{131.8s^3 + 54.51s^2 + 26.31s + 1} \quad (10)$$

5. Propane

a) Top

Best poles for model function: All real, 2, Zero, Integrator

$$i = \frac{-37.06s - 0.004775}{5307000000s^4 + 110600000s^3 + 20530s^2 + s} \quad (11)$$

b) Bottom

Best poles for model function: All real, 2, Zero, Integrator

$$j = \frac{0.001027s + 0.00003914}{1690s^2 + 10.42s + 1} \quad (12)$$

The transfer function equation development for all the components are selected based on the best fit of model output where the percentage of the best fit approaching 100%. These equations will be used to develop the control loop of forward and inverse neural network controller.

## **CHAPTER 5**

### **CONCLUSION AND RECOMMENDATION**

In conclusion, the feed forward neural network control system has the ability to predict the top and bottom composition of debutanizer column online as well as to improve the quality monitoring of product. It can be justified or proved based on the results obtained for neural network development where most of the MSE value and regression for all five components is approaching the target. The results for equation based neural network also seem well.

As a recommendation, the R-values can be improved to approach 1 by increase the number of hidden neurons and/or increase the number of input values, if more relevant information is available.

## REFERENCE

- Basheer, I., & Hajmeer, M, 2000, "Artificial neural networks: fundamentals, computing, design, and application", *Journal of microbiological methods*, **43(1)**, 3-31.
- Beale, M., Hagan, M. T., & Demuth, H. B, 1992, "Neural network toolbox", *Neural Network Toolbox, The Math Works*, 5-25.
- Cybenko, G, 1989, "Approximation by superpositions of a sigmoidal function". *Mathematics of control, signals and systems*, **2(4)**, 303-314.
- de Canete, J. F., Gonzalez-Perez, S., & del Saz-Orozco, P, 2008, "Artificial neural networks for identification and control of a lab-scale distillation column using LABVIEW". *World Academy of Science, Engineering and Technology*, **47(15)**, 64-69.
- Fortuna, L., Graziani, S., & Xibilia, M. G., 2005, "Soft sensors for product quality monitoring in debutanizer distillation columns". *Control Engineering Practice*,
- Ge, Z., & Song, Z, 2010, "A comparative study of just-in-time-learning based methods for online soft sensor modeling", *Chemometrics and Intelligent Laboratory Systems*, **104(2)**, 306-317.
- Gokhale, V., Hurowitz, S., & Riggs, J. B, 1995, "A comparison of advanced distillation control techniques for a propylene/propane splitter". *Industrial & engineering chemistry research*, **34(12)**, 4413-4419.
- Hernandaz, E., & Arkun, Y, 1990, "Neural network modeling and an extended DMC algorithm to control nonlinear systems", Paper presented at the American Control Conference, 1990.
- Hornik, K., Stinchcombe, M., & White, H, 1989, "Multilayer feedforward networks are universal approximators", *Neural networks*, **2(5)**, 359-366.
- Hoskins, J. C., & Himmelblau, D, 1988, "Artificial neural network models of knowledge representation in chemical engineering", *Computers & Chemical Engineering*, **12(9)**, 881-890.
- Hunt, K., & Sbarbaro, D, 1991, "Neural networks for nonlinear internal model control", Paper presented at the Control Theory and Applications, IEE Proceedings

- Hussain, M. A, 1999, "Review of the applications of neural networks in chemical process control—simulation and online implementation". *Artificial intelligence in engineering*, **13(1)**, 55-68.
- Jiang, H., Yan, Z., & Liu, X, 2013, "Melt index prediction using optimized least squares support vector machines based on hybrid particle swarm optimization algorithm" *Neurocomputing*, **119(0)**, 469-477.
- Kano, M., Miyazaki, K., Hasebe, S., & Hashimoto, I, 2000, "Inferential control system of distillation compositions using dynamic partial least squares regression" *Journal of Process Control*, **10(2-3)**, 157-166.
- Lightbody, G., & Irwin, G, 1995, "Direct neural model reference adaptive control", *IEE Proceedings-Control Theory and Applications*, **142(1)**, 31-43.
- Liu, X., & Zhao, C, 2012, "Melt index prediction based on fuzzy neural networks and PSO algorithm with online correction strategy". *AIChE Journal*, **58(4)**, 1194-1202.
- Loh, A., Looi, K., & Fong, K, 1995, "Neural network modelling and control strategies for a pH process"., *Journal of Process Control*, **5(6)**, 355-362.
- MacMurray, J. C., & Himmelblau, D, 1995, "Modeling and control of a packed distillation column using artificial neural networks", *Computers & Chemical Engineering*, **19(10)**, 1077-1088.
- Mohamed Ramli, N., Hussain, M. A., Mohamed Jan, B., & Abdullah, B, 2014, "Composition Prediction of a Debutanizer Column using Equation Based Artificial Neural Network Model", *Neurocomputing*, **131**, 59-76.
- Morris, A., Montague, G., & Willis, M, 1994, "Artificial Neural Networks-Studies in-Process Modeling and Control", *Chemical engineering research & design*, **72(1)**, 3-19.
- Park, S., & Han, C, 2000a, "A nonlinear soft sensor based on multivariate smoothing procedure for quality estimation in distillation columns", *Computers & Chemical Engineering*, **24(2)**, 871-877.
- Park, S., & Han, C, 2000b, "A nonlinear soft sensor based on multivariate smoothing procedure for quality estimation in distillation columns", *Computers & Chemical Engineering*, **24(2-7)**, 871-877.
- Prasad, V., & Bequette, B. W, 2003, "Nonlinear system identification and model reduction using artificial neural networks", *Computers & Chemical Engineering*, **27(12)**, 1741-1754.
- Psichogios, D. C., & Ungar, L. H, 1991, "Direct and indirect model based control using artificial neural networks", *Industrial & engineering chemistry research*, **30(12)**, 2564-2573.

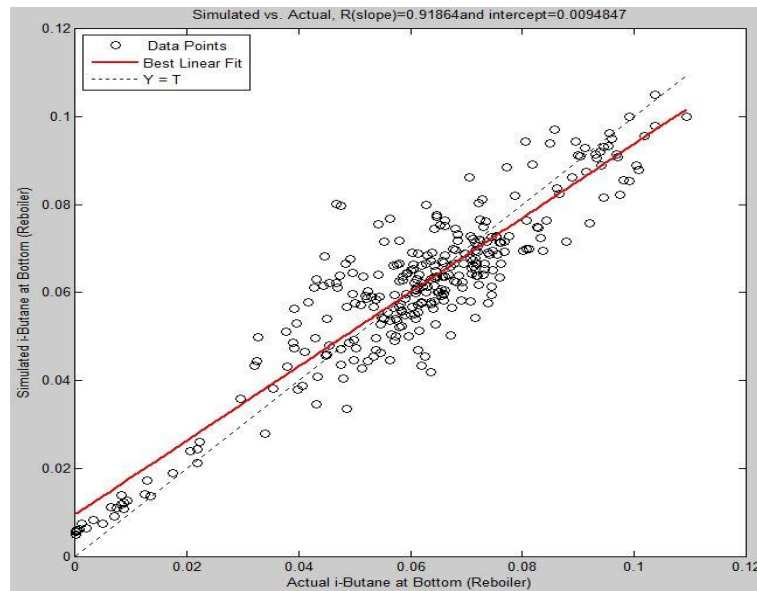
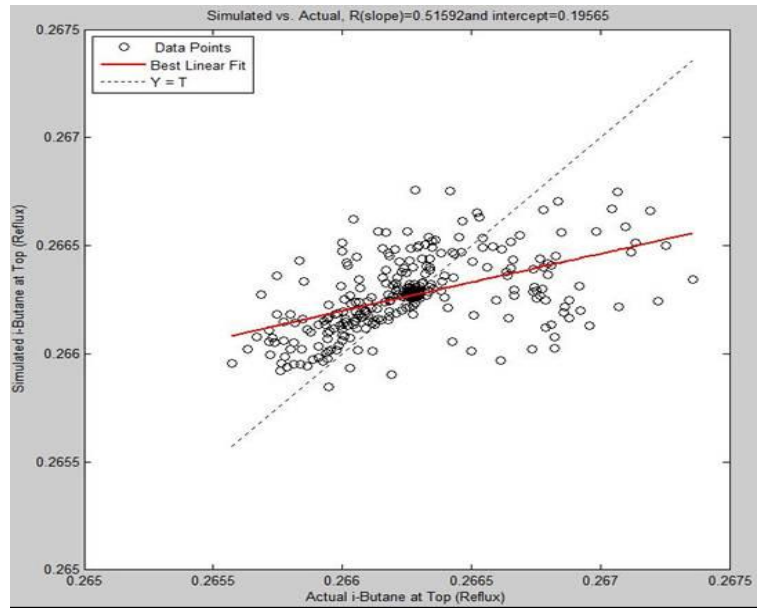
- Sharmin, R., Sundararaj, U., Shah, S., Vande Griend, L., & Sun, Y.-J, 2006, "Inferential sensors for estimation of polymer quality parameters: Industrial application of a PLS-based soft sensor for a LDPE plant", *Chemical Engineering Science*, **61(19)**, 6372-6384.
- Shi, J., & Liu, X, 2006, "Melt index prediction by weighted least squares support vector machines", *Journal of applied polymer science*, **101(1)**, 285-289.
- Singh, V., Gupta, I., & Gupta, H. O, 2007, "ANN-based estimator for distillation using Levenberg–Marquardt approach", *Engineering Applications of Artificial Intelligence*, **20(2)**, 249-259.
- Skogestad, S, 1997, "Dynamics and control of distillation columns: A tutorial introduction", *Chemical Engineering Research and Design*, **75(6)**, 539-562.
- Skogestad, S, 2004, "Control structure design for complete chemical plants", *Computers & Chemical Engineering*, **28(1-2)**, 219-234.
- Tan, Y., & Van Cauwenberghe, A. R, 1996, "Optimization techniques for the design of a neural predictive controller", *Neurocomputing*, **10(1)**, 83-96.
- Turner, P., Montague, G., & Morris, J, 1995, "Neural networks in dynamic process state estimation and non-linear predictive control".
- Watanabe, N 2014, "A comparison of neural network based control strategies for a CSTR", *Advanced Control of Chemical Processes 1994*, 377.
- Willis, M. J., Montague, G. A., Di Massimo, C., Tham, M. T., & Morris, A, 1992, "Artificial neural networks in process estimation and control", *Automatica*, **28(6)**, 1181-1187.
- Xuefeng, Y, 2010, "Hybrid artificial neural network based on BP-PLSR and its application in development of soft sensors", *Chemometrics and Intelligent Laboratory Systems*, **103(2)**, 152-159.
- Ydstie, B, (1990, "Forecasting and control using adaptive connectionist networks" *Computers & Chemical Engineering*, **14(4)**, 583-599.
- Zamprogna, E., Barolo, M., & Seborg, D. E, 2004, "Estimating product composition profiles in batch distillation via partial least squares regression" *Control Engineering Practice*, **12(7)**, 917-929.
- Zhang, M., & Liu, X, 2013, "A soft sensor based on adaptive fuzzy neural network and support vector regression for industrial melt index prediction", *Chemometrics and Intelligent Laboratory Systems*, **126(0)**, 83-90.
- Zilouchian, A., & Bawazeer, K, 2001, "Application of neural networks in oil refineries", *Intelligent Control Systems Using Soft Computing Methodologies*, 139-158.

# APPENDICES

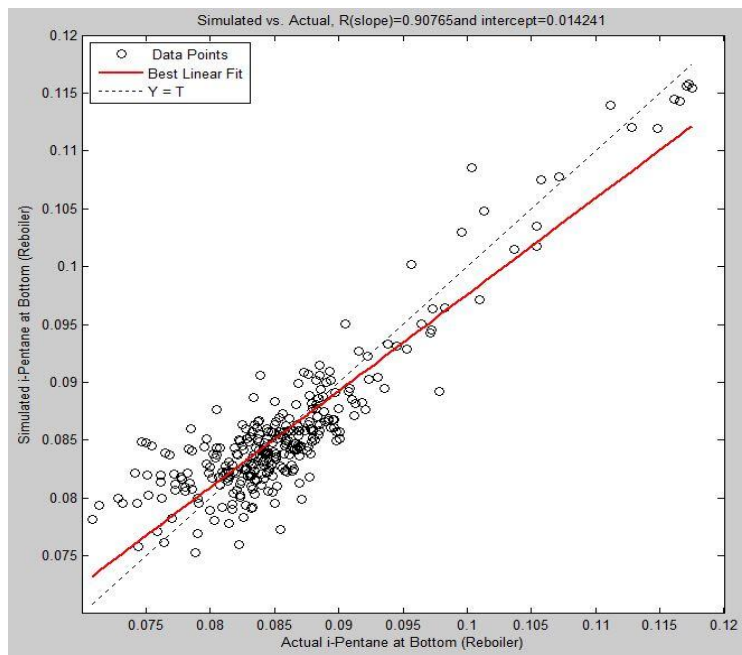
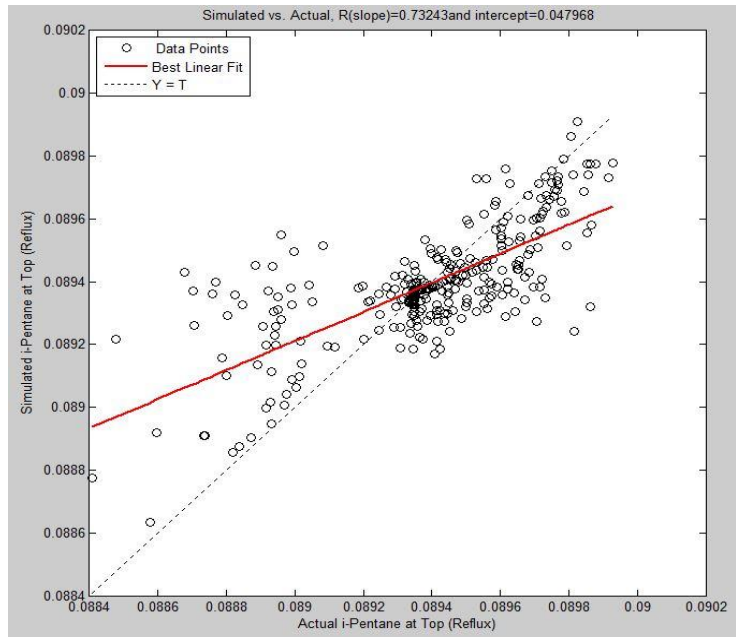
## Appendix 1: Top and Bottom Output Plot

### Forward Model Neural Network

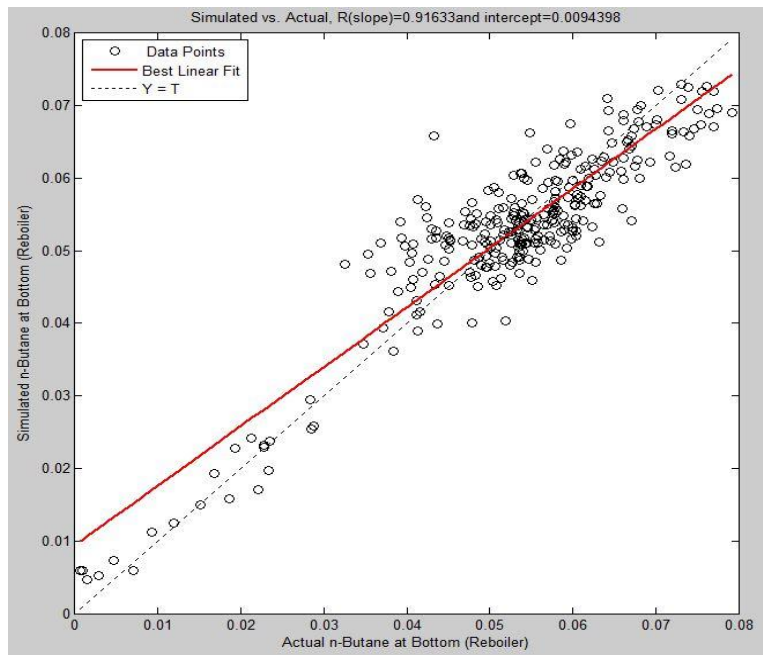
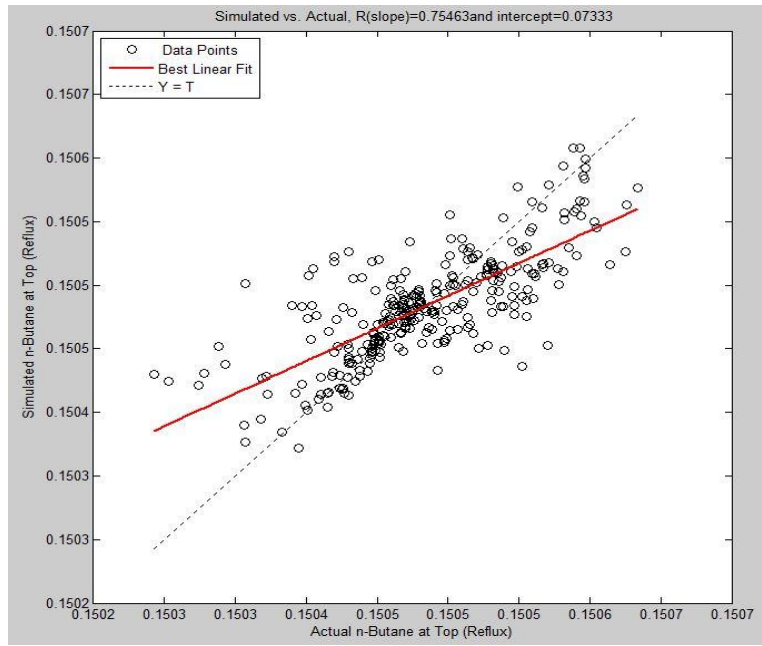
#### i. i-butane



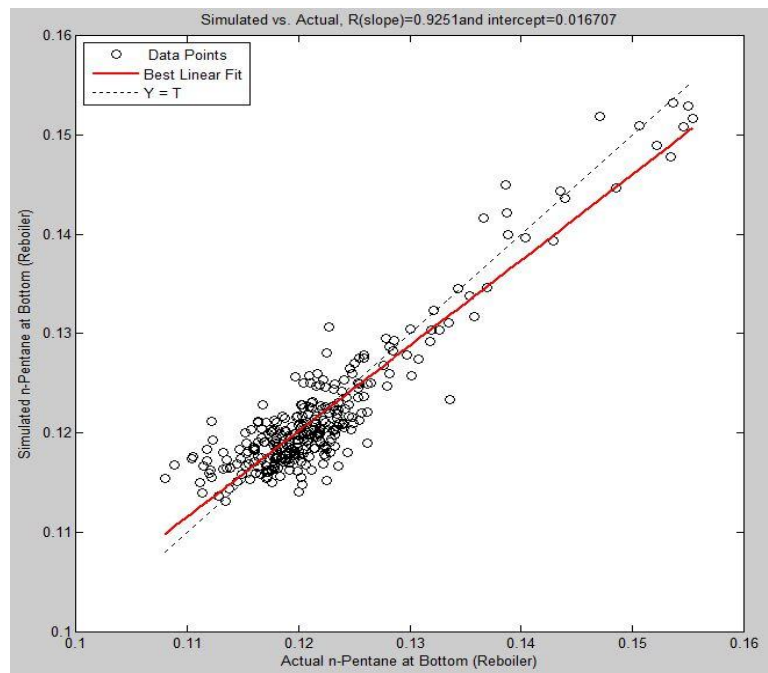
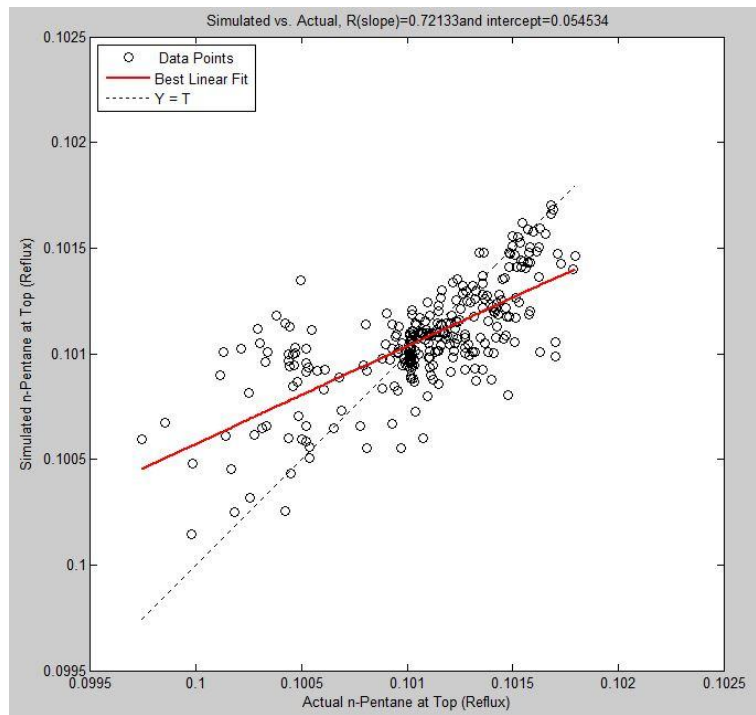
ii. i-pentane



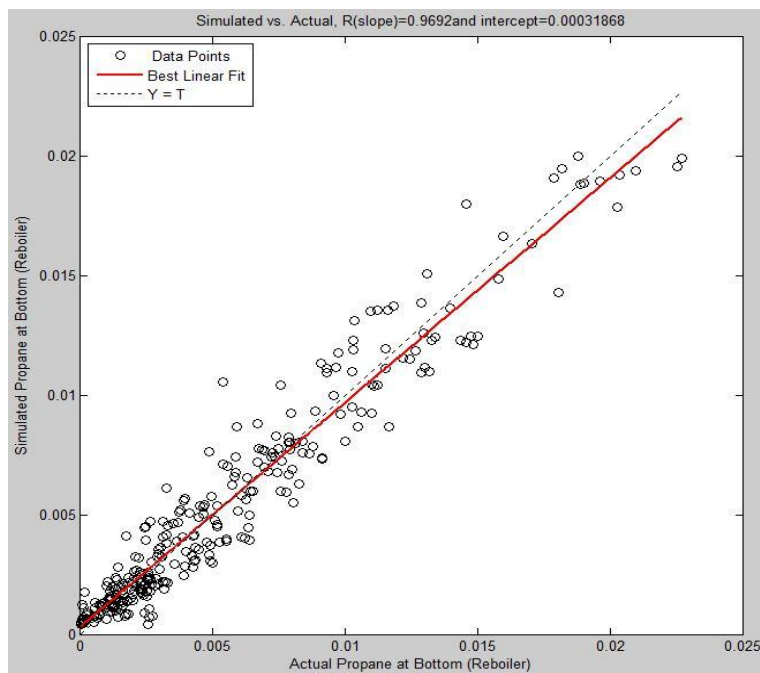
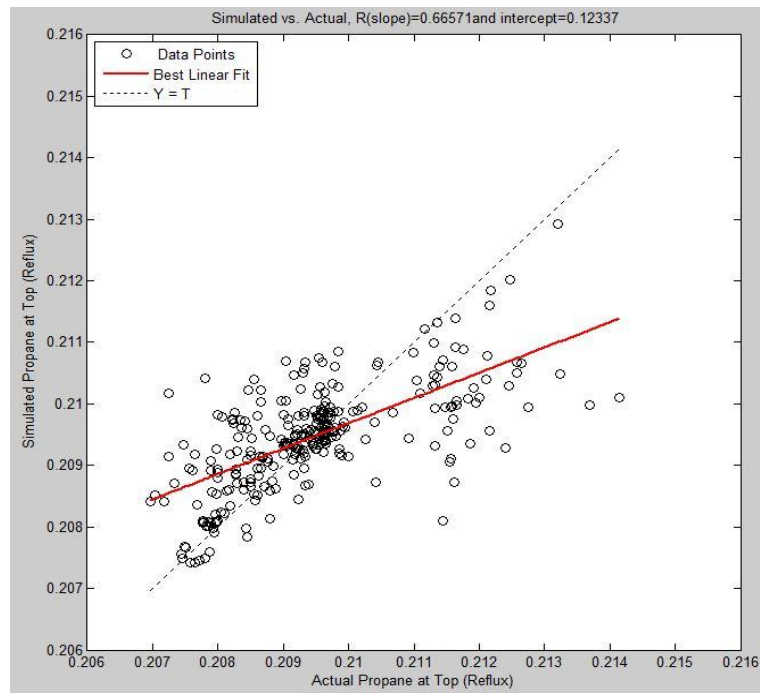
iii. n-butane



iv. n-pentane

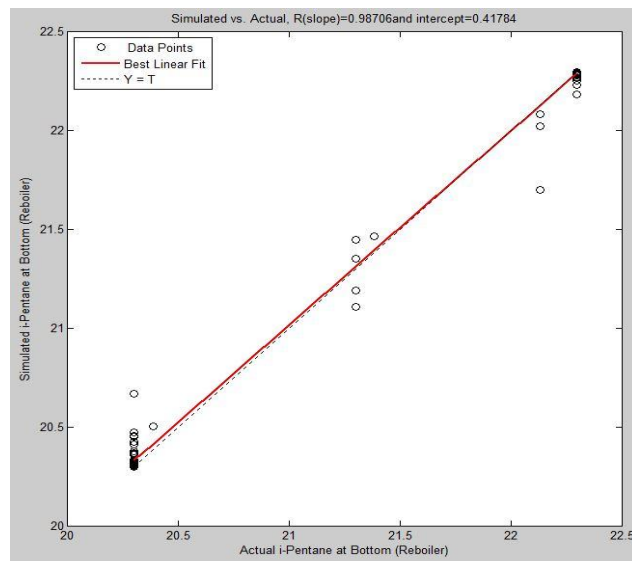
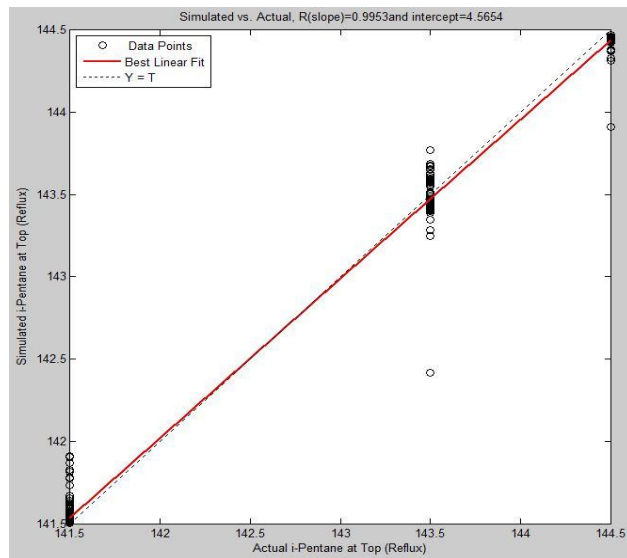


v. Propane

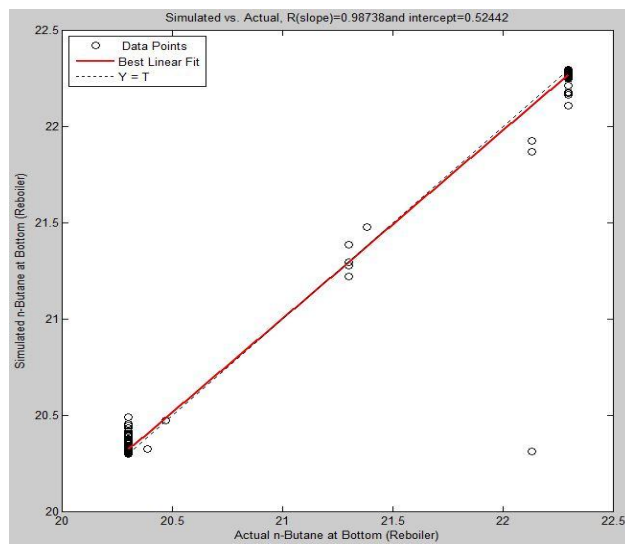
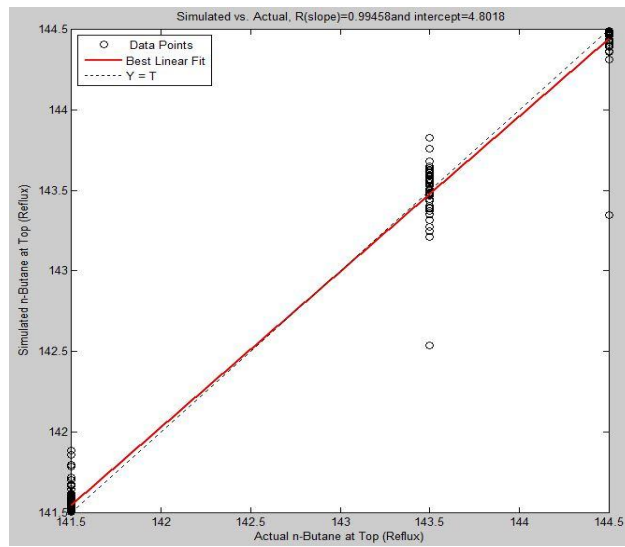




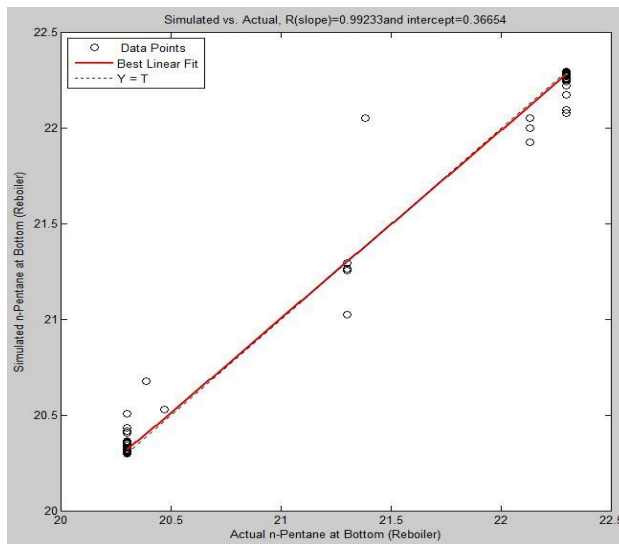
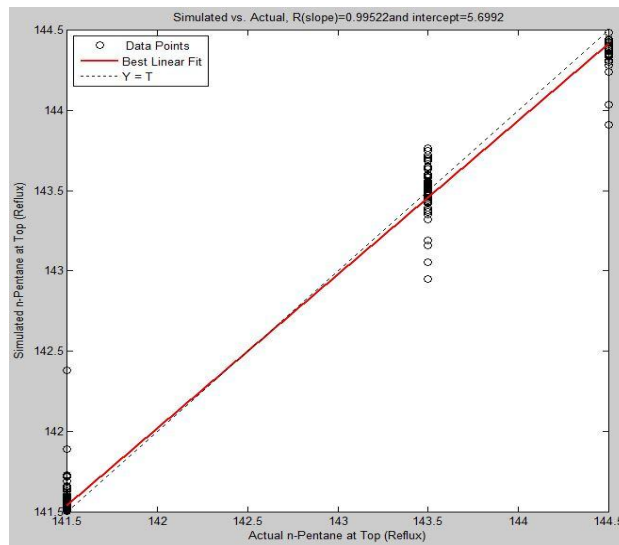
ii. i-pentane



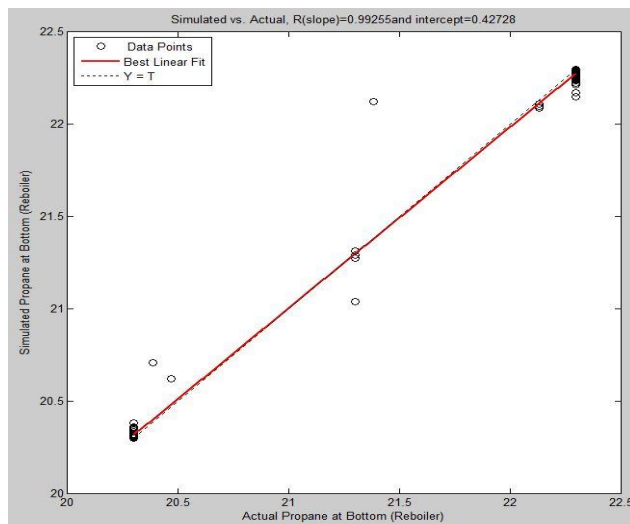
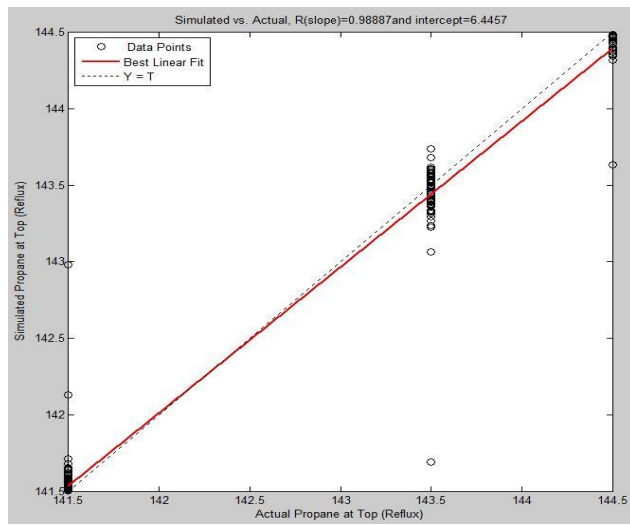
iii. n-butane



iv. n-pentane



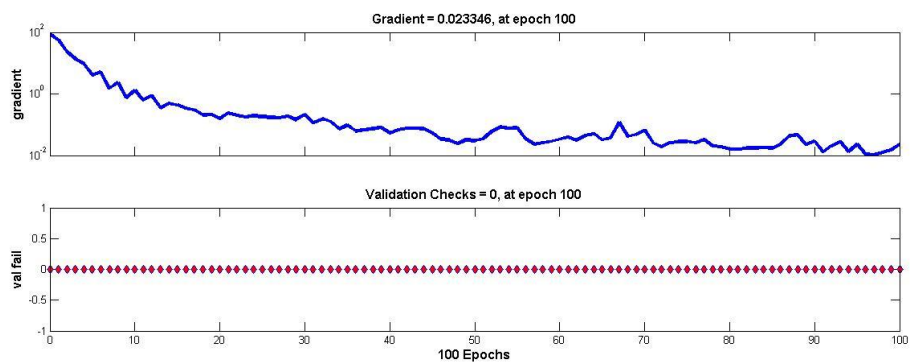
v. Propane



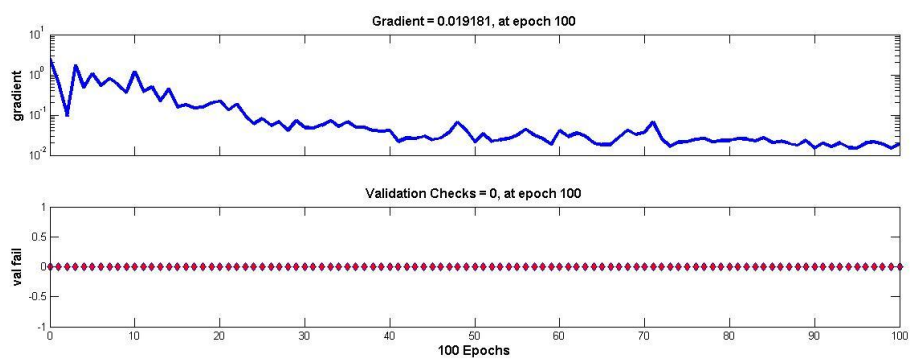
## Appendix 2: Training State

### Forward Model Neural Network

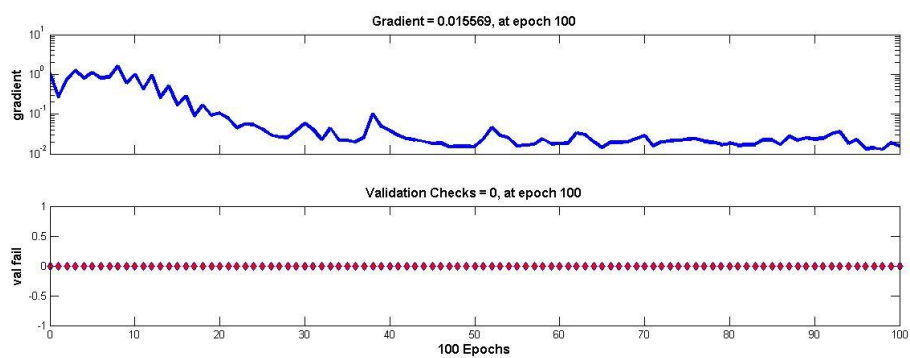
#### i. i-butane



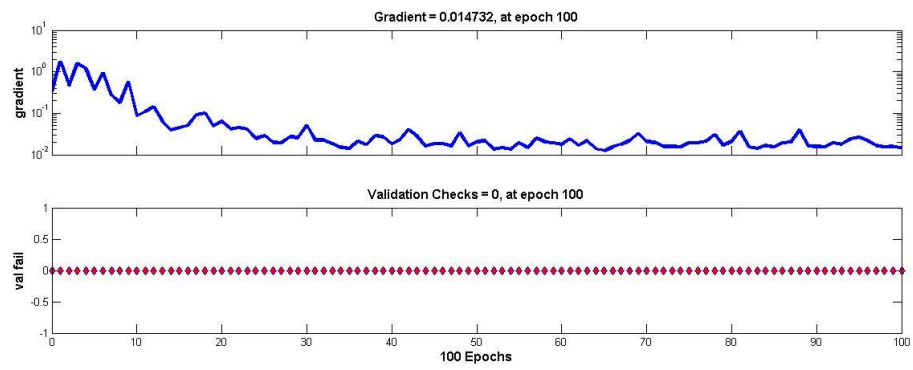
#### ii. i-pentane



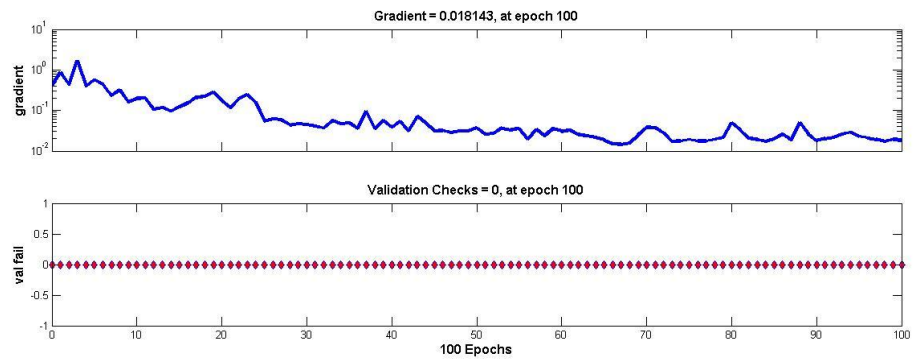
#### iii. n-butane



iv. n-pentane

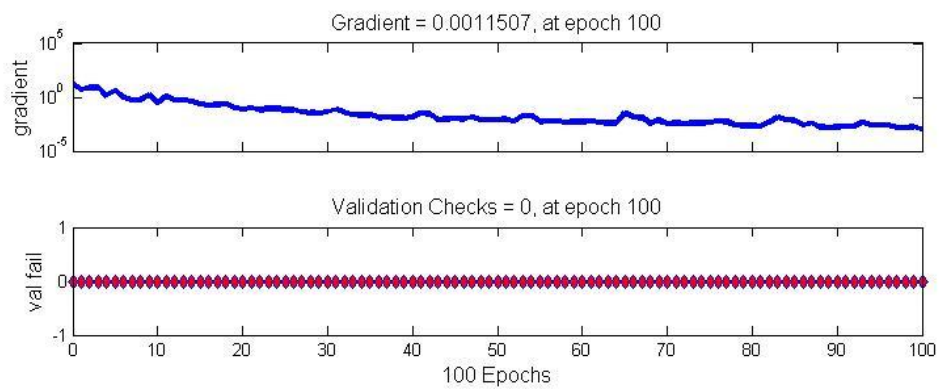


v. Propane

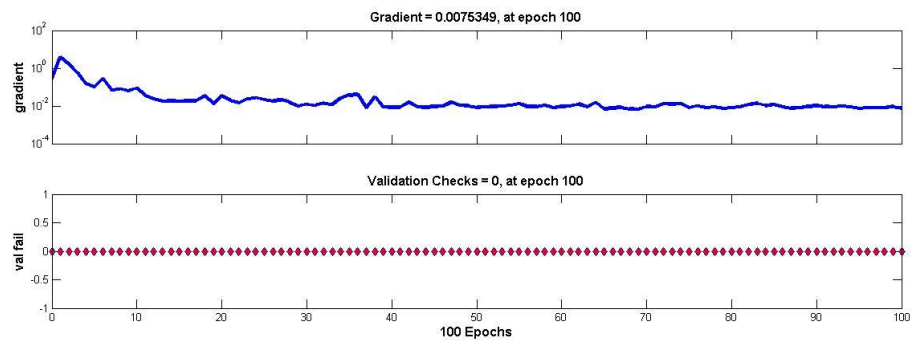


**Inverse Model Neural Network**

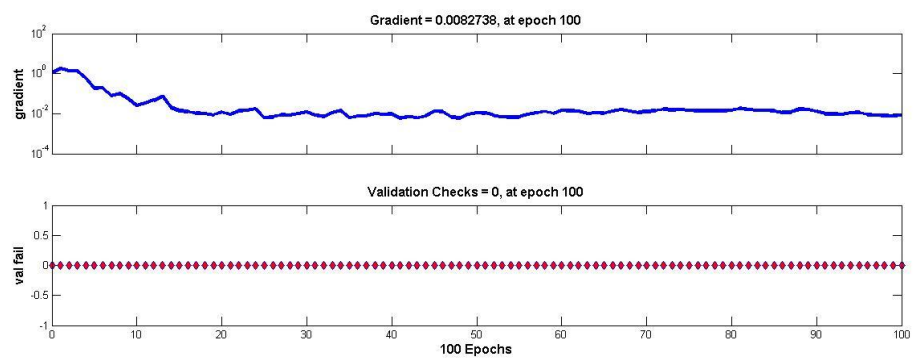
i. i-butane



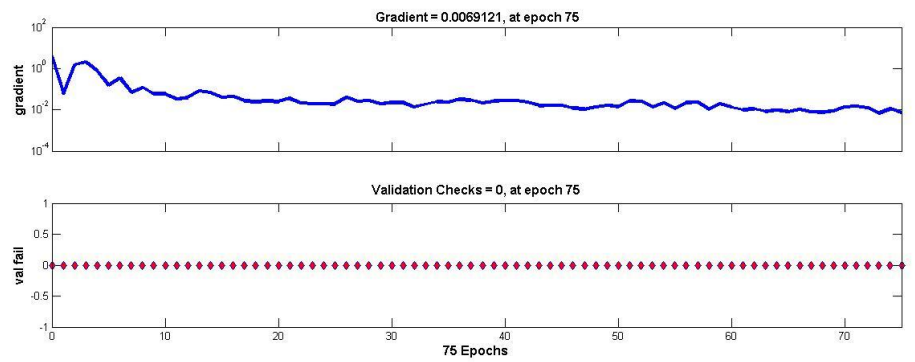
ii. i-pentane



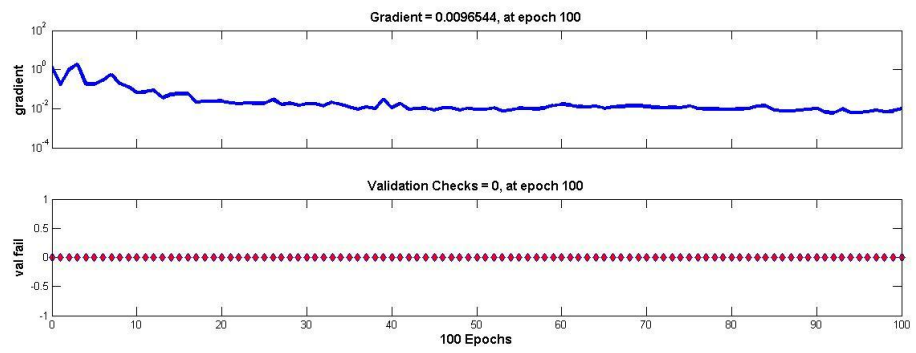
iii. n-butane



iv. n-pentane



v. Propane



### Appendix 3: Trial and Error Hidden Nodes

#### i-Butane

	4	8	12	16	20	24	28	32	36	40	44	48	52	56	60	64	68	72	76	80	
rmse_top_mol_fraction_training	0.0003	0.0003	0.0003	0.0003	0.0003	0.0003	0.0003	0.0003	0.0003	0.0003	0.0003	0.0003	0.0003	0.0003	0.0003	0.0003	0.0003	0.0003	0.0003	0.0003	0.0003
rmse_bottom_mol_fraction_training	0.0086	0.0086	0.0090	0.0089	0.0086	0.0087	0.0086	0.0088	0.0086	0.0090	0.0086	0.0088	0.0087	0.0091	0.0086	0.0087	0.0086	0.0089	0.0087	0.0087	0.0087
CDC_top_mol_fraction_training	45.0000	46.6667	48.0000	46.0000	45.0000	44.6667	47.0000	45.0000	45.6667	45.0000	45.3333	45.0000	46.3333	43.3333	46.3333	45.6667	45.0000	46.6667	46.0000	46.3333	46.3333
CDC_bottom_mol_fraction_training	56.0000	56.0000	53.6667	57.0000	56.0000	55.6667	56.3333	55.3333	55.3333	56.6667	56.3333	53.3333	56.6667	54.6667	57.0000	54.3333	56.0000	54.0000	55.3333	55.3333	55.3333
R_top_mol_fraction_training	0.5057	0.4956	0.5002	0.5165	0.5159	0.5149	0.5116	0.5028	0.5107	0.4858	0.4881	0.5136	0.5020	0.4895	0.5132	0.5109	0.5120	0.4944	0.5129	0.5129	0.4948
R_bottom_mol_fraction_training	0.9182	0.9184	0.9109	0.9129	0.9186	0.9162	0.9189	0.9155	0.9183	0.9106	0.9185	0.9161	0.9179	0.9079	0.9192	0.9179	0.9182	0.9142	0.9175	0.9175	0.9170
AIC_top_mol_fraction_training	-4494.5000	-4499.2000	-4415.7000	-4483.0000	-4484.6000	-4495.8000	-4437.0000	-4481.1000	-4482.1000	-4357.0000	-4487.3000	-4499.9000	-4518.6000	-4341.7000	-4443.4000	-4513.0000	-4510.7000	-4463.6000	-4501.3000	-4485.7000	-4485.7000
AIC_bottom_mol_fraction_training	-1771.4000	-1776.2000	-1827.4000	-1754.3000	-1768.0000	-1752.2000	-1762.4000	-1745.8000	-1782.3000	-1715.8000	-1761.7000	-1795.0000	-1751.5000	-1773.8000	-1772.9000	-1789.9000	-1765.9000	-1769.8000	-1739.5000	-1786.9000	-1786.9000
BIC_top_mol_fraction_training	-4479.6000	-4484.3000	-4400.8000	-4468.2000	-4469.7000	-4481.0000	-4422.1000	-4466.2000	-4467.3000	-4342.2000	-4472.5000	-4485.0000	-4503.7000	-4326.9000	-4428.5000	-4498.1000	-4495.8000	-4448.8000	-4486.5000	-4470.9000	-4470.9000
BIC_bottom_mol_fraction_training	-1756.6000	-1761.4000	-1812.6000	-1739.4000	-1753.2000	-1737.4000	-1747.5000	-1730.9000	-1767.4000	-1700.9000	-1746.9000	-1780.2000	-1736.7000	-1759.0000	-1758.1000	-1775.0000	-1751.0000	-1755.0000	-1724.7000	-1772.1000	-1772.1000
MAPE_top_mol_fraction_training	0.0002	-0.0001	-0.0003	0.0001	-0.0001	0.0000	0.0003	0.0009	-0.0006	0.0014	-0.0004	0.0002	0.0000	-0.0001	0.0005	0.0000	-0.0014	0.0000	0.0000	0.0000	-0.0001
MAPE_bottom_mol_fraction_training	2.5147	3.3606	2.1410	2.3336	2.8359	3.0170	2.7145	2.2769	2.5854	2.1471	2.4259	2.5861	2.7433	2.5490	2.9009	2.7315	2.7049	1.9034	2.7466	2.6522	2.6522
Cp_top_mol_fraction_training	0.5057	0.4956	0.5002	0.5165	0.5159	0.5149	0.5116	0.5028	0.5107	0.4858	0.4881	0.5136	0.5020	0.4895	0.5132	0.5109	0.5120	0.4944	0.5129	0.5129	0.4948
Cp_bottom_mol_fraction_training	0.9182	0.9184	0.9109	0.9129	0.9186	0.9162	0.9189	0.9155	0.9183	0.9106	0.9185	0.9161	0.9179	0.9097	0.9192	0.9179	0.9182	0.9142	0.9175	0.9175	0.9170

#### i-Pentane

	4	8	12	16	20	24	28	32	36	40	44	48	52	56	60	64	68	72	76	80	
rmse_top_mol_fraction_training	0.0002	0.0002	0.0002	0.0002	0.0002	0.0002	0.0002	0.0002	0.0002	0.0002	0.0002	0.0002	0.0002	0.0002	0.0002	0.0002	0.0002	0.0002	0.0002	0.0002	0.0002
rmse_bottom_mol_fraction_training	0.0037	0.0033	0.0034	0.0033	0.0035	0.0032	0.0032	0.0031	0.0031	0.0032	0.0031	0.0031	0.0031	0.0031	0.0031	0.0033	0.0031	0.0031	0.0035	0.0032	0.0030
CDC_top_mol_fraction_training	55.3333	54.3333	62.6667	62.0000	61.3333	60.0000	58.3333	62.6667	58.3333	62.0000	60.3333	64.3333	63.0000	60.3333	61.0000	60.0000	59.6667	60.6667	58.0000	60.0000	60.0000
CDC_bottom_mol_fraction_training	53.6667	57.6667	57.3333	58.0000	60.0000	57.6667	59.6667	58.0000	57.0000	58.0000	55.6667	54.0000	56.6667	58.0000	56.6667	60.6667	56.6667	56.6667	60.0000	59.0000	59.0000
R_top_mol_fraction_training	0.5915	0.6239	0.6808	0.6731	0.6937	0.6946	0.6893	0.7121	0.7059	0.6933	0.7321	0.6935	0.7017	0.7324	0.6524	0.7327	0.6844	0.6647	0.6982	0.7029	0.7029
R_bottom_mol_fraction_training	0.8649	0.8947	0.8882	0.8943	0.8832	0.9025	0.9059	0.9062	0.9096	0.8998	0.9062	0.9067	0.9121	0.9077	0.8939	0.9070	0.9120	0.8859	0.9002	0.9171	0.9171
AIC_top_mol_fraction_training	-4586.1000	-4558.3000	-4480.8000	-4571.7000	-4475.4000	-4486.9000	-4470.8000	-4492.3000	-4458.0000	-4472.3000	-4473.9000	-4434.7000	-4487.1000	-4451.8000	-4487.6000	-4496.9000	-4486.0000	-4539.3000	-4458.3000	-4466.3000	-4466.3000
AIC_bottom_mol_fraction_training	-2705.6000	-2604.8000	-2565.9000	-2478.4000	-2594.7000	-2504.8000	-2549.3000	-2560.8000	-2584.4000	-2521.1000	-2558.9000	-2532.9000	-2546.5000	-2517.2000	-2535.7000	-2538.6000	-2582.6000	-2605.5000	-2634.9000	-2558.4000	-2558.4000
BIC_top_mol_fraction_training	-4571.3000	-4543.4000	-4465.9000	-4556.9000	-4460.5000	-4472.1000	-4456.0000	-4477.5000	-4443.2000	-4457.5000	-4459.1000	-4419.9000	-4472.3000	-4437.0000	-4472.7000	-4482.1000	-4471.2000	-4524.5000	-4443.4000	-4451.5000	-4451.5000
BIC_bottom_mol_fraction_training	-2690.8000	-2590.0000	-2551.1000	-2463.5000	-2579.9000	-2490.0000	-2534.4000	-2546.0000	-2569.6000	-2506.3000	-2544.0000	-2518.1000	-2531.7000	-2502.4000	-2520.8000	-2523.7000	-2567.8000	-2590.7000	-2620.1000	-2543.5000	-2543.5000
MAPE_top_mol_fraction_training	-0.0046	0.0005	-0.0104	-0.0005	-0.0031	-0.0027	-0.0020	0.0020	-0.0043	-0.0025	-0.0023	-0.0023	-0.0041	-0.0006	0.0025	-0.0063	-0.0078	-0.0020	0.0025	0.0000	-0.0040
MAPE_bottom_mol_fraction_training	0.1774	0.0393	-0.0487	-0.0906	0.0476	-0.0782	-0.1651	-0.0342	-0.0225	-0.1113	-0.0344	-0.0997	-0.0281	-0.0977	-0.0411	-0.0328	0.0137	0.0420	-0.0906	0.1192	0.1192
Cp_top_mol_fraction_training	0.5915	0.6293	0.6808	0.6731	0.6937	0.6946	0.6893	0.7121	0.7059	0.6933	0.7321	0.6935	0.7017	0.7324	0.6542	0.7327	0.6844	0.6647	0.6982	0.7029	0.7029
Cp_bottom_mol_fraction_training	0.8649	0.8947	0.8882	0.8943	0.8832	0.9025	0.9059	0.9062	0.9096	0.8998	0.9062	0.9067	0.9121	0.9077	0.8939	0.9070	0.9120	0.8859	0.9002	0.9171	0.9171

## n-Butane

	4	8	12	16	20	24	28	32	36	40	44	48	52	56	60	64	68	72	76	80
rmse_top_mol_fraction_training	0.0000	0.0000	0.0000	0.0000	0.0000	0.0000	0.0000	0.0000	0.0000	0.0000	0.0000	0.0000	0.0000	0.0000	0.0000	0.0000	0.0000	0.0001	0.0000	0.0000
rmse_bottom_mol_fraction_training	0.0064	0.0061	0.0058	0.0059	0.0056	0.0056	0.0055	0.0056	0.0054	0.0055	0.0069	0.0054	0.0054	0.0057	0.0086	0.0054	0.0065	0.0185	0.0055	0.0113
CDC_top_mol_fraction_training	53.6667	54.3333	59.6667	52.6667	61.0000	62.0000	57.0000	59.6667	60.0000	62.0000	58.0000	59.3333	61.6667	59.0000	58.3333	63.0000	56.6667	53.3333	59.0000	56.3333
CDC_bottom_mol_fraction_training	55.0000	54.3333	58.0000	54.3333	56.3333	56.6667	57.3333	54.0000	56.6667	55.0000	57.0000	55.3333	60.0000	59.6667	52.3333	61.0000	54.6667	54.6667	61.0000	55.6667
R_top_mol_fraction_training	0.6147	0.6574	0.6794	0.6615	0.7116	0.7186	0.6889	0.7324	0.7147	0.7546	0.7051	0.7291	0.7277	0.7015	0.6380	0.7265	0.6929	0.1568	0.7058	0.7204
R_bottom_mol_fraction_training	0.8864	0.8979	0.9085	0.9057	0.9138	0.9131	0.9165	0.9135	0.9193	0.9163	0.8951	0.9202	0.9198	0.9120	0.8104	0.9205	0.8815	0.7086	0.9160	0.7579
AIC_top_mol_fraction_training	-5461.7000	-5474.1000	-5401.6000	-5409.9000	-5345.0000	-5295.3000	-5345.8000	-5293.1000	-5327.4000	-5319.1000	-5375.7000	-5307.3000	-5325.9000	-5340.1000	-5309.7000	-5315.3000	-5341.6000	-4946.8000	-5349.2000	-5356.6000
AIC_bottom_mol_fraction_training	-2099.6000	-2075.6000	-2094.4000	-2087.0000	-2087.2000	-2144.0000	-2103.8000	-2076.5000	-2062.3000	-2111.0000	-2121.7000	-2041.4000	-2105.5000	-2120.2000	-1932.6000	-2073.1000	-2159.8000	-1979.0000	-2101.7000	-1856.6000
BIC_top_mol_fraction_training	-5446.8000	-5459.3000	-5386.8000	-5395.1000	-5330.2000	-5280.5000	-5330.9000	-5278.3000	-5312.5000	-5304.3000	-5360.8000	-5292.5000	-5311.1000	-5325.3000	-5294.9000	-5300.5000	-5326.8000	-4932.0000	-5334.4000	-5341.8000
BIC_bottom_mol_fraction_training	-2084.8000	-2060.8000	-2079.6000	-2072.2000	-2072.4000	-2129.1000	-2089.0000	-2061.7000	-2047.4000	-2096.2000	-2106.9000	-2026.5000	-2090.7000	-2105.4000	-1917.8000	-2058.2000	-2145.0000	-1964.2000	-2086.9000	-1841.8000
MAPE_top_mol_fraction_training	-0.0005	0.0003	0.0000	0.0004	-0.0004	-0.0002	-0.0002	-0.0006	-0.0005	-0.0002	-0.0004	-0.0001	-0.0004	0.0000	0.0008	-0.0003	0.0000	0.0415	-0.0001	0.0003
MAPE_bottom_mol_fraction_training	0.4413	0.8918	1.1036	-0.0084	0.6105	0.0808	-0.2099	0.7266	0.9688	0.6719	-68.6627	0.5758	0.6159	1.3435	2.1339	-0.1374	-1.0922	16.9797	1.0360	6.0904
Cp_top_mol_fraction_training	0.6147	0.6574	0.6794	0.6615	0.7116	0.7186	0.6889	0.7324	0.7147	0.7546	0.7051	0.7291	0.7277	0.7015	0.6380	0.7265	0.6929	0.1568	0.7058	0.7204
Cp_bottom_mol_fraction_training	0.8864	0.8979	0.9085	0.9057	0.9138	0.9131	0.9165	0.9135	0.9193	0.9163	0.8951	0.9202	0.9198	0.9120	0.8104	0.9205	0.8815	0.7086	0.9160	0.7579

## n-Pentane

	4	8	12	16	20	24	28	32	36	40	44	48	52	56	60	64	68	72	76	80
rmse_top_mol_fraction_training	0.0003	0.0003	0.0003	0.0003	0.0003	0.0003	0.0003	0.0003	0.0003	0.0003	0.0003	0.0003	0.0003	0.0003	0.0003	0.0003	0.0003	0.0003	0.0004	0.0004
rmse_bottom_mol_fraction_training	0.0033	0.0032	0.0032	0.0031	0.0030	0.0030	0.0030	0.0031	0.0029	0.0030	0.0029	0.0030	0.0028	0.0028	0.0030	0.0029	0.0031	0.0030	0.0035	0.0034
CDC_top_mol_fraction_training	52.6667	52.3333	60.6667	54.0000	52.6667	58.6667	62.6667	57.6667	56.0000	53.3333	59.0000	58.3333	52.3333	57.3333	49.6667	53.6667	60.0000	58.6667	53.3333	54.0000
CDC_bottom_mol_fraction_training	50.6667	62.3333	55.0000	57.3333	59.6667	61.0000	59.0000	55.3333	59.3333	59.6667	57.3333	57.0000	61.3333	61.0000	59.6667	60.0000	59.3333	54.6667	58.6667	56.6667
R_top_mol_fraction_training	0.6007	0.5945	0.6976	0.6579	0.6683	0.6750	0.7034	0.6946	0.7213	0.6528	0.7123	0.6870	0.6544	0.6891	0.5408	0.7027	0.6805	0.6669	0.4536	0.4224
R_bottom_mol_fraction_training	0.9069	0.9111	0.9089	0.9175	0.9202	0.9242	0.9226	0.9143	0.9251	0.9238	0.9289	0.9223	0.9348	0.9324	0.9230	0.9294	0.9143	0.9214	0.8947	0.9016
AIC_top_mol_fraction_training	-4359.9000	-4389.4000	-4257.3000	-4360.9000	-4300.8000	-4305.6000	-4301.4000	-4350.4000	-4297.0000	-4335.5000	-4282.3000	-4391.8000	-4370.2000	-4317.7000	-4391.9000	-4323.7000	-4289.2000	-4276.0000	-4192.9000	-4232.6000
AIC_bottom_mol_fraction_training	-2872.1000	-2740.3000	-2750.5000	-2675.9000	-2623.9000	-2561.9000	-2588.5000	-2594.3000	-2551.3000	-2602.1000	-2562.0000	-2602.3000	-2614.9000	-2598.3000	-2630.9000	-2578.3000	-2609.0000	-2651.3000	-2651.6000	-2521.1000
BIC_top_mol_fraction_training	-4345.1000	-4374.6000	-4242.4000	-4346.1000	-4285.9000	-4290.8000	-4286.5000	-4335.5000	-4282.1000	-4320.7000	-4267.5000	-4377.0000	-4355.3000	-4302.9000	-4377.1000	-4308.8000	-4274.4000	-4261.1000	-4178.1000	-4217.7000
BIC_bottom_mol_fraction_training	-2857.3000	-2725.5000	-2735.6000	-2661.1000	-2609.1000	-2547.0000	-2573.7000	-2579.5000	-2536.5000	-2587.3000	-2547.1000	-2587.5000	-2600.0000	-2583.5000	-2616.1000	-2563.4000	-2594.2000	-2636.5000	-2636.8000	-2506.3000
MAPE_top_mol_fraction_training	0.0017	-0.0029	0.0075	-0.0028	0.0008	-0.0019	0.0007	-0.0040	-0.0037	-0.0032	-0.0044	-0.0031	-0.0016	-0.0016	0.0055	-0.0018	-0.0031	0.0015	0.0014	0.0244
MAPE_bottom_mol_fraction_training	0.0211	-0.0060	-0.0204	-0.0245	-0.0382	-0.0797	-0.0384	-0.0339	-0.0763	-0.0115	0.0101	-0.0256	-0.0300	0.0526	0.0455	-0.0928	-0.1297	0.0016	-0.1126	-0.2080
Cp_top_mol_fraction_training	0.6007	0.5945	0.6976	0.6579	0.6683	0.6750	0.7034	0.6946	0.7213	0.6528	0.7123	0.6870	0.6544	0.6891	0.5408	0.7027	0.6805	0.6669	0.4536	0.4224
Cp_bottom_mol_fraction_training	0.9069	0.9111	0.9089	0.9175	0.9202	0.9242	0.9226	0.9143	0.9251	0.9238	0.9289	0.9223	0.9348	0.9324	0.9230	0.9294	0.9143	0.9214	0.8947	0.9016

## Propane

	4	8	12	16	20	24	28	32	36	40	44	48	52	56	60	64	68	72	76
rmse_top_mol_fraction_training	0.0011	0.0011	0.0011	0.0010	0.0011	0.0010	0.0011	0.0010	0.0010	0.0010	0.0011	0.0010	0.0010	0.0010	0.0010	0.0010	0.0010	0.0010	0.0010
rmse_bottom_mol_fraction_training	0.0017	0.0016	0.0014	0.0014	0.0014	0.0014	0.0013	0.0013	0.0013	0.0013	0.0013	0.0012	0.0013	0.0033	0.0014	0.0014	0.0013	0.0013	0.0013
CDC_top_mol_fraction_training	51.6667	54.6667	54.6667	56.0000	59.0000	59.6667	57.0000	55.3333	60.0000	60.0000	58.3333	62.6667	61.6667	58.0000	56.6667	55.0000	59.3333	53.0000	55.3333
CDC_bottom_mol_fraction_training	54.0000	54.6667	53.0000	53.6667	53.0000	53.3333	51.3333	56.3333	49.3333	55.0000	51.3333	57.3333	52.0000	47.6667	52.6667	54.3333	58.3333	51.3333	53.6667
R_top_mol_fraction_training	0.5111	0.5536	0.5893	0.6256	0.6058	0.6427	0.5833	0.6472	0.6387	0.6649	0.6124	0.6657	0.6266	0.6516	0.6231	0.6425	0.6653	0.6504	0.6294
R_bottom_mol_fraction_training	0.9410	0.9478	0.9617	0.9613	0.9604	0.9614	0.9661	0.9641	0.9630	0.9674	0.9639	0.9692	0.9650	0.8412	0.9563	0.9614	0.9665	0.9636	0.9632
AIC_top_mol_fraction_training	-3727.2000	-3613.5000	-3593.2000	-3612.0000	-3581.0000	-3595.6000	-3607.0000	-3555.8000	-3588.0000	-3567.8000	-3625.5000	-3544.1000	-3658.4000	-3597.2000	-3613.8000	-3573.2000	-3581.7000	-3612.5000	-3615.9000
AIC_bottom_mol_fraction_training	-2872.0000	-2784.1000	-2787.9000	-2782.4000	-2841.1000	-2749.1000	-2787.3000	-2797.1000	-2764.7000	-2826.4000	-2790.7000	-2788.8000	-2802.6000	-3044.3000	-2830.8000	-2789.4000	-2781.1000	-2820.5000	-2743.4000
BIC_top_mol_fraction_training	-3712.3000	-3598.7000	-3578.4000	-3597.2000	-3566.2000	-3580.8000	-3592.2000	-3540.9000	-3573.1000	-3553.0000	-3610.7000	-3529.3000	-3643.6000	-3582.3000	-3599.0000	-3558.4000	-3566.8000	-3597.7000	-3601.1000
BIC_bottom_mol_fraction_training	-2857.2000	-2769.3000	-2773.0000	-2767.6000	-2826.3000	-2734.3000	-2772.4000	-2782.2000	-2749.9000	-2811.5000	-2775.9000	-2774.0000	-2787.7000	-3029.5000	-2816.0000	-2774.6000	-2766.3000	-2805.7000	-2728.6000
MAPE_top_mol_fraction_training	0.0025	-0.0024	0.0073	0.0043	0.0004	0.0019	0.0107	0.0122	-0.0043	0.0055	-0.0006	-0.0001	-0.0010	-0.0001	0.0133	0.0075	0.0105	0.0093	0.0007
MAPE_bottom_mol_fraction_training	-0.7292	2.5060	0.8798	3.4848	7.6994	-57.0482	1.6140	5.5691	-3.2852	-0.8478	-0.3281	0.7860	0.6067	-4611.1000	-3.0917	3.0636	1.5997	7.1872	0.4371
Cp_top_mol_fraction_training	0.5111	0.5536	0.5893	0.6256	0.6058	0.6427	0.5833	0.6472	0.6387	0.6649	0.6124	0.6657	0.6266	0.6516	0.6231	0.6425	0.6653	0.6504	0.6294
Cp_bottom_mol_fraction_training	0.9410	0.9478	0.9617	0.9613	0.9604	0.9614	0.9661	0.9641	0.9630	0.9674	0.9639	0.9692	0.9650	0.8412	0.9563	0.9614	0.9665	0.9636	0.9632

## Appendix 4: Overall Algorithm/Coding for neural network

### n-Butane

```
clc;
clear all;
close all;

%Load Data
A=xlsread('n-butane all');
P_tr=A(:,1:10);
T_tr=A(:,11:12);

nntwarn off;

% Training set
[Pn_tr, Pmin_tr, Pmax_tr] = premmx(P_tr);
[Tn_tr, Tmin_tr, Tmax_tr] = premmx(T_tr);

%Setup network
net=newff(minmax(Pn_tr), [10 40 2], {'tansig','tansig','tansig'}, 'trainrp','learnqdm','mse');
net.trainParam.show=10;
net.trainParam.epochs=100;
net.trainParam.goal=1e-2;

%Train network with early stopping
rand('seed',419877);
net = init(net);
[net, tr] = train(net,Pn_tr,Tn_tr);

%Simulate network
an2=sim(net,Pn_tr); % Training
at2 = postmnmx(an2, Tmin_tr, Tmax_tr);

%-----graphs-----

figure(1)
[slope5,intercept5,R5] = postreg(at2(1,:),T_tr(1,:)); % Top Mol Fraction
ylabel('Simulated n-Butane at Top'),xlabel('Actual n-Butane at Top'),...
title([' Simulated vs. Actual, R(slope)=', num2str(R5),'and intercept=',num2str(intercept5)]);

figure(2)
[slope6,intercept6,R6] = postreg(at2(2,:),T_tr(2,:));% Bottom Mol Fraction
ylabel('Simulated n-Butane at Bottom'), xlabel('Actual n-Butane at Bottom'),...
title(['Simulated vs. Actual, R(slope)=', num2str(R6),'and intercept=',num2str(intercept6)]);

figure(3) % Training
time = 1:length(T_tr(1,:));
plot(time,T_tr(1,:),'kd-', time,at2(1,:),'r-', 'LineWidth',0.5,...
      'MarkerEdgeColor','k',...
      'MarkerFaceColor','g',...
      'MarkerSize',4);
xlabel('Time'), ylabel('Top Mol Fraction:Training'),...
legend('Actual','Simulated')
title(['Actual and Simulated plot for Top Mol Fraction :Training']),

figure(4) % Training
time = 1:length(T_tr(2,:));
plot(time,T_tr(2,:),'kd-', time,at2(2,:),'r-', 'LineWidth',0.5,...
      'MarkerEdgeColor','k',...
      'MarkerFaceColor','g',...
      'MarkerSize',4);
xlabel('Time'), ylabel('Bottom Mol Fraction:Training'),...
legend('Actual','Simulated')
title(['Actual and Simulated plot for Bottom Mol Fraction:Training']),

%-----Training set performance measurement-----

% rmse calculation Training
[row1,col1] = size(T_tr);
error_col = zeros(row1,col1);
```

```

for i = 1:1:row1,
for j = 1:1:col1,
    error_col(i,j) = (at2(i,j) - T_tr(i,j))^2;
end
end
sum_error = sum(error_col(1,:));
rmse_top_mol_fraction_training = sqrt(sum_error/col1);
sum_error = sum(error_col(2,:));
rmse_bottom_mol_fraction_training = sqrt(sum_error/col1);

% CDC calculation for training
d1=zeros(1,col1-1);
w1=zeros(1,col1-1);
i=2;
for n=1:1:col1-1
    a=T_tr(1,i) - T_tr(1,i-1);
    b=at2(1,i) - at2(1,i-1);
    c=a*b;
    d1(:,i-1)=c;
    g=T_tr(2,i) - T_tr(2,i-1);
    h=at2(2,i) - at2(2,i-1);
    x=g*h;
    w1(:,i-1)=x;
    i=i+1;
end

D_top=zeros(1,col1-1);
D_botm=zeros(1,col1-1);
m=1;
for q=1:1:col1-1
    if d1(:,m)>0
        D_top(:,m)=1;
    else
        D_top(:,m)=0;
    end

    if w1(:,m)>0
        D_botm(:,m)=1;
    else
        D_botm(:,m)=0;
    end
    m=m+1;
end

[row2,col2] = size(D_top);
[row3,col3] = size(D_botm);
CDC_top_mol_fraction_training = (sum(D_top))*(100/(col2));
CDC_bottom_mol_fraction_training = (sum(D_botm))*(100/(col3));

% AIC and BIC calculation for training
[Coeff_top_mol_fraction,Errors_top_mol_fraction,LLF_top_mol_fraction,Innovations_top_mol_fraction,Sigmas_top_mol_fra
tion,Summary_top_mol_fraction]=garchfit(at2(1,:));
[Coeff_bottom_mol_fraction,Errors_bottom_mol_fraction,LLF_bottom_mol_fraction,Innovations_bottom_mol_fraction,Sigma
s_bottom_mol_fraction,Summary_bottom_mol_fraction]=garchfit(at2(2,:));
[AICt_trainng BICt_trainng]=aicbic(LLF_top_mol_fraction,4,col1);
[AICT_trainng BICT_trainng]=aicbic(LLF_bottom_mol_fraction,4,col1);

% MAPE calculation Training
[row1,col1] = size(T_tr);
Percentage_error = zeros(row1,col1);
for i = 1:1:row1,
    for j = 1:1:col1,
        Percentage_error(i,j) = ((at2(i,j) - T_tr(i,j))/at2(i,j))*100;
    end
end
sum_Percentage_error = sum(Percentage_error(1,:));
MAPE_top_mol_fraction_training = (sum_Percentage_error/col1);
sum_Percentage_error = sum(Percentage_error(2,:));
MAPE_bottom_mole_fraction_training = (sum_Percentage_error/col1);

% pearson correlation coeff calculation Training
[row1,col1] = size(T_tr);
Predicted = zeros(row1,col1);

```

```

Actual = zeros(row1,col1);
val1 = zeros(row1,col1);
val2 = zeros(row1,col1);
val3 = zeros(row1,col1);
for i = 1:1:row1,
    Ep=mean(at2(i,:));
Ea=mean(T_tr(i,:));
    for j = 1:1:col1,
        Predicted(i,j) = at2(i,j);
        Actual(i,j)=T_tr(i,j);
        val1(i,j)=(Predicted(i,j)-Ep)*(Actual(i,j)-Ea);
        val2(i,j)=(Predicted(i,j)-Ep)^2;
        val3(i,j)=(Actual(i,j)-Ea)^2;
    end
end

Cp_top_mol_fraction_training=(sum(val1(1,:)))/(sqrt(sum(val2(1,:))*sum(val3(1,:))));
Cp_bottom_mol_fraction_training=(sum(val1(2,:)))/(sqrt(sum(val2(2,:))*sum(val3(2,:))));

%-----display output-----
clc;
output.rmse_top_mol_fraction_training=rmse_top_mol_fraction_training;
output.rmse_bottom_mol_fraction_training=rmse_bottom_mol_fraction_training;
output.CDC_top_mol_fraction_training=CDC_top_mol_fraction_training;
output.CDC_bottom_mol_fraction_training=CDC_bottom_mol_fraction_training;
output.R_top_mol_fraction_training=R5;
output.R_bottom_mol_fraction_training=R6;
output.AIC_top_mol_fraction_training=AICt_trainng;
output.AIC_bottom_mol_fraction_training=AICT_trainng;
output.BIC_top_mol_fraction_training=BICt_trainng;
output.BIC_bottom_mol_fraction_training=BICT_trainng;
output.MAPE_top_mol_fraction_training=MAPE_top_mol_fraction_training;
output.MAPE_bottom_mol_fraction_training=MAPE_bottom_mole_fraction_training;
output.Cp_top_mol_fraction_training=Cp_top_mol_fraction_training;
output.Cp_bottom_mol_fraction_training=Cp_bottom_mol_fraction_training;

disp(output),

gensim(net);

```